Developing novel classes of protein kinase CK1δ inhibitors by fusing [1,2,4]triazole with different bicyclic heteroaromatic systems

Ilenia Grieco [a], Maicol Bissaro [b], Davide Benedetto Tiz [a], Daniel I. Perez [c], Conception Perez [d], Ana Martinez [c, e], Sara Redenti [a], Elena Mariotto [f], Roberta Bortolozzi [g], Giampietro Viola [f, g], Giorgio Cozza [h], Giampiero Spalluto [a], Stefano Moro [b], Stephanie Federico [a, *]

[a] Dipartimento di Scienze Chimiche e Farmaceutiche, Università degli Studi di Trieste, Via Licio Giorgieri 1, 34127, Trieste, Italy
[b] Molecular Modeling Section (MMS), Dipartimento di Scienze del Farmaco, Università degli Studi di Padova, via Marzolo 5, 35131, Padova, Italy
[c] Centro de Investigaciones Biologicas, CSIC, Ramiro de Maetzu 9, 28040, Madrid, Spain
[d] Instituto de Quimica Medica, CSIC, Juan de la Cierva 3, 28006, Madrid, Spain
[e] Centro de Investigacion Biomedica en Red en Enfermedades Neurodegenerativas (CIBERNED), Instituto Carlos III, 28031, Madrid, Spain
[f] Dipartimento di Salute della Donna e del Bambino, Laboratorio di Oncoematologia, Università di Padova, 35131, Padova, Italy
[g] Istituto di Ricerca Pediatrica (IRP), Corso Stati Uniti 4, 35128, Padova, Italy
[h] Dipartimento di Medicina Molecolare, Università degli Studi di Padova, Via U. Bassi 58/B, 35131, Padova, Italy

ARTICLE INFO

Article history:
Accepted 21 February 2021

Keywords:
Protein kinase CK1 delta
[1,2,4]triazolo[1,5-*c*]pyrimidine
[1,2,4]triazolo[1,5-*a*][1,3,5]triazine
BBB-PAMPA assay
Kinase molecular modeling
Neurodegenerative diseases

ABSTRACT

Protein kinase CK1δ expression and activity is involved in different pathological situations that include neuroinflammatory and neurodegenerative diseases. For this reason, protein kinase CK1δ has become a possible therapeutic target for these conditions. 5,6-fused bicyclic heteroaromatic systems that resemble adenine of ATP represent optimal scaffolds for the development of a new class of ATP competitive CK1δ inhibitors. In particular, a new series of [1,2,4]triazolo[1,5-*c*]pyrimidines and [1,2,4]triazolo[1,5-*a*][1,3,5] triazines was developed. Some crucial interactors have been identified, such as the presence of a free amino group able to interact with the residues of the hinge region at the 5- and 7- positions of the [1,2,4] triazolo[1,5-*c*]pyrimidine and [1,2,4]triazolo[1,5-*a*][1,3,5]triazine scaffolds, respectively; or the presence of a 3-hydroxyphenyl or 3,5-dihydroxyphenyl moiety at the 2- position of both nuclei. Molecular modeling studies identified the key interactions involved in the inhibitor-protein recognition process that appropriately fit with the outlined structure-activity relationship. Considering the fact that the CK1 protein kinase is involved in various pathologies in particular of the central nervous system, the interest in the development of new inhibitors permeable to the blood-brain barrier represents today an important goal in the pharmaceutical field. The best potent compound of the series is the 5-(7-amino-5-(benzylamino)-[1,2,4]triazolo[1,5-*a*][1,3,5]triazin-2-yl)benzen-1,3-diol (compound **51**, IC_{50} = 0.18 μM) that was predicted to have an intermediate ability to cross the membrane in our *in vitro* assay and represents an optimal starting point to both studies the therapeutic value of protein kinase CK1δ inhibition and to develop new more potent derivatives.

1. Introduction

Protein kinase CK1δ is a member of the protein kinase CK1 family of serine-threonine kinases. This family gives also the name to the homonym group of kinases which, in humans, beyond the other five CK1 isoforms, comprises Tau Tubulin Kinase (TTBK) and Vaccinia Related Kinase (VRK) families [1,2]. Deregulation of CK1δ is involved in the pathogenesis of several diseases [3], including sleep disorders [4,5], cancer [6–10] and infections [11,12]. In particular,

Abbreviations: CK1δ, protein kinase CK1 delta; BM, binding mode; HB, hydrogen bond; IE, interaction energy; MD, molecular dynamics; TM, transmembrane; TP, [1,2,4]triazolo[1,5-*c*]pyrimidine; TT, [1,2,4]triazolo[1,5-*a*][1,3,5]triazine; vdW, van der Waals.

* Corresponding author.
E-mail address: sfederico@units.it (S. Federico).

CK1δ is nowadays considered an appealing target in different neurodegenerative diseases [13–15], i.e. Alzheimer's disease (AD) [16–19], amyotrophic lateral sclerosis (ALS) [20–23], and Parkinson's disease [24–26] where it co-localizes with misphosphorylated proteins that are typical hallmarks of these diseases (tau protein; TDP-43, transactive response DNA-binding protein 43 KDa; and α-synuclein, respectively). Consequently, different CK1δ inhibitors were developed over the years and some of them are currently studied at the preclinical phase [27]. Firstly reported inhibitors showed low potency and non-optimal pharmacological properties, i.e. CK1-7 [28], D4476 [29], IC261 [30], while now different potent inhibitors are available but most of them lack of selectivity against CK1δ isoform. In fact, the existence of 6 different CK1 isoforms in humans (e.g. CK1α, CK1γ1, CK1γ2, CK1γ3, CK1δ and CK1ε) is the biggest challenge in development of inhibitors selective towards only the desired isoform, because they are highly conserved especially in their catalytic domain. In addition, isoforms are also present as different splice variants that mediate different activities but are structurally very similar each other [31]. Finally, CK1 activities were regulated also by their different localization, even at subcellular level [32]. For all these reasons, development of new CK1δ inhibitors is still an interesting challenge. The more interesting CK1δ pharmacological tools are PF-670462 (**I**) [33], PF-5006739 (**II**) [34], (R)-DRF053 (**III**) [35], SR-2890 (**IV**), SR-3029 (**V**) [36] and IGS-2.7 (**VI**) [20] (Fig. 1). In particular, PF-670462 (**I**), a 2-aminopyrimidine, was intensively used as pharmacological tool for CK1δ/ε inhibition (IC_{50}s of 14 and 7.7 nM, respectively [33]). Noteworthy, it demonstrated to attenuate fibrosis in idiopathic pulmonary fibrosis [37] and epithelial-to-mesenchymal transition in chronic obstructive pulmonary disease [38], both via inhibition of tumor growth factor β. The same compound was used by different groups to investigate CK1δ implication in AD mouse models [16,39] and cancer (i.e. bladder cancer [9] and chronic lymphocytic leukemia [40]) even if the most studied effect was that in the circadian rhythm [41–43]. Pfizer developed also the brain penetrant PF-5006739 (**II**, IC_{50} CK1δ = 3.9 nM, IC_{50} CK1ε = 17 nM) that was found to attenuate the opioid-seeking behavior in rodents [34]. Several CK1δ ATP competitive inhibitors have an adenine scaffold [9,35,36,44,45]. Among them, (R)-DRF053 (**III**, IC_{50} = 14 nM) [35] SR-2890 (**IV**, IC_{50} = 4 nM) and SR-3029 (**V**, IC_{50} = 44 nM) [36] display potent inhibitor properties against kinase. SR-3029 (**V**) demonstrated to inhibit growth of specific breast cancer cell lines where CK1δ resulted overexpressed or amplified [45,46]. Finally, the benzothiazole IGS-2.7 (**VI**, IC_{50} = 23 nM) [20] developed by Martinez's group was used to evaluate CK1δ inhibition as strategy for the treatment of ALS and frontotemporal dementia by targeting TDP-43 phosphorylation [21,22].

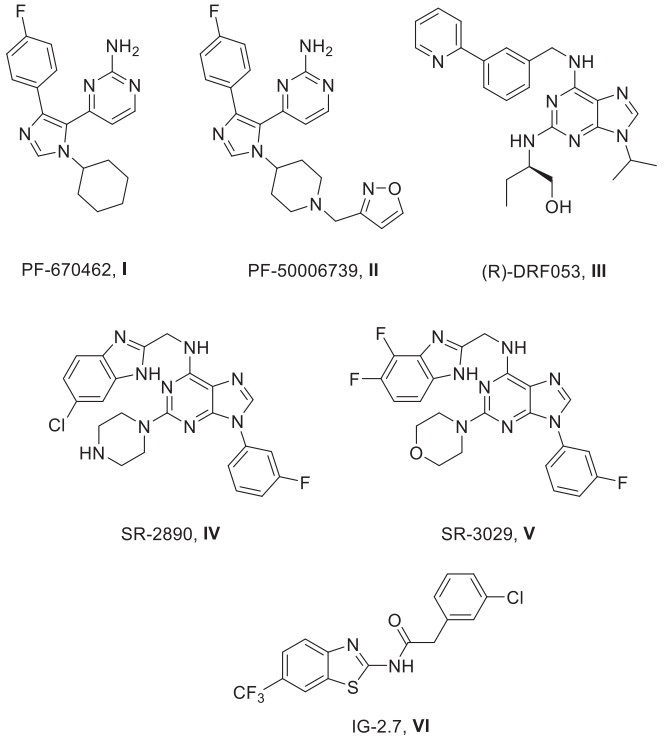

Fig. 1. Representative CK1δ inhibitors.

Over the years, we have developed [1,2,4]triazolo[1,5-*c*]pyrimidines (TP, **VII**) [47,48] and [1,2,4]triazolo[1,5-*a*][1,3,5]triazines (TT, **VIII**) [49–52] (Fig. 2) as adenosine receptor (AR) antagonists, Due to the obvious similarity between adenosine (the endogenous agonist of AR) and ATP (one of the substrates of kinases), herein reported a series of TP (compounds **1**–**36**) and TT (compounds **37**–**57**) with the aim of obtaining new ATP-competitive inhibitors for CK1δ kinase.

2. Chemistry

Synthesis of 2,5,8-trisubstituted [1,2,4]triazolo[1,5-c] pyrimidines.

All the 2,5,8-trisubstituted TP derivatives (**1**–**29**) have been synthesized following the strategy of Kyowa Hakko Kogyo Co., [53], adjusting it to our synthetic purposes as summarized below (Schemes 1–3).

Condensation between S-methylisothiourea (**58**) and diethyl ethoxymethylene malonate (**59**) in basic conditions led to the pyrimidine sodium salt **60**, which after treatment with phosphorous oxychloride under reflux afforded chloro derivative **61** that was immediately coupled with the required hydrazides (**62**–**76**) in the presence of DBU, to obtain derivatives **77**–**91**. The intramolecular cyclization that led to the [1,2,4]triazolo[1,5-*c*]pyrimidine system (**92**–**106**) was conducted using the trimethylsilyl ester of polyphosphoric acid as a dehydrating agent [54]. For those compounds presenting at the 2- position of the triazolo-pyrimidine scaffold polar groups susceptible to secondary reactions (e.g. OH for compounds **17**–**21** and NH_2 for compound **22**), a protective group was required in the initial steps of the synthetic pathway. So we decided to protect the hydroxyl groups with a benzyl group due to the mild conditions involved in its removal by catalytic hydrogenolysis (Scheme 2, reaction II). The same conditions were applied also in the palladium-catalyzed reduction of the nitro group (**9**) used to protect the amino group in compound **22** (Scheme 2, reaction III). Nucleophilic substitutions of methylthio group with primary amines (obtaining compounds **11**–**14**,**110**) were conducted heating the mixture in a sealed tube (Scheme 1). To obtain a free amino

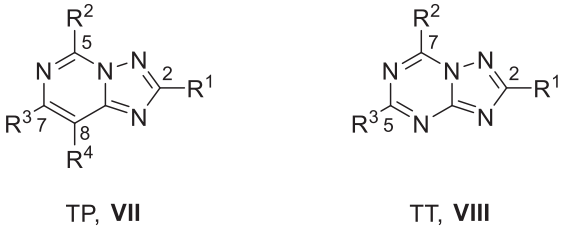

Fig. 2. [1,2,4]Triazolo[1,5-c]pyrimidine (**VII**) and [1,2,4]triazolo[1,5-a][1,3,5]triazine (**VIII**) nuclei developed in this work to find new CK1δ inhibitors.

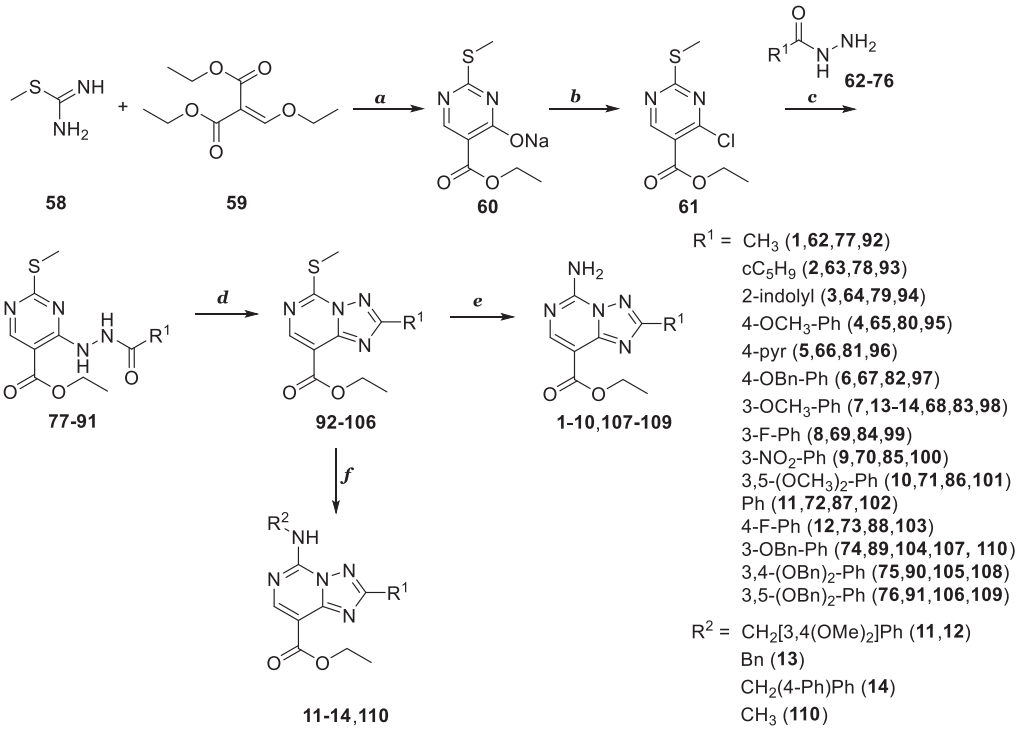

Scheme 1. Synthesis of the 2,5,8-trisubstituted [1,2,4]triazolo[1,5-*c*]pyrimidine nucleus and of final compounds **1**–**14**. *Reagents and conditions.* ***a:*** NaOH, H_2O, ethanol, rt, 24 h; ***b:*** $POCl_3$, rfx, 5 h; ***c:*** DBU, THF, rt, 12 h; ***d:*** P_2O_5, HMDSO, xylene, from rt to 90 °C, 2.5 h, rfx, 12 h; ***e:*** ammonia 7 N in methanol, ethanol, 70 °C, sealed tube, 3–12 h; ***f:*** R^2-NH_2, ethanol, 90 °C, sealed tube, 3–12 h.

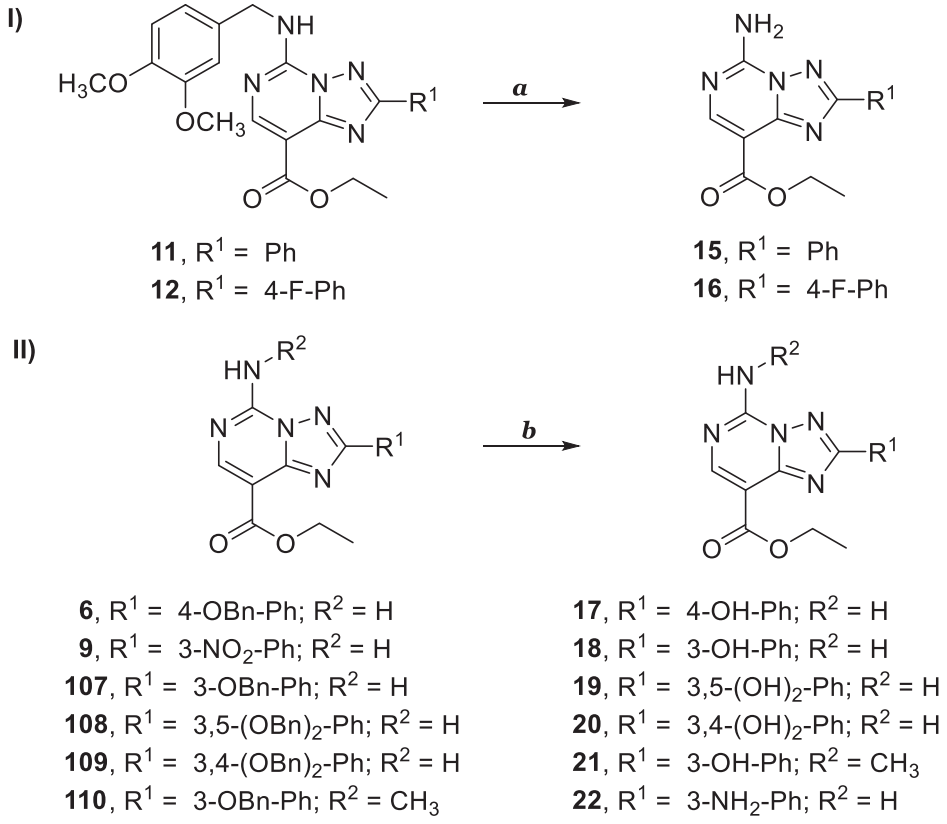

Scheme 2. Synthesis of final compounds **15**–**22**. *Reagents and conditions*. I) Deprotection of amino group at the 5-position, ***a:*** CF_3COOH, trifluoromethanesulfonic acid, anisole, rt, overnight; II) Deprotection of hydroxy groups and reduction of nitro group, ***b:*** Pd/C, ammonium formate, methanol, rfx, 3–12 h.

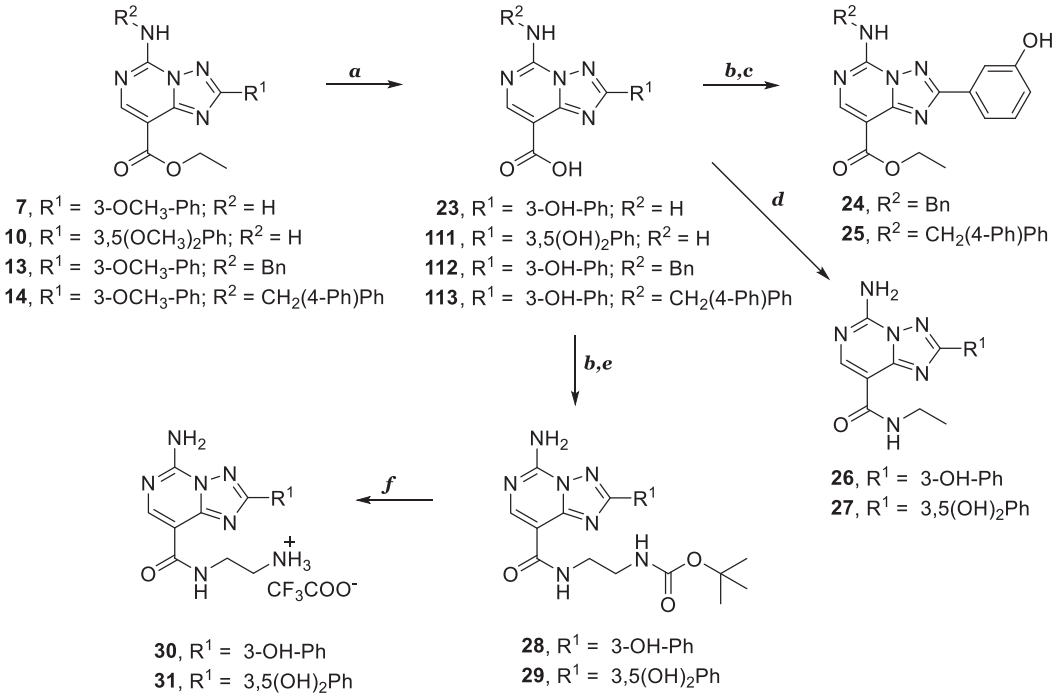

Scheme 3. Synthesis of final compounds **23**–**31**. *Reagents and conditions*. ***a:*** BBr_3 1 M in DCM, DCM, from −78 °C to rt, 12 h; ***b:*** $SOCl_2$, DMF, chloroform, rfx, 5 h; ***c:*** ethanol, rt, 12 h; ***d:*** $SOCl_2$, ethylamine, pyridine, THF, from 0 °C to rt, 12 h; ***e:*** $NH_2(CH_2)_2NHBOC$, Et_3N, THF, rt, 12 h; ***f:*** CF_3COOH 10% in DCM, rt, 2 h.

group at the 5-position, the 2-phenyl (**15**) and 2-(4-fluoro)phenyl (**16**) derivatives were obtained following the two-step strategy reported in the literature [47,53] which consists of the synthesis of the 3,4-dimethoxybenzylamino derivatives (**11,12**) and the subsequent deprotection with trifluoromethanesulfonic acid, anisole, and trifluoroacetic acid, leading to the desired derivatives **15** an **16** (Scheme 2, reaction I). This strategy allowed to avoid the possible ammonolysis of the ethyl ester [55], that could occur proceeding with a direct replacement of methylthio group with ammonia. Since the overall yields were not high, we tried to directly substitute the 5-methylthio derivatives **92**–**101** and **104**–**106** with ammonia using mild conditions (temperature not above 70 °C), obtaining the desired 5-amino derivatives **1**–**10**,**107**–**109** in a single step with acceptable yields most of the time (Scheme 1).

The final 5-benzylamino derivatives **24**–**25** were obtained from the 3-methoxyphenyl derivatives **13,14** as an alternative to the benzyl as hydroxyl protecting group that could have led to the undesired loss of the benzyl and 4-phenylbenzyl groups present at the 5-position during the deprotection step. Demethylation was achieved in 3–12 h using boron tribromide (BBr_3), the classical but harsh reagent used for this purpose. Unfortunately, the reactivity of BBr_3 led also to the hydrolysis of the ethyl ester at the 8-position, even using the minimum excess of reagent (1.1 equivalents) and maintaining the temperature below the 0 °C. So we decided to force the reaction using an excess of BBr_3 that ensured the complete consumption of starting material. Therefore, compounds **24**–**25** were obtained after re-esterification of **112**–**113**, *via* acyl chloride formation (Scheme 3). The same strategy was used to obtain 8-amido derivatives **26**–**29**, from compounds **7** and **10**, hydroxyl groups deprotection and ester hydrolysis were obtained in one step leading to compounds **23** and **111**. The reaction of the carboxylic acids with thionyl chloride and the desired amine afforded amido derivatives **26**–**29**. Finally, the *tert*-butyloxycarbonyl (BOC) group was removed by classical trifluoroacetic acid deprotection leading to the final compounds **30**–**31**.

Synthesis of 2,5,7-trisubstituted [1,2,4]triazolo[1,5-c] pyrimidines.

2,5,7-trisubstituted [1,2,4]triazolo[1,5-c]pyrimidines were obtained following the approach used by Schering Co. (Scheme 4) [56]. The commercially available 2-amino-4,6-dihydroxypyrimidine **114** was converted to the dichloride derivative **115** with phosphorus oxychloride and triethylamine in refluxing acetonitrile, which was, in turn, reacted with desired hydrazide (**68,71**) and diazabicycloundecene (DBU) to obtain *N'*-(2-amino-6-chloropyrimidin-4-yl)-3-hydrazide derivatives **116**–**117**. These compounds were then cyclized in dehydrating conditions by *N,O*-bis(trimethylsilyl)acetamide (BSA) leading to the 5-amino-7-chloro-[1,2,4]triazolo[1,5-*c*]-pyrimidines **118**–**119.** [57] Nucleophilic substitution of chlorine at the 7-position of the TP **118** with benzylamine in ethanol in the presence of base yielded derivative **32**. On the contrary, compound **119** was not soluble in ethanol and DMF was used as co-solvent, but instead, to obtain the desired compound **33**, the reaction afforded dimethylamino derivative **36**. Finally, compound **33** was achieved performing the reaction in butanol. All compounds (**32,33,36**) were then demethylated with boron tribromide to afford derivatives **34,35** and **37**.

Synthesis of 2,5,7-trisubstituted [1,2,4]triazolo[1,5-a][1,3,5] triazines.

In addition to 2,5,7-trisubstituted-[1,2,4]triazolo[1,5-*c*]pyrimidines also a series of [1,2,4]triazolo[1,5-*a*][1,3,5]triazines has been developed bearing the same or similar substitutions at equivalent positions. The synthesis started by reacting the commercially available 2,4,6-trichloro[1,3,5]triazine (**120**) with phenol under reflux for 5 h. The 2,4,6-triphenoxy[1,3,5]triazine **121** was reacted with the required arylhydrazides (**65,68,71,72,122**) and DBU to give 4,6-diphenoxy-[1,3,5]triazin-2-yl-hydrazides **123**–**127**, that successively underwent dehydrative cyclization with phosphorus pentoxide and HMDSO in xylene at reflux, yielding the 2-substituted 5,7-diphenoxy[1,2,4]triazolo[1,5-*a*][1,3,5]triazines **128**–**132** (Scheme 5) [54,58]. Addition of methanolic ammonia led

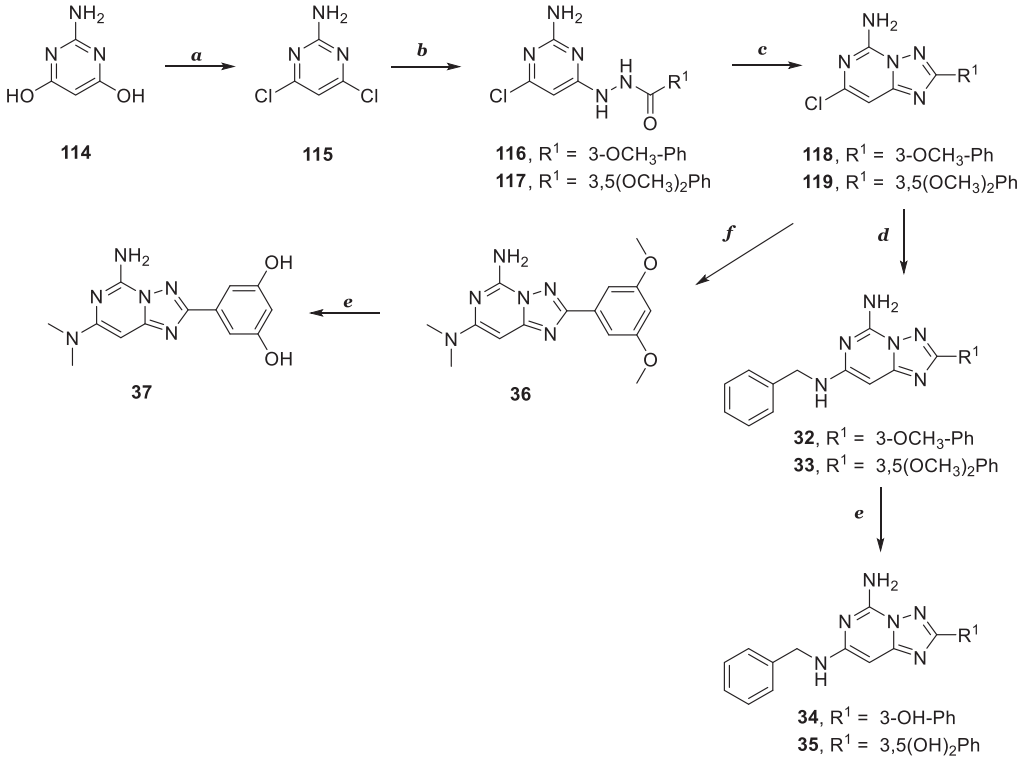

Scheme 4. Synthesis of the 2,5,7-trisubstituted [1,2,4]triazolo[1,5-*c*]pyrimidine nucleus and final compounds **32**–**37**. *Reagents and conditions*. ***a:*** $POCl_3$, Et_3N, acetonitrile, rfx, 1 h; ***b:*** hydrazide (**68** or **71**), DBU, THF, rt, 12 h; ***c:*** BSA, rfx, 12 h; ***d:*** for **34** benzylamine, K_2CO_3, ethanol, 95 °C, sealed tube, 4 days; for **35** benzylamine, K_2CO_3, butanol, 100 °C, sealed tube, 36 h; ***e:*** BBr_3 1 M in DCM, DCM, from −78 °C to rt, 12h; ***f:*** benzylamine, K_2CO_3, ethanol, DMF, 100 °C, sealed tube, 3 days.

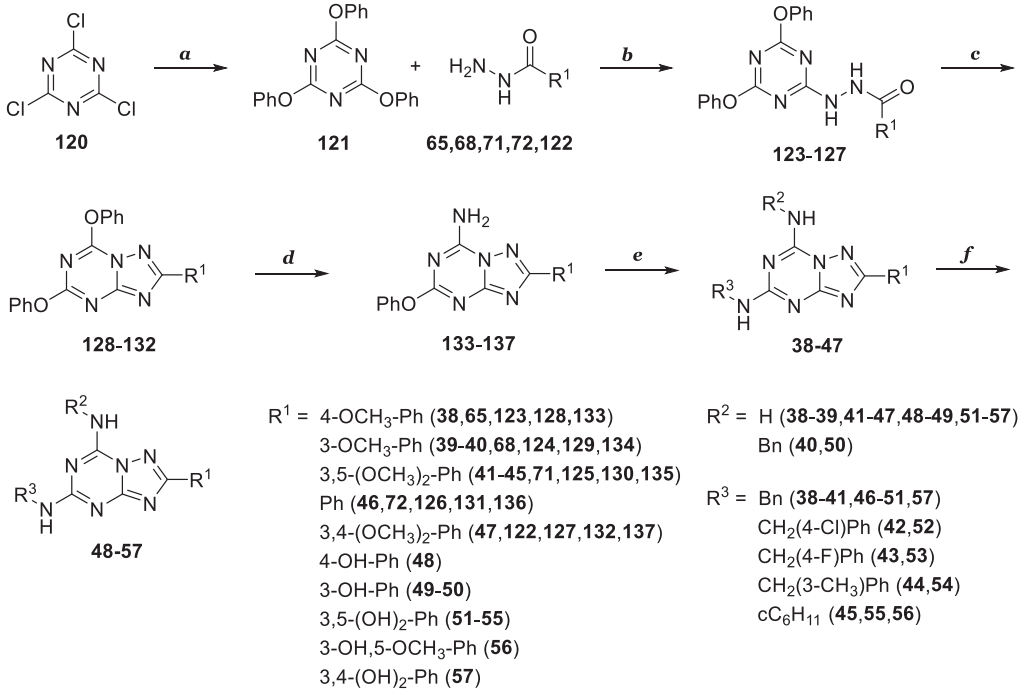

Scheme 5. Synthesis of the 2,5,7-trisubstituted [1,2,4]triazolo[1,5-*a*][1,3,5]triazine nucleus and final compounds **38**–**57**. *Reagents and conditions*. ***a:*** phenol, rfx, 5 h; ***b:*** DBU, THF, rt, 12 h; ***c:*** P_2O_5, HMDSO, xylene, from rt to 90 °C, 2.5 h, rfx, 2–4 h; ***d:*** ammonia 7 N in methanol, methanol, rt, 2 h; ***e:*** *Method A.* desired amine, ethanol, 95–100 °C, sealed tube, 24–72 h. *Method B.* butanol, MW, 170 °C, 100W, 2 h (compounds **42**–**45**); ***f:*** BBr_3 1 M in DCM, DCM, from −78 °C to rt, 12 h.

to the corresponding 7-amino derivatives **133**–**137**, while nucleophilic substitution at the 5-position with benzylamines occurred after heating the mixture in ethanol in a sealed tube at 95–100 °C for days (compounds **38**–**47**) [52]. During the synthesis of the 3-

methoxy derivative **39**, also the N^5,N^7-bisbenzylamino derivative **40** was isolated and characterized. Finally, removal of the methoxy group with an excess of boron tribromide afforded the hydroxyphenyl derivatives **48**–**57**.

3. Structure-activity relationship (SAR) studies

Investigations at the 2 position of the [1,2,4]triazolo[1,5-c] pyrimidine nucleus [1,2,4]Triazolo[1,5-*c*]pyrimidine nucleus is an adenine-like nucleus that represents a good starting point to develop new ATP-competitive CK1δ inhibitors. Thus, different ethyl 5-amino-[1,2,4]triazolo[1,5-*c*]pyrimidines-8-carboxylates (**1**–**10**,**15**–**20**,**22**) with substituents at the 2 positions of different size and nature were synthetized and tested at a fixed dose of 40 μM on truncated CK1δ (aa 1–294) using a luminescent kinase assay (Table 1) that uses luciferase to give a luminescence signal proportional to the unreacted amount of ATP in the enzymatic reaction. Because kinase was truncated at residue 294, all CK1δ autophosphorylation sites are not present in this protein, thus only the peptide substrate could be phosphorylated. A threshold of 40 μM allows to include also not so potent inhibitors that is essential at this stage where no SAR is available. IC_{50}s were determined only for compounds that displayed an inhibition of kinase activity more than 50% at that concentration.

As reported in Table 1, all compounds can inhibit CK1δ to some extent. A large aromatic moiety such indole seems to not give favorable interactions with kinase (22.4% inhib. at 40 μM) but smaller moieties, both aromatic and aliphatic, displayed higher kinase activity inhibition.

[a]Parallel artificial membrane permeability assay-blood brain barrier (PAMPA- BBB), central nervous system (CNS), CNS + means that compound was predicted able to cross the BBB by passive permeation, CNS- means that compound was predicted unable to cross the BBB by passive permeation, CNS ±means that permeability value was lower than limit for CNS+ and upper than limit for CNS-; [b]data represent the mean ± SD of 3 independent experiments performed in duplicate; [c]data represent the % of inhibition of kinase activity expressed as a mean ± SD of 2 independent experiments performed in duplicate at 40 μM concentration; [d]inhibition curve could not be obtained for this compound, thus it was a false positive. n.d. not determined.

Table 1
Inhibitory activity of 2-substituted TP (**1**–**10**,**15**–**20**,**22**) towards CK1δ.

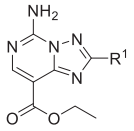

1-10,15-20,22

Cmpd	R^1	PAMPA BBB[a]	IC_{50} μM[b] (% inhib. at 40 μM)[c]
1	-CH_3	CNS-	15.17 ± 5.70 (66.6% ± 1.1)
2	-cC_5H_9	CNS+	12.32 ± 5.17 (76.8% ± 6.8)
3	-2-indolyl	CNS+	n.d. (22.4% ± 3.5)
15	-Ph	CNS+	8.67 ± 4.73 (62.2% ± 9.2)
16	-(4-F)Ph	n.d.	n.d. (44.7% ± 12.3)
5	-4-pyr	CNS ±	20.19 ± 5.57 (59.7% ± 6.6)
6	-(4-OBn)Ph	n.d.	n.d. (39.7% ± 7.4)
4	-(4-OCH_3)Ph	CNS ±	n.d.[d] (50.3% ± 9.35)
17	-(4-OH)Ph	CNS ±	n.d. (39.3% ± 19.1)
7	-(3-OCH_3)Ph	n.d.	25.00 ± 5.04 (52.0% ± 9.2)
8	-(3-F)Ph	CNS+	15.24 ± 5.00 (53.7% ± 4.4)
9	-(3-NO_2)Ph	n.d.	n.d. (21.6% ± 10.3)
22	-(3-NH_2)Ph	CNS-	16.59 ± 5.03 (66.8% ± 12.2)
18	-(3-OH)Ph	CNS-	2.06 ± 0.28 (88.9% ± 0.3)
20	-(3,4-$(OH)_2$)Ph	CNS-	4.75 ± 0.35 (98.0% ± 0.3)
10	-(3,5-$(OCH_3)_2$)Ph	n.d.	n.d. (18.8% ± 15.1)
19	-(3,5-$(OH)_2$)Ph	CNS ±	0.48 ± 0.20 (97.8% ± 5.3)

A simple phenyl ring, compound **15**, led to an IC_{50} of 8.67 μM. Substitution with a 4-pyridyl ring led to a detrimental effect in terms of inhibitory activity (**5**, IC_{50} = 20.19 μM). Different groups were then introduced at the *para* or *meta* positions of the phenyl ring. The most interesting results were obtained with 3-aminophenyl derivative **22** (IC_{50} = 16.59 μM) and especially with 3-hydroxyphenyl compound **18** which exhibited an IC_{50} of 2.06 μM. These results provided the first information about the requirement of a polar H-bond donor group with a specific orientation to gain an affinity towards the kinase. Hydroxyl group at the *para* position led to a compound with a residual kinase activity of only 39.3%.

Focusing our attention on the hydroxyl group, disubstituted derivatives were explored: the *meta*,*para*-disubstituted derivative **20** resulted less active than the *meta*-derivative **18** (**20**, IC_{50} = 4.75 μM *vs.* **18**, IC_{50} = 2.06 μM), while more effective than the *para*- (**17**) and the not substituted phenyl derivative (**15**). Notably, with the 3,5-dihydroxy-substituted derivative **19**, we reached the submicromolar range of inhibiting concentrations (IC_{50} = 0.48 μM), with a 4-fold increase in inhibition potency if compared with the mono-*meta*- substituted derivative **18** (IC_{50} = 2.06 μM).

To rationalize the molecular basis responsible for such a different inhibitory profile shown by this first series of 2-substituted TP derivates, molecular docking calculations were performed, providing an atomistic description of the ligand possible bound states. In detail, as accurately described in the Experimental Section of the manuscript, for each docking-predicted binding pose, the ligand-protein electrostatic and hydrophobic contributions to binding were computed and graphically represented in the form of heatmaps. Two colorimetric scales were exploited to quantitatively represent the magnitude of these two different interactions (i.e. IE_{ele} and IE_{hyd}), computed between the kinase binding site residues (x-axis) and each of the TP derivates taken into consideration (y-axis). As reported in Fig. 3-A, compounds able to significantly inhibit the enzymatic activity of CK1δ are all characterized by the presence of strong electrostatic interactions with the residues belonging to the kinase hinge region (E83, L84, and L85) and with the two negative charged amino acids located in the inner portion of the catalytic cleft (E52 and D149). The aliphatic residues defining the ceil and the floor of the binding site (respectively I15, I23 and L135, I148) mediate instead the greatest hydrophobic stabilizing contacts. For the most potent derivative of this series, specifically, compound **19**, the docking predicted binding mode was reported in Fig. 3-B, highlighting how the TP scaffold is tightly anchored to the backbone of the kinase hinge region by a bidentate hydrogen bond pattern, closely mimicking the interactivity of the physiological substrate ATP. The 3,5-dihydroxyl functional groups introduced on the phenyl ring at the 2-position mediate in turn a double hydrogen bond interaction, respectively with residue E52 and D149.

To better understand the ligands recognition mechanism, however, the pivotal role played by solvent molecules must be taken into consideration and integrated into traditional in-silico tools, for example molecular docking protocols, which otherwise would poorly treat this aspect. For this reason, an all-atoms molecular dynamics (MD) simulation has been collected starting from the unliganded form of CK1δ protein kinase (PDB ID: 5IH4) and it has been subsequently analyzed with AquaMMapS, an in-house developed algorithm able to characterize the hydrodynamic behavior of water molecules within the target binding site. AquaMMapS results, graphically reported on the rounded box present in

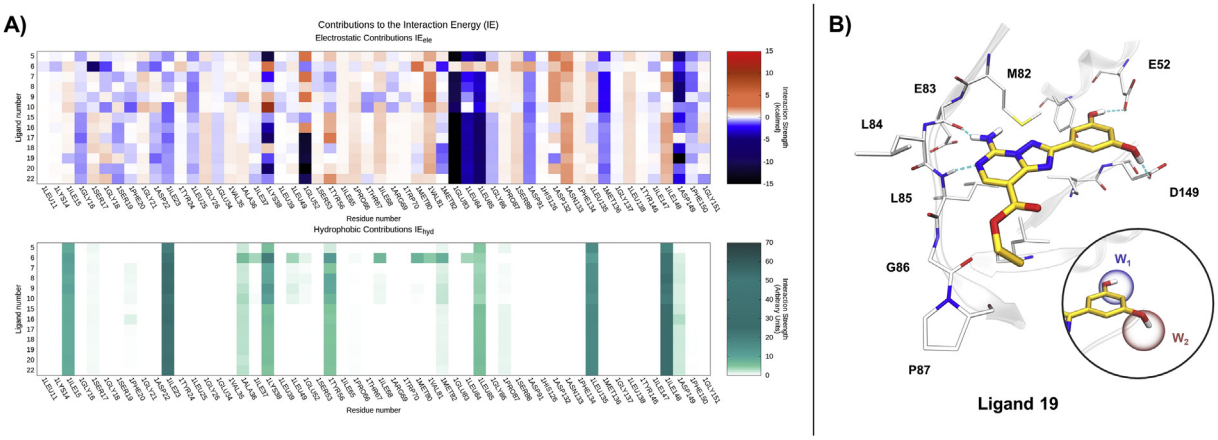

Fig. 3. Panel A. Interaction Energy (IE) fingerprints shown as heat maps reporting the electrostatic (IE_{ele}) and hydrophobic (IE_{hyd}) interaction between each 2-substituted TP derivate (y-axis) and each CK1δ binding site residue (x-axis). The intensity of the electrostatic interactions is rendered by a colorimetric scale going from blue to red (for negative to positive values) while for the hydrophobic interactions a scale going from white to dark green (for low to high values) is exploited. Panel B. Representation of the docking-predicted structure of the complex between protein kinase CK1δ (grey) and compound **19** (orange). Hydrogen bond interactions are depicted as cyan dotted lines. The rounded box contains a zoomed view within the inner portion of the kinase binding site, showing the stable hydration sites predicted using AquaMMapS analysis. The solvent stationary behavior with each of these regions is rendered by a colorimetric scale going from blue to red (for high to low % O_{RMSF} values).

Fig. 3-B, have highlighted the presence in the inner portion of CK1δ catalytic pocket of two important hydration sites populated by stationary solvent molecules, respectively W_1 (% O_{RMSF} = 74) and W_2 (% O_{RMSF} = 21). Intriguingly, the two polar phenolic functionalities introduced in the TP derivative **19** perfectly occupy regions W_1 and W_2, allowing us to hypothesize how the displacement of stationary water molecules could contribute, along with the tight network of hydrogen bond interactions described above, to the submicromolar potency of the compound.

Investigations at the 8 position of the [1,2,4]triazolo[1,5-c]pyrimidine nucleus.

Exploration at the 8-position was performed maintaining the best substitutions at the 2-position of the TP scaffold highlighted in the previous series, that is the 3-hydroxyphenyl and 3,5-dihydroxyphenyl moieties.

The ethyl ester of compounds **7** and **10** was hydrolyzed to the corresponding carboxylic acid and then three different amides were synthesized (ethyl **26**–**27**, N-BOC-aminoethyl **28**–**29**, aminoethyl **30**–**31**) to explore if stabilizing interactions could be reached in that part of the kinase pocket (Table 2). Also the carboxylic acid **23** (R^1 = -(3OH)Ph) has been assayed but resulted less active than the corresponding ethyl ester (**23**, IC_{50} = 26.75 μM *vs.* **18**, IC_{50} = 2.06 μM). Instead, the introduction of an amido moiety led to improved inhibition potencies of both ethylamido derivative **26** (IC_{50} = 0.32 μM) and aminethylamido derivative **30** (IC_{50} = 1.26 μM), while BOC protected compound **28** did not affect enzyme activity at low concentrations. Interestingly, a different behavior was observed for 3,5-dihydroxyphenyl derivatives (**27**,**29**,**31**): aminethylamido derivative was more potent than the corresponding ethylamido compounds (**27**, IC_{50} = 0.99 μM *vs.* **31**, IC_{50} = 0.21 μM) but showed a similar potency to the ester **19** (IC_{50} = 0.48 μM). Notably, an IC_{50} of 5.32 μM was determined for BOC protected compound **29**, denoting that very different interactions occurred when this substitution is coupled with 3,5-dihydroxyphenyl moiety at the 2-position with respect to a single *meta* hydroxyl group (**28**, % inhib. at 40 μM = 16.8).

Table 2
Inhibitory activity of 8-substituted TP (**23**,**26**–**31**) towards CK1δ.

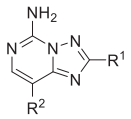

23,**26-31**

Cmpd	R^1	R^2	PAMPABBB[a]	IC_{50} μM[b] (% inhib. at 40 μM)[c]
23	-(3-OH)Ph	-COOH	CNS-	26.75 ± 6.03 (75.8% ± 1.8)
26	-(3-OH)Ph	$-CONHC_2H_5$	CNS ±	0.32 ± 0.10 (90.4% ± 4.6)
27	$-(3,5-(OH)_2)Ph$	$-CONHC_2H_5$	CNS-	0.99 ± 0.12 (86.1% ± 4.7)
28	-(3-OH)Ph	$-CONH(CH_5)_2NHBOC$	n.d.	n.d. (16.8% ± 25.9)
29	$-(3,5-(OH)_2)Ph$	$-CONH(CH_5)_2NHBOC$	CNS-	5.32 ± 1.02 (84.2% ± 0.4)
30	-(3-OH)Ph	$-CONH(CH_5)_2NH_2$	CNS+	1.26 ± 0.19 (93.0% ± 4.6)
31	$-(3,5-(OH)_2)Ph$	$-CONH(CH_5)_2NH_2$	CNS-	0.21 ± 0.09 (93.6% ± 11.5)

[a]CNS + means that compound was predicted able to cross the BBB by passive permeation, CNS- means that compound was predicted unable to cross the BBB by passive permeation, CNS ±means that permeability value was lower than limit for CNS+ and upper than limit for CNS-; [b]data represent the mean ± SD of 3 independent experiments performed in duplicate; [c]data represent the % of inhibition of kinase activity expressed as a mean ± SD of 2 independent experiments performed in duplicate at 40 μM concentration. n.d.: not determined.

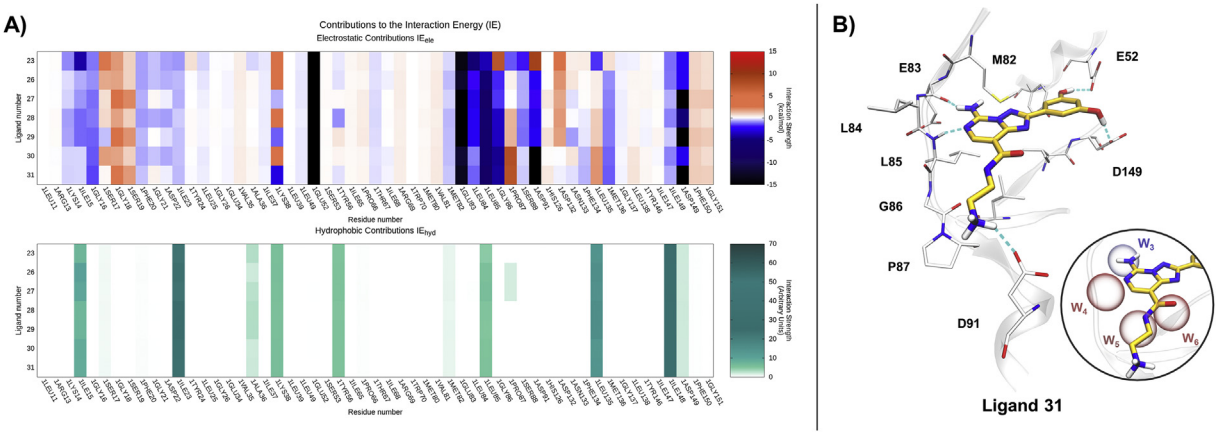

Fig. 4. Panel A. Interaction Energy (IE) fingerprints shown as heat maps reporting the electrostatic (IE_{ele}) and hydrophobic (IE_{hyd}) interaction between each 8-substituted TP derivate (y-axis) and each CK1δ binding site residue (x-axis). The intensity of the electrostatic interactions is rendered by a colorimetric scale going from blue to red (for negative to positive values) while for the hydrophobic interactions a scale going from white to dark green (for low to high values) is exploited. Panel B. Representation of the docking-predicted structure of the complex between protein kinase CK1δ (grey) and compound **31** (orange). Hydrogen bond interactions are depicted as cyan dotted lines. The rounded box contains a zoomed view within the vestibular region of the kinase binding site, showing the stable hydration sites predicted using AquaMMapS analysis. The solvent stationary behavior with each of these regions is rendered by a colorimetric scale going from blue to red (for high to low % O_{RMSF} values).

In-silico studies have confirmed how modification at the 8-position of the TP scaffold only marginally affects the binding modes of the analyzed derivatives. As shown on the IE maps reported in Fig. 4-A, the main electrostatic (IE_{ele}) and hydrophobic (IE_{hyd}) interactions with the protein kinase binding site residues, as discussed in the previous paragraph, are all conserved. The reason for this lies in the fact that the substituents in position 8 protrude towards the external region of the catalytic site, partially exposed to the solvent, and therefore they do not alter the crucial interactivity with the kinase hinge region. The predicted binding mode for compound **31**, the most potent derivative of this series, has been reported in Fig. 4-B, highlighting a salt bridge interaction taking place between the positively charged aminoethylamido moiety introduced at the 8-position of the TP scaffold and the negative charged residue D91, located in the vestibular region of CK1δ binding site. The role of solvent molecules during binding was taken into consideration also in this case and, as reported on the rounded box present in Fig. 4-B, four regions populated by stationary water molecules were identified by AquaMMapS analysis in the proximity to the kinase hinge region, respectively W_3 (% O_{RMSF} = 57), W_4 (% O_{RMSF} = 18), W_5 (% O_{RMSF} = 26) and W_6 (% O_{RMSF} = 18). The polar free amino group at the 5-position of the TP scaffold, similarly to what happens with the physiological substrate ATP, perfectly occupies region W_3, the one characterized by the more stationary water behavior. Moreover, the polar atoms belonging to the amide functionality inserted at the 8-position respectively perturb the other two regions W_5 and W_6, although it is reasonable to hypothesize how the contribution to binding brought by their displacement could be less impacting, considering the greater solvent turbulence experienced within these spots.

Investigations at the 5 position of the [1,2,4]triazolo[1,5-c]pyrimidine nucleus.

To assess if a substitution at the 5-position of the TP scaffold is tolerated, the free amino group was substituted with methyl (**21**), benzyl (**13**,**24**), and 4-phenyl-benzyl groups (**14**,**25**), while veratryl compounds **11**–**12** are intermediates for the synthesis of compounds **15**–**16** that were purified and assayed. From what can be seen from Table 3, the substitution at the 5-position led to inactive compounds at 40 μM, even when one of the best substituents is present at the 2-position (e.g. R^1 = -(3-OH)Ph) such as in compounds **21**, **24**–**25**.

Molecular docking calculations were then exploited to assess the impact of modification at the 5-position of the TP scaffold. As noticeable in Fig. 5-A, the IE fingerprint depicts a completely disrupted electrostatic (IE_{ele}) and hydrophobic (IE_{hyd}) interactions pattern with the residues composing CK1δ binding site. The reason for this is observable in Fig. 4-B, showing how even the smallest methyl substituent, present in derivative **21,** prevents the crucial hydrogen bond interactions with the hinge region residues E83 and L85. Moreover, modification at this specific position impairs the ability of the compound to effectively displace stationary water molecules populating regions W_3, W_5, and W_6.

Investigations at the 7 position of the [1,2,4]triazolo[1,5-c]pyrimidine nucleus.

Another opportunity with the [1,2,4]triazolo[1,5-*c*]pyrimidine scaffold is to investigate the 7-position, thus, few compounds have been synthesized bearing the free amino group at the 5-position and the *meta* or 3,5-di- hydroxyl substitutions on the phenyl ring at the 2-position. At the 7-position benzylamino or dimethylamino moieties were introduced (**34**–**35**,**37**). Again, also the protected

Table 3
Inhibitory activity of 5-substituted TP (**11**–**14**,**21**,**24**–**25**) towards CK1δ..

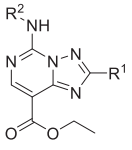

11-14,**21**,**24-25**

Cmpd	R^1	R^2	% inhib. at 40 μM[a]
11	-Ph	-CH_2(3,4-(OCH_3)$_2$)Ph	35.7% ± 9.3
12	-(4-F)Ph	-CH_2(3,4-(OCH_3)$_2$)Ph	11.3% ± 8.1
13	-(3-OCH_3)Ph	-Bn	10.9% ± 2.3
14	-(3-OCH_3)Ph	-CH_2(4-Ph)Ph	17.5% ± 19.7
21	-(3-OH)Ph	-CH_3	7.1% ± 7.1
24	-(3-OH)Ph	-Bn	1.2% ± 3.5
25	-(3-OH)Ph	-CH_2(4-Ph)Ph	9.0% ± 11.6

[a] Data represent the % of inhibition of kinase activity expressed as a mean ± SD of 2 independent experiments performed in duplicate at 40 μM concentration.

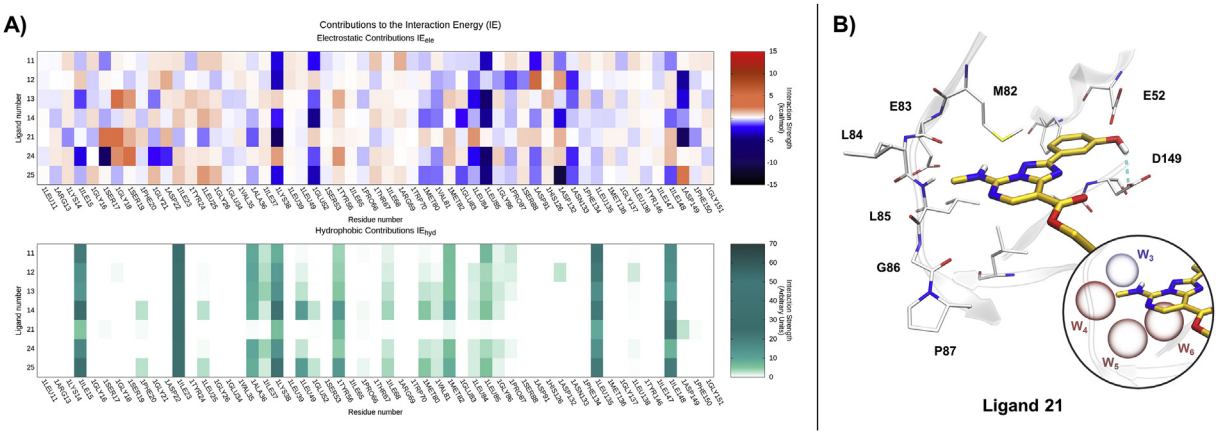

Fig. 5. Panel A. Interaction Energy (IE) fingerprints shown as heat maps reporting the electrostatic (IE_{ele}) and hydrophobic (IE_{hyd}) interaction between each 8-substituted TP derivate (y-axis) and each CK1δ binding site residue (x-axis). The intensity of the electrostatic interactions is rendered by a colorimetric scale going from blue to red (for negative to positive values) while for the hydrophobic interactions a scale going from white to dark green (for low to high values) is exploited. Panel B. Representation of the docking-predicted structure of the complex between protein kinase CK1δ (grey) and compound **21** (orange). Hydrogen bond interactions are depicted as cyan dotted lines. The rounded box contains a zoomed view within the vestibular region of the kinase binding site, showing the stable hydration sites predicted using AquaMMapS analysis. The solvent stationary behavior with each of these regions is rendered by a colorimetric scale going from blue to red (for high to low % O_{RMSF} values).

Table 4
Inhibitory activity of 7-substituted TP (**32**–**37**) towards CK1δ..

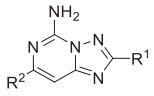

32-37

Cmpd	R^1	R^2	PAMPA BBB[a]	IC_{50} μM[b] (% inhib. at 40 μM)[c]
32	-(3-OCH_3)Ph	-NHBn	n.d.	n.d. (−12.7% ± 4.5)
33	-(3,5-(OCH_3)$_2$)Ph	-NHBn	n.d.	n.d. (19.4% ± 15.5)
36	-(3,5-(OCH_3)$_2$)Ph	-N(CH_3)$_2$	n.d.	n.d. (33.5% ± 9.9)
34	-(3-OH)Ph	-NHBn	CNS+	0.30 ± 0.07 (75.2% ± 7.6)
35	-(3,5-(OH)$_2$)Ph	-NHBn	CNS ±	0.74 ± 0.08 (80.2% ± 5.6)
37	-(3,5-(OH)$_2$)Ph	-N(CH_3)$_2$	n.d.	n.d. (−22.1% ± 2.5)

[a] CNS + means that compound was predicted able to cross the BBB by passive permeation, CNS- means that compound was predicted unable to cross the BBB by passive permeation, CNS ±means that permeability value was lower than limit for CNS+ and upper than limit for CNS-.
[b] Data represent the mean ± SD of 3 independent experiments performed in duplicate.
[c] Data represent the % of inhibition of kinase activity expressed as a mean ± SD of 2 independent experiments performed in duplicate at 40 μM concentration. n.d.: not determined.

methoxy derivatives (**32**–**33**,**36**) were tested for their ability to inhibit CK1δ.

As expected (Table 4), compounds with masked hydroxyl groups at the 2-position (**32**–**33**,**36**) were inactive at a concentration of 40 μM (% inhib. at 40 μM 33.5–12.7). Interestingly, when free hydroxyl groups are present, compounds displayed a submicromolar potency towards CK1δ, and monosubstitution on the phenyl ring seems to be favorable with respect to 3,5-dihydroxy substitution (**34**, IC_{50} = 0.30 μM *vs*. **35**, IC_{50} = 0.74 μM). When a dimethylamino moiety, instead of a benzylamino moiety, was introduced at the 7-position, the compound remains inactive also when free hydroxyl groups were present at the phenyl ring at the 2-position (**37**, % inhib. at 40 μM = −22.1). These results revealed that 7-position gives a valuable opportunity to develop new compounds in order to draw SAR for this series. In fact, from a synthetic point of view, it is easier to develop 7-substituted TP (5 synthetic steps) than 8-substituted TP (7 synthetic steps).

In-silico investigations, as reported in Fig. 6-A, confirmed how only benzylamino functionality is tolerated at the 7-position of the TP scaffold, while dimethylamino derivates deeply perturb the previously discussed IE fingerprint, especially as regards the IE_{ele} component. Also, in this case, compounds interactivity with CK1δ hinge region residues has proved to be an essential pharmacophoric feature. As it is possible to appreciate in Fig. 6-B, by the docking-predicted binding mode for derivative **35**, the mono-substituted amino group at the 7 position allows enriching the hinge region recognition motif of a further hydrogen bond interaction, mediated with the residue L85 carbonyl group. On the contrary, a di-substituted amino group at the same position not only prevents this specific interaction but also disrupts the canonical hinge region hydrogen bond network, due to a steric repulsion mediated by the dimethylamino group. As regards AquaMMapS analysis, the rounded box depicted in Fig. 6-B highlights a different pattern of stationary water molecules displacement for this series, if compared to the previously discussed 8-substituted TP derivates. In particular, the amino moiety introduced at the 7-position closely occupy the W_4 region, which is located in proximity to the key residue L85, while W_5, and W_6 stationary solvent spots are completely unperturbed.

Investigations on the [1,2,4]triazolo[1,5-a][1,3,5]triazine nucleus.

Finally, due to the good results obtained with the 7-substituted TP, we decided to explore another scaffold, which bears an additional nitrogen atom at the 8 position of TP, leading to the [1,2,4]triazolo[1,5-*a*][1,3,5]triazine nucleus. There is good expertise on the chemistry of this nucleus in our group [49–52,59], thus we decided to perform investigations at the 5-position of the TT ring that is equivalent to the 7-position in TP.

Table 5 shows that the simple phenyl ring at the 2-position of the TT scaffold was not sufficient to confer potency against CK1δ. As we can observe, the presence of a hydroxyl group on the phenyl ring at the 2-position has been confirmed to confer affinity to the kinase (compounds **49**,**51**–**57**). In particular, again we can see in the 5-benzyl series that the best results were obtained with the *meta*-(**49**, IC_{50} = 0.46 μM) and 3,5-disubstituted derivatives (**51**, IC_{50} = 0.18 μM), probably due to the formation of important

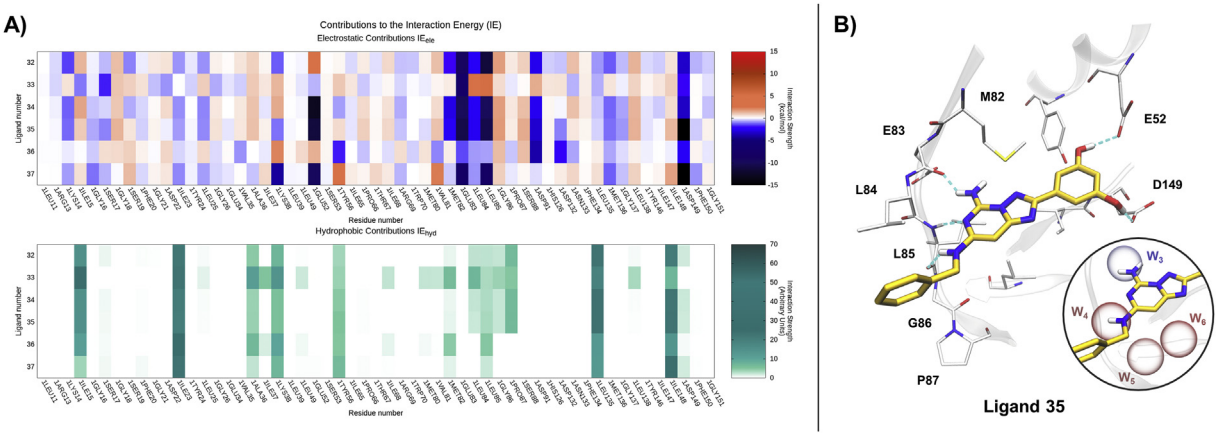

Fig. 6. Panel A. Interaction Energy (IE) fingerprints shown as heat maps reporting the electrostatic (IE_{ele}) and hydrophobic (IE_{hyd}) interaction between each 7-substituted TP derivate (y-axis) and each CK1δ binding site residue (x-axis). The intensity of the electrostatic interactions is rendered by a colorimetric scale going from blue to red (for negative to positive values) while for the hydrophobic interactions a scale going from white to dark green (for low to high values) is exploited. Panel B. Representation of the docking-predicted structure of the complex between protein kinase CK1δ (grey) and compound **35** (orange). Hydrogen bond interactions are depicted as cyan dotted lines. The rounded box contains a zoomed view within the vestibular region of the kinase binding site, showing the stable hydration sites predicted using AquaMMapS analysis. The solvent stationary behavior with each of these regions is rendered by a colorimetric scale going from blue to red (for high to low % O_{RMSF} values).

interactions between the hydroxyl group and an amino acid residue of the ATP-binding pocket. Potency towards kinase raise from 4-OH (**48**, IC_{50} = 1.32 μM), 3,4-$(OH)_2$ (**57**, IC_{50} = 0.91 μM), 3-OH (**49**, IC_{50} = 0.46 μM) and 3,5-$(OH)_2$ (**51**, IC_{50} = 0.18 μM).

It is worth noticing that all the methoxy derivatives (**38**–**45**) resulted nearly inactive at the concentration used in the screening assay (40 μM), with the only exception of the 3,4-dimethoxy derivative **47** (IC_{50} = 5.65 μM). We can also notice that even in this case the introduction of substituents on the amino group at the 7-position of TT (that corresponds to the 5-position in TP) have a detrimental effect in terms of potency: in fact, both derivative **40**, isolated as side-product of the nucleophilic substitution at the 5-

Table 5
Inhibitory activity of 5-substituted TT (**38**–**57**) towards CK1δ..

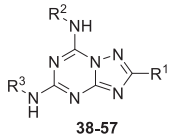

38-57

Cmpd	R^1	R^2	R^3	PAMPABBB[a]	IC_{50} μM[b] (% inhib. at 40 μM)[c]
46	Ph	-H	-Bn	CNS+	n.d. (39.7% ± 14.4)
38	-(4-OCH_3)Ph	-H	-Bn	n.d.	n.d. (15.6% ± 21.9)<
48	-(4-OH)Ph	-H	-Bn	CNS-	1.32 ± 0.51 (70.4% ± 11.2)
39	-(3-OCH_3)Ph	-H	-Bn	n.d.	n.d. (18.1% ± 7.7)
40	-(3-OCH_3)Ph	-Bn	-Bn	n.d.	n.d. (−10.3% ± 14.7)
49	-(3-OH)Ph	-H	-Bn	CNS+	0.46 ± 0.15 (84.2% ± 9.6)
50	-(3-OH)Ph	-Bn	-Bn	n.d.	n.d. (−8.5% ± 2.9)
47	-(3,4-$(OCH_3)_2$)Ph	-H	-Bn	CNS+	5.65 ± 1.34 (72.4% ± 2.4)
57	-(3,4-$(OH)_2$)Ph	-H	-Bn	CNS+	0.91 ± 0.30 (93.8% ± 10.5)
41	-(3,5-$(OCH_3)_2$)Ph	-H	-Bn	n.d.	n.d. (4.5% ± 2.3)
42	-(3,5-$(OCH_3)_2$)Ph	-H	-CH_2(4-Cl)Ph	n.d.	n.d. (9.7% ± 10.4)
43	-(3,5-$(OCH_3)_2$)Ph	-H	-CH_2(4-F)Ph	n.d.	n.d. (10.5% ± 13.8)
44	-(3,5-$(OCH_3)_2$)Ph	-H	-CH_2(3-CH_3)Ph	n.d.	n.d. (13.9% ± 3.9)
45	-(3,5-$(OCH_3)_2$)Ph	-H	-cC_6H_{11}	n.d.	n.d. (41.9% ± 23.5)
51	-(3,5-$(OH)_2$)Ph	-H	-Bn	CNS ±	0.18 ± 0.04 (85.3% ± 4.4)
52	-(3,5-$(OH)_2$)Ph	-H	-CH_2(4-Cl)Ph	CNS+	0.75 ± 0.06 (95.8% ± 2.5)
53	-(3,5-$(OH)_2$)Ph	-H	-CH_2(4-F)Ph	CNS ±	0.47 ± 0.10 (87.0% ± 12.2)
54	-(3,5-$(OH)_2$)Ph	-H	-CH_2(3-CH_3)Ph	CNS ±	0.53 ± 0.11 (79.7% ± 9.3)
55	-(3,5-$(OH)_2$)Ph	-H	-cC_6H_{11}	CNS ±	0.67 ± 0.16 (89.3% ± 5.1)
56	- (3-OCH_3)(5-OH)Ph	-H	-cC_6H_{11}	CNS+	3.30 ± 1.17 (68.6% ± 28.0)

[a] CNS + means that compound was predicted able to cross the BBB by passive permeation, CNS- means that compound was predicted unable to cross the BBB by passive permeation, CNS ±means that permeability value was lower than limit for CNS+ and upper than limit for CNS-.
[b] Data represent the mean ± SD of 3 independent experiments performed in duplicate.
[c] Data represent the % of inhibition of kinase activity expressed as a mean ± SD of 2 independent experiments performed in duplicate at 40 μM concentration. n.d.: not determined.

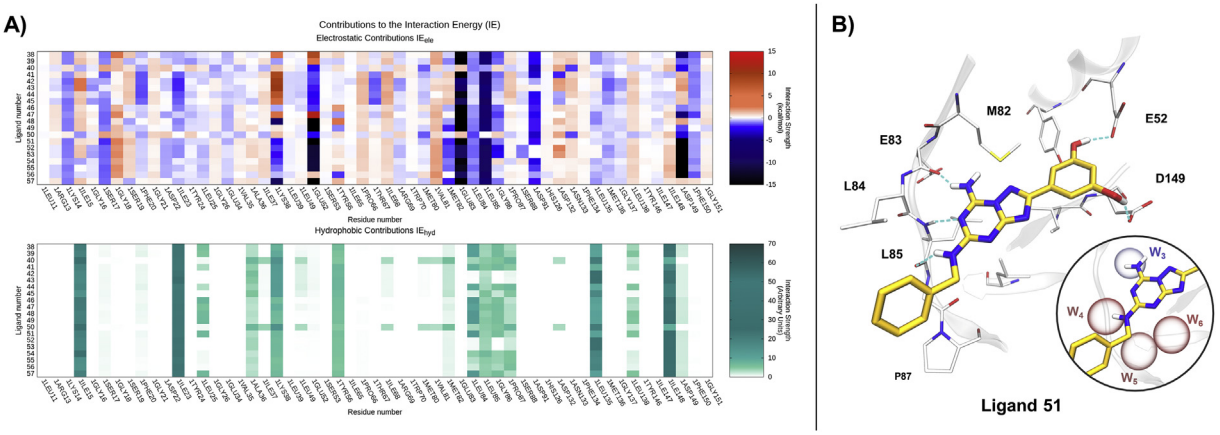

Fig. 7. Panel A. Interaction Energy (IE) fingerprints shown as heat maps reporting the electrostatic (IE_{ele}) and hydrophobic (IE_{hyd}) interaction between each 5-substituted TT derivate (y-axis) and each CK1δ binding site residue (x-axis). The intensity of the electrostatic interactions is rendered by a colorimetric scale going from blue to red (for negative to positive values) while for the hydrophobic interactions a scale going from white to dark green (for low to high values) is exploited. Panel B. Representation of the docking-predicted structure of the complex between protein kinase CK1δ (grey) and compound **51** (orange). Hydrogen bond interactions are depicted as cyan dotted lines. The rounded box contains a zoomed view within the vestibular region of the kinase binding site, showing the stable hydration sites predicted using AquaMMapS analysis. The solvent stationary behavior with each of these regions is rendered by a colorimetric scale going from blue to red (for high to low % O_{RMSF} values).

position, and the corresponding hydroxyl-derivative **50**, presenting a benzylamino group also at the 7-position, have no effects on CK1δ activity at 40 μM. Finally, the introduction of substituents on the phenyl ring of the benzylamino group at the 5-position, led to compounds **52**–**54** still active in the submicromolar range (IC_{50}s = 0.75, 0.47 and 0.53 μM for compounds **52**,**53** and **54**, respectively), also, an aromatic ring seems to not be essential because the introduction of a cyclohexylamino moiety in compound **55** displayed an IC_{50} of 0.67 μM, comparable to that of benzylamino derivatives **52**–**54**. During deprotection of compound **45** to **55**, mono-deprotected derivative **56** was isolated: as expected, it was remarkably more potent than the corresponding fully protected compound **45** and less potent than the completely deprotected compound **55** (**45**, % inhib. at 40 μM = 41.9 vs. **56**, IC_{50} = 3.30 μM vs. **55**, IC_{50} = 0.67 μM).

Molecular docking studies were finally exploited to investigate the impact of TP scaffold replacement with the closely related TT nucleus, in terms of CK1δ binding mechanism. The IE fingerprints depicted in Fig. 7-A clearly show how most of the TT derivates herein reported conserving the key interactions which have been previously validated as crucial for the kinase recognition and inhibition, both as regards the IE_{ele} and the IE_{ele} components. The binding mode for compound **51**, as reported in Fig. 7-B, appears almost completely superimposable to that previously described for compound **31**. In detail, a tridentate hydrogen bond network tightly anchors the TT heterocyclic scaffold to the protein kinase hinge domain (residues E83 and L85), while the resorcinol-like substituent at the 2-position engaged a double hydrogen bond interaction with the negatively charged amino acids buried within the catalytic cleft (residues E52 and D91). Moreover, the benzylamino group inserted at the 5-position of the TT scaffold and protruding towards the binding site vestibular regions, adopts a conformation nearly indistinguishable from that described for the same substituent, when inserted at the 7-position of the TP scaffold. As a

Table 6
Competition binding assay KINOMEscan™ [60]. Data are reported as % of binding to kinases with respect to a positive control at a concentration of compound **51** of 10 μM.

Cmpd	CK1α_1	CK1α_{1L}	CK1γ_1	CK1γ_2	CK1γ_3	CK1δ	CK1ε
51	3.2	14	32	20	14	14	1.4

Finally, compound **51** displayed to be not cytotoxic against three different types of non-tumoral cells (IC_{50} > 10 μM, Table 7).

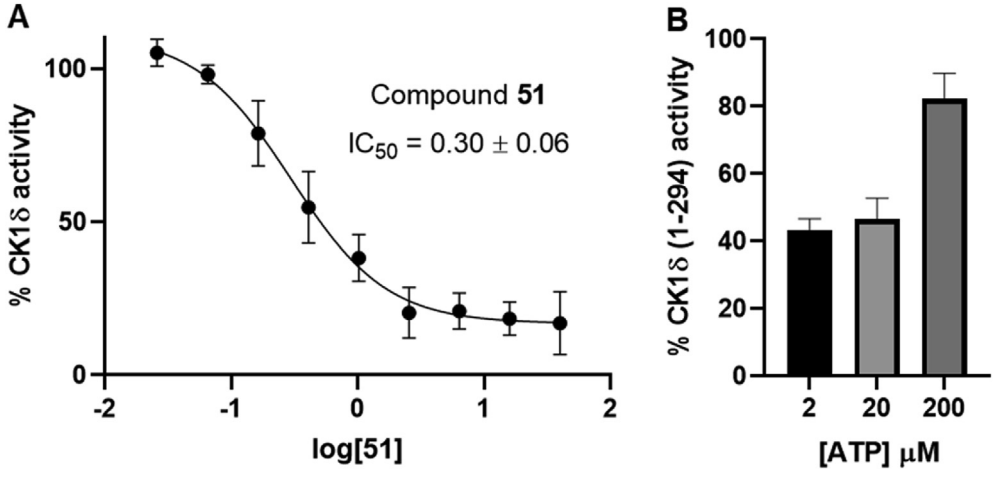

Fig. 8. Panel A. Concentration–inhibition curve of compound **51** at full-length CK1δ. Panel B. Truncated CK1δ activity at different concentrations of ATP (e.g. 2, 20 and 200 μM).

Table 7
Cytotoxicity of compound **51** in non-tumoral cells.

	IC_{50} (μM) [a]		
	$PBL_{resting}$ [b]	PBL_{PHA} [c]	Human fibroblast
51	>10	>10	>10

[a] Compound concentration required to inhibit cell growth by 50%.
[b] PBL not stimulated with PHA.
[c] PBL stimulated with PHA.

consequence, also the solvent displacement profile for this last series, reported on the rounded box of Fig. 7-B, doesn't show a remarkable difference with respect to the previous one.

The binding mechanism of ligand **51**, the most potent derivative identified through this medicinal chemistry optimization campaign, was further investigated using MD simulations, in such a way to fully address the ligand-receptor conformational flexibility while explicitly accounting for the solvent contribution during the binding process. In detail, supervised molecular dynamics (SuMD), an in-house developed computational protocol, was exploited to collect a MD trajectory describing compound **51** recognition mechanism, from the unbound to the bound state, in a very competitive timescale.

The SuMD trajectory collected, along with all the geometric and energetic analysis performed, has been graphically summarized in a synchronized video, reported on supplementary materials (Video1). As noticeable from the two upper panels, few ns are sufficient for the TT derivative to approach the vestibular region of CK1δ binding site, where it engages the first interaction with the residues located on the kinase N-lobe. On the contrary, ligand accommodation within the catalytic pocket required a long negotiation, as evincible by the important repulsive interactions occurring in the first 40 ns of the SuMD simulation. Once this important energy barrier has been overcome, the ligand experiences the first contact with the kinase hinge region residues and quickly converges towards molecular docking anticipated bound state, reproducing both the hydrogen bond network as well as the interactivity with AquaMMapS-predicted hydration sites.

Supplementary video related to this article can be found at https://doi.org/10.1016/j.ejmech.2021.113331Video 1. In the end, considering the promising nature characterizing derivative **51** it was firstly tested against full length CK1δ confirming the high inhibitor activity showing an IC_{50} of 0.30 μM (Fig. 8-A). Then its mechanism of action was investigated by determining truncated CK1δ activity at different ATP concentrations. In Fig. 8-B it is possible to observe an increase in kinase activity with increasing concentrations of ATP, demonstrating that compound **51** has an ATP competitive behavior. In order to asses compound **51** selectivity it was tested at a fixed dose of 10 μM against a panel of 452 kinases (Table S1) comprised all other CK1 isoforms (Table 6). Compound **51** displayed a quite good selectivity, only 17 off-target kinases, excepted for CK1 isoforms, were found by this screening, but unfortunately as showed in Table 6, the compound binds all CK1 isoforms, denoting its ability to interact with common features of these family.

4. Prediction of blood-brain barrier (BBB) permeability

As mentioned before, since CK1δ is considered a potential target for therapeutic intervention in CNS diseases and one of the main obstacles for the treatment of the diseases of the CNS is the drug's penetration into the BBB at therapeutic concentrations [61], we decided to apply the Parallel Artificial Membrane Permeability Assay (PAMPA) to predict the BBB-permeability of most active developed triazolo derivatives [62]. As we can see from Tables 1–5, many of the tested 2,5,8-trisubstituted TPs (**18**–**20** and **26**–**31**), presenting one or more hydroxyl groups on the scaffold, found difficult to pass the BBB in the *in vitro* assay, excepted for compound **30**, that even if bears an additional polar moiety at the 8-position (a free amino group) resulted to passively permeate the BBB in this assay. However, the same substitutions at the 2-position on the TT scaffold (**48**–**57**) or the 2,5,7-trisubstituted TPs (**34**,**35**) are better tolerated, probably for the presence of the benzylamino moiety at the 5 (TT) or 7 (TP) positions, leading to more BBB-permeable derivatives (i.e. **34**,**49**,**52**) and, thus, representing a valuable starting point for further structural optimizations and biological evaluations.

5. Conclusions

In summary, in this work a new series of [1,2,4]triazolo[1,5-*c*]pyrimidines and [1,2,4]triazolo[1,5-*a*][1,3,5]triazines have been developed as protein kinase CK1δ inhibitors. Substitutions on all positions have been investigated: 2,5,7 and 8 for the [1,2,4]triazolo[1,5-*c*]pyrimidine scaffold and 2,5,and 7 for the [1,2,4]triazolo[1,5-*a*][1,3,5]triazine one. Structure-activity relationship for these compounds revealed that a free amino group is required at the 5 position of the [1,2,4]triazolo[1,5-*c*]pyrimidine nucleus (and at the correspondent position in the triazolo-triazine ring, position 7) while at the 2 position an opportunely substituted phenyl ring can tune kinase inhibitory activity. In particular, the insertion of hydroxy groups at the 3 and 5 positions gave optimal interactions in the catalytic binding cleft, confirmed by molecular modeling studies. Prediction of passive blood-brain barrier permeability of most potent compounds highlighted some promising compounds which could be used as tools for the study of protein kinase CK1δ implications in neuroinflammatory and neurodegenerative disease, as also as hit compounds for a more focused structural optimization.

6. Experimental Section

6.1. Chemistry

6.1.1. General chemistry

Reagents were obtained from commercial suppliers and used without further purification. Reactions were monitored by TLC, on precoated silica gel plates (Macherey-Nagel, 60FUV254) or aluminum oxide plates (Macherey-Nagel, 60NUV254). Final compounds and intermediates were purified by flash chromatography using stationary phases silica gel (Macherey-Nagel, silica 60, 240–400 mesh) or (Macherey-Nagel, aluminum oxide 90 neutral, 50–200 μm). When used, light petroleum ether refers to the fractions boiling at 40–60 °C. Melting points were determined with a Stuart SMP10 melting point apparatus and were not corrected. The ^{1}H NMR and ^{13}C NMR spectra were determined in $CDCl_3$, DMSO-d_6, D_2O or CD_3OD solutions and recorded on Jeol GX 270 MHz, Jeol 400 MHz, Varian 400 MHz or Varian 500 MHz spectrometers; chemical shifts (δ scale) are reported in parts per million (ppm) and referenced to residual solvent peak, with splitting patterns abbreviated to: s (singlet), d (doublet), dd (doublet of doublets), dt (doublet of triplets), t (triplet), m (multiplet) and bs (broad signal). Coupling constants (*J*) are given in Hz. MS-ESI analysis were performed using ESI Bruker 4000 Esquire spectrometer while for the accurate mass the instrument microTOF-Q – Bruker have been used. Compound purities were determined by two different methods: method A) HPLC-DAD (*Waters* 515 HPLC pump; *Waters* PDA 2998 Detector) using Luna C8(2) HPLC column (150 × 4.6 mm, particle size 3 μm). Isocratic elution was performed for 40 min at a flow rate of 300 μL/min in water-methanol 30:70. UV absorption

was detected from 220 to 400 nm using a diode array detector; purity was determined at the maximum absorption wavelength of the compound and at 254 nm. Method B) HPLC (Agilent Technologies 1260 Infinity; UV-VIS detector) using column (Zorbax Eclipse Plus, C18, 95 Å, 3,5 μm, 4,6 × 100 mm). Elution gradient was performed for 20 min at a flow rate of 1 mL/min from water-methanol 40:60 to 20:80, detection was determined at 254 nm.

Synthesis of 2,5,8-trisubstituted [1,2,4]triazolo[1,5-c]pyrimidines (**1**–**31**).

Synthesis of 4-hydroxy-2-methylthio-5-carbethoxypyrimidine sodium salt (**60**).

To a solution of 34.4 g (0.860 mol) of sodium hydroxide in 215 mL of water at 20 °C were added 59.8 g of 2-methyl-2-thiopseudourea hemisulfate (**58**, 0.430 mol). The mixture was stirred for 5 min, by which time most of the pseudothiourea had dissolved. Diethyl ethoxymethylenemalonate (**59**, 0.430 mol, 92.9 g), dissolved in 500 mL of ethanol, was added under stirring for 1 h. After the addition was completed, stirring was continued for 3 h and then the solid mixture was allowed to stand for 24 h. Finally, the mixture was filtered and washed using the minimum amount of water to give a pink solid (81.2 g). Yield 40%; mp > 300 °C. ^{1}H NMR (400 MHz, D_2O): δ 8.35 (s, 1H), 4.16 (q, J = 7.1 Hz, 2H), 2.33 (s, 3H), 1.20 (t, J = 7.1 Hz, 3H).

General procedure for the synthesis of ethyl 4-(2-hydrazido)-2-(methylthio)pyrimidine-5-carbocarboxylate derivatives (**77**–**91**).

To 10.0 g (42 mmol) of dried **60** were added 30 mL of phosphoryl oxychloride dropwise at 0 °C. After the addition was completed, the mixture was refluxed for 5 h. The excess of phosphoryl oxychloride was then removed under reduced pressure and ice and cold water were added to the solid residue (150 mL). The mixture was extracted with diethylether (3 × 50 mL), dried over sodium sulfate anhydrous and the solvent was removed by evaporation under reduced pressure to give the 4-chloro-2-methylthio-5-carbethoxypyrimidine (**61**), which was readily used in the next step without purification. The chloropyrimidine obtained (**61**) and 74 mmol of the required hydrazide (**62**–**76**) were dissolved in 60 mL THF, while 74 mmol of DBU were added dropwise at 0 °C. The mixture was stirred at room temperature overnight. The solvent was then removed, the residue was dissolved in dichloromethane (300 mL) and the resulting solution was washed with water (3 × 100 mL). The organic layer was dried over anhydrous sodium sulfate, concentrated under reduced pressure, and purified by flash chromatography.

*ethyl 4-(2-acetylhydrazinyl)-2-(methylthio)pyrimidine-5-carboxylate (**77**)*: flash chromatography eluent: light petroleum-EtOAc 6:4. Yield 42% (4.76 g); pale yellow solid; mp 155 °C (EtOEt-light petroleum). ^{1}H NMR (400 MHz; $CDCl_3$): 10.17 (s, 1H), 9.60 (s, 1H), 8.62 (s, 1H), 4.30 (q, J = 7.0 Hz, 2H), 2.46 (s, 3H), 1.92 (s, 3H), 1.29 (t, J = 7.1 Hz, 3H). ES-MS (methanol) m/z: 293.0 $[M+Na]^+$.

*ethyl 4-[2-(cyclopentancarbonyl)hydrazinyl]-2-(methylthio)pyrimidine-5-carboxylate (**78**)*: flash chromatography eluent: light petroleum-EtOAc 8:2. Yield 24% (3.27 g); pale yellow solid; mp 127 °C (EtOEt-light petroleum). ^{1}H NMR (270 MHz, $CDCl_3$): δ 10.05 (bs, 1H), 8.67 (s, 1H), 8.20 (bs, 1H), 4.35 (q, J = 7.0 Hz, 2H), 2.80–2.57 (m, 1H), 2.52 (s, 3H), 2.06–1.49 (m, 8H), 1.37 (t, J = 7.0 Hz, 3H). ES-MS (methanol) m/z: 323.0 $[M-H]^-$.

*ethyl 4-[2-(1H-indol-2-carbonyl)hydrazinyl]-2-(methylthio)pyrimidine-5-carboxylate (**79**)*: flash chromatography eluent: light petroleum-EtOAc 8:2. Yield 46% (7.18 g); pale yellow solid; mp 253–255 °C (EtOEt-light petroleum). ^{1}H NMR (400 MHz, DMSO-d_6): δ 11.71 (s, 1H), 10.69 (s, 1H), 9.76 (s, 1H), 8.68 (s, 1H), 7.65 (d, J = 8.0 Hz, 1H), 7.43 (d, J = 8.3 Hz, 1H), 7.27 (d, J = 1.3 Hz, 1H), 7.20 (t, J = 7.6 Hz, 1H), 7.05 (t, J = 7.3 Hz, 1H), 4.34 (q, J = 7.1 Hz, 2H), 2.29 (s, 3H), 1.33 (t, J = 7.1 Hz, 3H). ES-MS (methanol) m/z: 370.0 $[M-H]^-$.

*ethyl 4-(2-(4-methoxybenzoyl)hydrazinyl)-2-(methylthio)pyrimidine-5-carboxylate (**80**)*: flash chromatography eluent: light petroleum-EtOAc 6:4. Yield 57% (8.68 g); white solid; mp 186 °C (EtOEt-light petroleum). ^{1}H NMR (400 MHz, $CDCl_3$): δ 10.57 (s, 1H), 9.71 (s, 1H), 8.66 (s, 1H), 7.88 (d, J = 8.8 Hz, 2H), 7.04 (d, J = 8.8 Hz, 2H), 4.33 (q, J = 7.1 Hz, 2H), 3.81 (s, 3H), 2.31 (s, 3H), 1.32 (t, J = 7.1 Hz, 3H). ES-MS (methanol) m/z: 361.0 $[M-H]^-$.

*ethyl 4-(2-isonicotinoylhydrazinyl)-2-(methylthio)pyrimidine-5-carboxylate (**81**)*: flash chromatography eluent: EtOAc-light petroleum 8:2. Yield 24% (4.12 g); white solid; mp 203–206 °C (EtOEt-light petroleum). ^{1}H NMR (270 MHz, DMSO-d_6): δ 11.04 (bs, 1H), 9.85 (bs, 1H), 8.80 (d, J = 4.7 Hz, 2H), 8.70 (s, 1H), 7.81 (d, J = 4.7 Hz, 2H), 4.35 (q, J = 7.1 Hz, 2H), 2.34 (s, 3H), 1.34 (t, J = 7.1 Hz, 3H). ES-MS (methanol) m/z: 333.9 $[M+H]^+$, 355.9 $[M+Na]^+$.

*ethyl 4-(2-(4-(benzyloxy)benzoyl)hydrazinyl)-2-(methylthio)pyrimidine-5-carboxylate (**82**)*: flash chromatography eluent: DCM-EtOAc 9:1. Yield 40% (7.46 g); yellow solid; mp 202–205 °C (EtOEt-light petroleum). ^{1}H NMR (400 MHz, DMSO-d_6): δ 10.58 (bs, 1H), 9.75 (bs, 1H), 8.67 (s, 1H), 7.89 (d, J = 7.9 Hz, 2H), 7.47–7.35 (m, 5H), 7.14 (d, J = 7.9 Hz, 2H), 5.19 (s, 2H), 4.34 (q, J = 6.6 Hz, 2H), 2.33 (s, 3H), 1.33 (t, J = 6.6 Hz, 3H). ES-MS (methanol) m/z: 439.2 $[M+H]^+$, 461.1 $[M+Na]^+$, 477.1 $[M+K]^+$.

*ethyl 4-(2-(3-methoxybenzoyl)hydrazinyl)-2-(methylthio)pyrimidine-5-carboxylate (**83**)*: flash chromatography eluent: from DCM-EtOAc 95:5 to DCM-MeOH 9:1.Yield 43% (6.54 g); white solid; mp 145–150 °C (EtOEt-light petroleum). ^{1}H NMR (400 MHz, $CDCl_3$): δ 10.34 (bs, 1H), 8.88 (bs, 1H), 8.71 (s, 1H), 7.44–7.33 (m, 3H), 7.10 (bs, 1H), 4.39 (q, J = 7.1 Hz, 2H), 3.87 (s, 3H), 2.49 (s, 3H), 1.41 (t, J = 7.1 Hz, 3H). ES-MS (methanol) m/z: 363.1 $[M+H]^+$, 385.1 $[M+Na]^+$.

*ethyl 4-(2-(3-fluorobenzoyl)hydrazinyl)-2-(methylthio)pyrimidine-5-carboxylate (**84**)*: flash chromatography eluent: DCM-EtOAc 9:1. Yield 66% (9.7 g); white solid; mp 175 °C (EtOEt-light petroleum). ^{1}H NMR (400 MHz, $CDCl_3$): δ 10.82 (s, 1H), 9.78 (s, 1H), 8.67 (s, 1H), 7.75 (d, J = 7.8 Hz, 1H), 7.67 (dt, J = 8.0 Hz, J = 2.4 Hz, 1H), 7.61–7.55 (m, 1H), 7.45 (td, J = 8.0, J = 2.4 Hz, 1H), 4.33 (q, J = 7.1 Hz, 2H), 2.33 (s, 3H), 1.32 (t, J = 7.1 Hz, 3H). ES-MS (methanol) m/z: 351.0 $[M+H]^+$, 373.0 $[M+Na]^+$.

*ethyl 4-(2-(3-nitrobenzoyl)hydrazinyl)-2-(methylthio)pyrimidine-5-carboxylate (**85**)*: flash chromatography eluent: from light petroleum-EtOAc 9:1 to 4:6. Yield 63% (10.0 g); white solid; mp 204–208 °C (EtOEt-light petroleum). ^{1}H NMR (400 MHz, DMSO-d_6): δ 11.14 (s, 1H), 9.90 (s, 1H), 8.74 (s, 1H), 8.70 (s, 1H), 8.49–8.44 (m, 1H), 8.36–8.31 (m, 1H), 7.86 (t, J = 8.0 Hz, 1H), 4.36 (q, J = 7.1 Hz, 2H), 2.35 (s, 3H), 1.34 (t, J = 7.1 Hz, 3H).). ES-MS (methanol) m/z: 378.3 $[M+H]^+$, 400.3 $[M+Na]^+$.

*ethyl 4-(2-(3,5-dimethoxybenzoyl)hydrazinyl)-2-(methylthio)pyrimidine-5-carboxylate (**86**)*: flash chromatography eluent: from DCM-EtOAc 9.8:0.2 to DCM-EtOAc 9:1. Yield 21% (5,76 g, reaction performed on 70 mmol of **60**); white solid; mp 194 °C (EtOAc-light petroleum). ^{1}H NMR (400 MHz, $CDCl_3$) δ 10.28 (d, J = 5.1 Hz, 1H), 8.77 (d, J = 5.1 Hz, 1H), 8.72 (s, 1H), 6.97 (d, J = 2.2 Hz, 2H), 6.63 (t, J = 2.2 Hz, 1H), 4.39 (q, J = 7.1 Hz, 2H), 3.84 (s, 6H), 2.49 (s, 3H), 1.41 (t, J = 7.1 Hz, 3H). ES-MS (methanol) m/z: 393.2 $[M+H]^+$.

*ethyl 4-(2-benzoylhydrazinyl)-2-(methylthio)pyrimidine-5-carboxylate (**87**)*: flash chromatography eluent: DCM-EtOAc 95:5. Yield 34% (4.75 g); white solid; mp 168 °C (EtOEt-light petroleum). ^{1}H NMR (270 MHz, $CDCl_3$): δ 10.43 (bs, 1H), 8.96 (bs, 1H), 8.75 (s, 1H), 7.91 (d, J = 7.5 Hz, 2H), 7.67–7.41 (m, 3H), 4.43 (q, J = 7.2 Hz, 2H), 2.52 (s, 3H), 1.44 (t, J = 7.2 Hz, 3H). ES-MS (methanol) m/z: 331.0 $[M-H]^-$.

*ethyl 4-(2-(4-fluorobenzoyl)hydrazinyl)-2-(methylthio)pyrimidine-5-carboxylate (**88**)*: flash chromatography eluent: DCM-EtOAc 9:1. Yield 28%; white solid; mp 200 °C (EtOEt-light petroleum). ^{1}H NMR (270 MHz, DMSO-d_6): δ 10.77 (bs, 1H), 9.78 (bs, 1H), 8.68 (s,

1H), 7.98 (dd, $J_H = 8.8$, $J_{HF} = 5.6$ Hz, 2H), 7.37 (t, $J_{H,HF} = 8.8$ Hz, 2H), 4.34 (q, $J = 7.0$ Hz, 2H), 2.33 (s, 3H), 1.33 (t, $J = 7.0$ Hz, 3H). ES-MS (methanol) *m/z*: 348.9 [M − H]$^-$.

*ethyl 4-(2-(3-(benzyloxy)benzoyl)hydrazinyl)-2-(methylthio)pyrimidine-5-carboxylate (**89**):* flash chromatography eluent: DCM-EtOAc 9:1. Yield 34% (6.17 g); white solid; mp 117 °C (EtOEt-light petroleum). ^{1}H NMR (270 MHz, DMSO-d_6): δ 10.72 (bs, 1H), 9.77 (bs, 1H), 8.68 (s, 1H), 7.71−7.11 (m, 9H), 5.17 (s, 2H), 4.34 (q, $J = 7.1$ Hz, 2H), 2.33 (s, 3H), 1.33 (t, $J = 7.1$ Hz, 3H). ES-MS (methanol) *m/z*: 438.9 [M+H]$^+$, 460.8 [M+H]$^+$.

*ethyl 4-(2-(3,4-bis(benzyloxy)benzoyl)hydrazinyl)-2-(methylthio) pyrimidine-5-carboxylate (**90**):* flash chromatography eluent: from DCM-light petroleum 9.5:0.5 to DCM-EtOAc 8:2. Yield 30% (6.86 g); white solid; mp 186 °C (EtOEt-light petroleum). ^{1}H NMR (270 MHz, DMSO-d_6): δ 10.59 (bs, 1H), 9.74 (bs, 1H), 8.68 (s, 1H), 7.62 (s, 1H), 7.60−7.26 (m, 11H), 7.20 (d, $J = 8.4$ Hz, 1H), 5.21 (d, $J = 9.9$ Hz, 4H), 4.35 (q, $J = 6.7$ Hz, 2H), 2.31 (s, 3H), 1.33 (t, $J = 6.7$ Hz, 3H). ES-MS (methanol) *m/z*: 544.9 [M+H]$^+$, 566.9 [M+Na]$^+$.

*ethyl 4-(2-(3,5-bis(benzyloxy)benzoyl)hydrazinyl)-2-(methylthio) pyrimidine-5-carboxylate (**91**):* flash chromatography eluent: from DCM-EtOAc 9:1 to DCM-EtOAc 8.5:1.5. Yield 54% (12.35 g); white solid; mp 184−188 °C (EtOEt-light petroleum). ^{1}H NMR (400 MHz, DMSO-d_6): δ 10.69 (s, 1H), 9.77 (s, 1H), 8.68 (s, 1H), 7.49−7.33 (m, 10H), 7.16 (s, 2H), 6.91 (s, 1H), 5.16 (s, 4H), 4.35 (q, $J = 7.0$ Hz, 2H), 2.33 (s, 3H), 1.34 (t, $J = 7.0$ Hz, 3H). ES-MS (methanol) *m/z*: 545.2 [M+H]$^+$, 567.3 [M+Na]$^+$. MW 544.62.

General procedure for the synthesis of 2-substituted 5-(methylthio)-[1,2,4]triazolo[1,5-*c*]pyrimidine-8-carboxylate derivatives (**92**−**106**).

Method A: To 150 mL of dry xylene were added 0.030 mol of phosphorus pentoxide and hexamethyldisiloxane, and the mixture was heated at 90 °C for 2 h. Pyrimidine hydrazides (0.010 mol) were then added, and the reaction was refluxed for 2 days. After that, the solvent was removed under reduced pressure, and the residue was dissolved in EtOAc (200 mL) and washed with water (3 × 70 mL)). The organic layer was then dried over anhydrous sodium sulfate, concentrated under reduced pressure, and purified by flash chromatography.

Method B: The mixture of phosphorous pentoxyde [0.045 mol (Method **B$_1$**) or 0.075 mol (Method **B$_2$**)] and hexamethyldisiloxane [0.045 mol (Method **B$_1$**) or 0.075 mol (Method **B$_2$**)] in anhydrous xylene (150 mL) was heated to 90 °C over 1.5 h and then stirred for 1 h at 90 °C, under argon atmosphere. The well-dried hydrazides compounds (**62**−**76**) (0.015 mol, 1 equivalent) were then added to the clear solution and the temperature is increased to reflux and stirred for 2−3 h. The solvent was then removed, the residue dissolved in DCM (300 mL) and the resulting solution was washed with water (3 × 100 mL). The organic layer was concentrated, dried over anhydrous sodium sulfate and purified to afford the desired compounds.

*ethyl 2-methyl-5-(methylthio)-[1,2,4]triazolo[1,5-c]pyrimidine-8-carboxylate (**92**):* Method A. Flash chromatography eluent: light petroleum-EtOAc 6:4. Yield 32% (0.807 g); pale yellow solid; mp 120 °C (EtOEt-light petroleum). ^{1}H NMR (400 MHz, $CDCl_3$): δ 8.76 (s, 1H), 4.50 (q, $J = 7.1$ Hz, 2H), 2.78 (s, 3H), 2.70 (s, 3H), 1.44 (t, $J = 7.1$ Hz, 3H). ES-MS (methanol) *m/z*: 225.0 [M + H-(CH_2CH_3)]$^+$, 253.0 [M+H]$^+$, 275.0 [M+Na]$^+$.

*ethyl 2-cyclopentyl-5-(methylthio)-[1,2,4]triazolo[1,5-c]pyrimidine-8-carboxylate (**93**):* Method A. Flash chromatography eluent: light petroleum-EtOAc 8:2. Yield 28% (0.858 g); white solid; mp 95 °C (EtOEt-light petroleum). ^{1}H NMR (400 MHz, $CDCl_3$): δ 8.74 (s, 1H), 4.49 (q, $J = 7.1$ Hz, 2H), 3.48 (p, $J = 8.3$ Hz, 1H), 2.77 (s, 3H), 2.21−2.13 (m, 2H), 2.09−1.99 (m, 2H), 1.90−1.82 (m, 2H), 1.76−1.67 (m, 2H), 1.44 (d, $J = 7.1$ Hz, 3H). ES-MS (methanol) *m/z*: 307.1 [M+H]$^+$, 329.1 [M+Na]$^+$.

*ethyl 2-(1-H-indol-2-yl)-5-(methylthio)-[1,2,4]triazolo[1,5-c]pyrimidine-8-carboxylate (**94**):* Method A. Flash chromatography eluent: light petroleum-EtOAc 7:3. Yield 28% (0.989 g); yellow solid; mp 187−190 °C (EtOEt-light petroleum). ^{1}H NMR (400 MHz, $CDCl_3$): δ 9.39 (s, 1H), 8.80 (s, 1H), 7.71 (d, $J = 8.0$ Hz, 1H), 7.50−7.45 (m, 2H), 7.31−7.27 (m, 1H), 7.17−7.13 (m, 1H), 4.54 (q, $J = 7.1$ Hz, 2H), 2.82 (s, 3H), 1.49 (t, $J = 7.1$ Hz, 3H). ES-MS (methanol) *m/z*: 354.1 [M+H]$^+$, 376.0 [M+Na]$^+$.

*ethyl 2-(4-methoxyphenyl)-5-(methylthio)-[1,2,4]triazolo[1,5-c] pyrimidine-8-carboxylate (**95**):* Method A. Flash chromatography eluent: DCM (stationary phase: aluminium oxide). Yield 57% (1.96 g); white solid; mp 182−184 °C (EtOEt-light petroleum). ^{1}H NMR (400 MHz, $CDCl_3$): δ 8.78 (s, 1H), 8.35 (d, $J = 8.9$ Hz, 2H), 7.01 (d, $J = 8.9$ Hz, 2H), 4.52 (q, $J = 7.1$ Hz, 2H), 3.88 (s, 3H), 2.80 (s, 3H), 1.49 (t, $J = 7.1$ Hz, 3H). ES-MS (methanol) *m/z*: 345.2 [M+H]$^+$, 367.1 [M+Na]$^+$.

*ethyl 2-(pyridin-4-yl)-5-(methylthio)-[1,2,4]triazolo[1,5-c]pyrimidine-8-carboxylate (**96**):* Method B$_1$. Flash chromatography eluent: DCM-MeOH 97:3. Yield 8% (0.252 g); white solid; mp 183−185 °C (EtOEt-light petroleum). ^{1}H NMR (400 MHz, DMSO-d_6): δ 8.83−8.81 (m, 3H), 8.14 (dd, $J = 4.4$, 1.6 Hz, 2H), 4.43 (q, $J = 7.1$ Hz, 2H), 2.80 (s, 3H), 1.40 (t, $J = 7.1$ Hz, 3H). ES-MS (methanol) *m/z*: 316.4 [M+H]$^+$, 338.3 [M+Na]$^+$.

*ethyl 2-(4-(benzyloxy)phenyl)-5-(methylthio)-[1,2,4]triazolo[1,5-c]pyrimidine-8-carboxylate (**97**):* Method B$_1$. Flash chromatography eluent: DCM. Yield 7% (0.294 g); white solid; mp 190−192 °C (EtOEt-light petroleum). ^{1}H NMR (400 MHz, $CDCl_3$): δ 8.79 (s, 1H), 8.37 (d, $J = 8.7$ Hz, 2H), 7.56−7.30 (m, 5H), 7.09 (d, $J = 8.7$ Hz, 2H), 5.14 (s, 2H), 4.53 (q, $J = 7.1$ Hz, 2H), 2.80 (s, 3H), 1.49 (t, $J = 7.1$ Hz, 3H). ES-MS (methanol) *m/z*: 421.0 [M+H]$^+$, 443.0 [M+Na]$^+$, 458.9 [M+K]$^+$.

*ethyl 2-(3-methoxyphenyl)-5-(methylthio)-[1,2,4]triazolo[1,5-c] pyrimidine-8-carboxylate (**98**):* Method B$_2$. Flash chromatography eluent: light petroleum-EtOAc 8:2. Yield 59% (2.03 g)); white solid; mp 154 °C (EtOEt-light petroleum). ^{1}H NMR (270 MHz, $CDCl_3$): δ 8.80 (s, 1H), 8.06−7.87 (m, 2H), 7.41 (t, $J = 7.8$ Hz, 1H), 7.06 (dd, $J = 7.8$, 2.7 Hz, 1H), 4.53 (q, $J = 7.1$ Hz, 2H), 3.93 (s, 3H), 2.81 (s, 3H), 1.49 (t, $J = 7.1$ Hz, 3H). ES-MS (methanol) *m/z*: 345.4 [M+H]$^+$, 367.3 [M+Na]$^+$.

*ethyl 2-(3-fluorophenyl)-5-(methylthio)-[1,2,4]triazolo[1,5-c]pyrimidine-8-carboxylate (**99**):* Method B$_2$. Flash chromatography eluent: light petroleum-EtOAc 95:5 (stationary phase: aluminium oxide). Yield 14% (0.465 g); white solid; mp 153−156 °C (EtOEt-light petroleum). ^{1}H NMR (400 MHz, $CDCl_3$): 8.81 (s, 1H), 8.20 (m, 1H), 8.12−8.09 (m, 1H), 7.47 (td, $J = 8.0$, $J_{HF} = 5.7$ Hz, 1H), 7.23−7.17 (m, 1H), 4.53 (q, $J = 7.1$ Hz, 2H), 2.81 (s, 3H), 1.49 (t, $J = 7.1$ Hz, 3H). ES-MS (methanol) *m/z*: 333.0 [M+H]$^+$.

*ethyl 2-(3-nitrophenyl)-5-(methylthio)-[1,2,4]triazolo[1,5-c]pyrimidine-8-carboxylate (**100**)*: Method B$_2$. Flash chromatography eluent: DCM-light petroleum 8:2 (stationary phase: aluminium oxide). Yield 7% (0.252 g); white solid; mp 210−215 °C (EtOEt-light petroleum). ^{1}H NMR (400 MHz, $CDCl_3$): δ 9.23 (s, 1H), 8.84 (s, 1H), 8.77−8.72 (m, 1H), 8.39−8.33 (m, 1H), 7.70 (t, $J = 8.0$ Hz, 1H), 4.54 (q, $J = 7.1$ Hz, 2H), 2.83 (s, 3H), 1.49 (t, $J = 7.1$ Hz, 3H). ES-MS (methanol) *m/z*: 332.3 [M + H-(CH_2CH_3)]$^+$, 360.3 [M+H]$^+$, 382.3 [M+Na]$^+$.

*ethyl 2-(3,5-dimethoxyphenyl)-5-(methylthio)-[1,2,4]triazolo[1,5-c]pyrimidine-8-carboxylate (**101**)*: Method B$_2$. Flash chromatography eluent: light petroleum-EtOAc from 8:2 to 6:4. Yield: 12% (0.43 g, starting from 10 mmol of **86**); white solid; mp 206−208 °C (EtOAc-light petroleum). ^{1}H NMR (400 MHz, $CDCl_3$) δ 8.80 (s, 1H), 7.57 (d, $J = 2.1$ Hz, 2H), 6.61 (t, 1H), 4.53 (q, $J = 7.1$ Hz, 2H), 3.90 (s, 6H), 2.81 (s, 3H), 1.49 (t, $J = 7.1$ Hz, 3H).^{13}C NMR (101 MHz, $CDCl_3$) δ 166.24, 163.26, 161.09, 158.13, 150.59, 148.10, 131.45, 110.72, 106.08, 104.18, 62.03, 55.78, 14.47, 13.80. ES-MS (methanol) *m/z*:

375.1 $[M+H]^+$, 397.1 $[M+Na]^+$.

*ethyl 2-phenyl-5-(methylthio)-[1,2,4]triazolo[1,5-c]pyrimidine-8-carboxylate (**102**):* Method B_1. Flash chromatography eluent: light petroleum-EtOAc from 9:1 to 4:6 (stationary phase: aluminium oxide). Yield 16% (0.503 g); white solid; mp 169–171 °C (EtOEt-light petroleum). ^{1}H NMR (270 MHz, $CDCl_3$): δ 8.80 (s, 1H), 8.41 (m, 2H), 7.51 (m, 3H), 4.53 (q, J = 6.5 Hz, 2H), 2.81 (s, 3H), 1.49 (t, J = 6.5 Hz, 3H). ES-MS (methanol) m/z: 315.2 $[M+H]^+$, 337.2 $[M+Na]^+$, 353.1 $[M+K]^+$.

*ethyl 2-(4-fluorophenyl)-5-(methylthio)-[1,2,4]triazolo[1,5-c]pyrimidine-8-carboxylate (**103**):* Method B_1. Flash chromatography eluent: DCM-EtOAc from 95:5. Yield 6% (0.199 g); white solid; mp 188–190 °C (EtOEt-light petroleum). ^{1}H NMR (270 MHz, $CDCl_3$): δ 8.80 (s, 1H), 8.41 (dd, J_H = 8.2 Hz, J_{HF} = 5.7 Hz, 2H), 7.18 (t, $J_{H,HF}$ = 8.2Hz, 2H), 4.53 (q, J = 7.1 Hz, 2H), 2.80 (s, 3H) 1.48 (t, J = 7.1 Hz, 3H). ES-MS (methanol) m/z: 332.9 $[M+H]^+$, 354.9 $[M+Na]^+$, 370.8 $[M+K]^+$.

*ethyl 2-(3-(benzyloxy)phenyl)-5-(methylthio)-[1,2,4]triazolo[1,5-c]pyrimidine-8-carboxylate (**104**):* Method B_1. Flash chromatography eluent: light petroleum-EtOAc 8:2. Yield 7% (0.294 g); white solid; mp 167–169 °C (EtOEt-light petroleum). ^{1}H NMR (270 MHz, $CDCl_3$): δ 8.81 (s, 1H), 8.03 (d, J = 8.0 Hz, 2H), 7.57–7.30 (m, 6H), 7.12 (d, J = 6.6 Hz, 1H), 5.18 (s, 2H), 4.53 (q, J = 7.1 Hz, 2H), 2.81 (s, 3H), 1.49 (t, J = 7.1 Hz, 3H). ES-MS (methanol) m/z: 421.4 $[M+H]^+$, 443.3 $[M+Na]^+$.

*ethyl 2-(3,4-bis(benzyloxy)phenyl)5-(methylthio)-[1,2,4]triazolo [1,5-c]pyrimidine-8 carboxylate (**105**):* Method B_1. Flash chromatography eluent: DCM-EtOAc 99:1. Yield 6% (0.342 g); white solid; mp 170–172 °C (EtOEt-light petroleum). ^{1}H NMR (270 MHz; $CDCl_3$): δ 8.80 (s, 1H), 8.08–7.97 (m, 2H), 7.57–7.28 (m, 10H), 7.08–6.99 (m, 1H), 5.34–5.17 (m, 4H), 4.59–4.48 (q, J = 6.5 Hz, 2H), 2.81 (s, 3H), 1.55–1.43 (t, J = 6.5 Hz, 3H). ES-MS (methanol) m/z: 527.2 $[M+H]^+$, 549.2 $[M+Na]^+$, 565.1 $[M+K]^+$.

*ethyl 2-(3,5-bis(benzyloxy)phenyl)5-(methylthio)-[1,2,4]triazolo [1,5-c]pyrimidine-8 carboxylate (**106**):* Method B_2. Flash chromatography eluent: light petroleum-EtOAc 8:2. Yield 5% (0.263 g); white solid; mp 170–175 °C (EtOEt-light petroleum). ^{1}H NMR (400 MHz, $CDCl_3$): δ 8.80 (s, 1H), 7.69 (s, 2H), 7.53 7.30 (m, 10H), 6.76 (s, 1H), 5.14 (s, 4H), 4.53 (q, J = 7.0 Hz, 2H), 2.80 (s, 3H), 1.48 (t, J = 7.0 Hz, 3H). ES-MS (methanol) m/z: 527.3 $[M+H]^+$, 549.2 $[M+Na]^+$.

General procedure for the preparation of 2-substituted 5-amino-[1,2,4]triazolo[1,5-*c*]pyrimidine-8-carboxylate derivatives (**1**–**10**, **107**–**109**).

1 mL of methanolic ammonia 7 N and 4 mL of ethanol were added to 0.5 mmol of **92**–**101**,**104**–**106** and the mixture was heated at 70 °C in a sealed tube for 3–12 h. The solvent was then removed under vacuum and the solid purified by flash chromatography.

*ethyl 5-amino-2-methyl-[1,2,4]triazolo[1,5-c]pyrimidine-8-carboxylate (**1**)*: flash chromatography eluent: light petroleum-EtOAc 8:2. Yield 52% (57 mg); white solid; mp 238–241 °C (EtOEt-light petroleum). ^{1}H NMR (270 MHz, DMSO-d_6): δ 8.90–8.35 (m, 3H), 4.30 (q, J = 7.1 Hz, 2H), 2.51 (s, 3H), 1.31 (t, J = 7.1 Hz, 3H). ^{1}H NMR (270 MHz, DMSO-d_6/D_2O) δ: 8.44 (s, 1H), 4.27 (bs, 2H), 2.46 (s, 3H), 1.27 (bs, 3H). ^{13}C NMR (101 MHz, DMSO-d_6): δ 164.5, 163.5, 152.2, 151.6, 150.2, 103.0, 60.5, 14.80, 14.70. ES-MS (methanol) m/z: 222.4 $[M+H]^+$, 244.4 $[M+Na]^+$. HRMS (ESI-TOF) m/z: $C_9H_{11}N_5O_2$ experimental 244.0803 $[M+Na]^+$, theoretical 244.0804 $[M+Na]^+$, Δ = 0.0001. Purity HPLC (Method A): 98.1%.

*ethyl 5-amino-2-cyclopentyl-[1,2,4]triazolo[1,5-c]pyrimidine-8-carboxylate (**2**):* flash chromatography eluent: light petroleum-EtOAc 1:1. Yield 27% (37 mg); white solid; mp 179–181 °C (EtOEt-light petroleum). ^{1}H NMR (400 MHz, $CDCl_3$): δ 8.60 (s, 1H), 6.74 (bs, 2H), 4.29 (q, J = 7.1 Hz, 2H), 3.36–3.28 (m, 1H), 2.09–2.00 (m, 2H), 1.98–1.85 (m, 2H), 1.83–1.73 (m, 2H), 1.73–1.61 (m, 2H), 1.31 (t, J = 7.1 Hz, 3H). ^{13}C NMR (101 MHz, DMSO-d_6): δ 171.6, 163.4, 152.0, 151.7, 150.2, 103.1, 60.5, 39.0, 32.4, 25.8, 14.7. ES-MS (methanol) m/z: 276.1 $[M+H]^+$, 298.1 $[M+Na]^+$. HRMS (ESI-TOF) m/z: $C_{13}H_{17}N_5O_2$ experimental 298.1271 $[M+Na]^+$, theoretical 298.1274 $[M+Na]^+$, Δ = 0.0003. Purity HPLC (Method A): 99.0%.

*ethyl 5-amino-2-(1H-indol-2-yl)-[1,2,4]triazolo[1,5-c]pyrimidine-8-carboxylate (**3**):* flash chromatography eluent: light petroleum-EtOAc 6:4. Yield 16% (26 mg); white solid; mp 296–299 °C (EtOEt-light petroleum). ^{1}H NMR (400 MHz, DMSO-d_6): δ 11.80 (s, 1H), 8.95–8.30 (m, 3H), 7.66 (d, J = 7.9 Hz, 1H), 7.55 (d, J = 8.1 Hz, 1H), 7.19–7.15 (m, 2H), 7.06 (t, J = 7.3 Hz, 1H), 4.35 (q, J = 7.1 Hz, 2H), 1.36 (t, J = 7.1 Hz, 3H). ^{13}C NMR (101 MHz, DMSO-d_6): δ 163.2, 159.4, 152.4, 152.2, 150.4, 137.8, 128.7, 128.2, 123.3, 121.4, 120.2, 112.8, 110.0, 103.4, 60.6, 14.8. ES-MS (methanol) m/z: 323.2 $[M+H]^+$, 345.1 $[M+Na]^+$. HRMS (ESI-TOF) m/z: $C_{16}H_{14}N_6O_2$ experimental 345.1072 $[M+Na]^+$, theoretical 345.1070 $[M+Na]^+$, Δ = 0.0002. Purity HPLC (Method A): 96.2%.

*ethyl 5-amino-2-(4-methoxyphenyl)-[1,2,4]triazolo[1,5-c]pyrimidine-8-carboxylate (**4**):* flash chromatography eluent: DCM-MeOH 98:2. Yield 40% (63 mg); white solid; mp 232 °C (EtOEt-light petroleum). ^{1}H NMR (270 MHz, DMSO-d_6): δ 8.90 (s, 1H), 8.65–8.28 (m, 2H), 8.18 (d, J = 8.8 Hz, 2H), 7.13 (d, J = 8.8 Hz, 2H), 4.33 (q, J = 7.1 Hz, 2H), 3.85 (s, 3H), 1.35 (t, J = 7.1 Hz, 3H). ^{13}C NMR (68 MHz, DMSO-d_6): δ 163.86, 163.23, 161.43, 152.07, 151.97, 150.19, 128.99, 122.53, 114.46, 102.98, 60.18, 55.36, 14.25. ES-MS (methanol) m/z: 314.1 $[M+H]^+$, 336.1 $[M+Na]^+$. HRMS (ESI-TOF) m/z: $C_{15}H_{15}N_5O_3$ experimental 314.1247 $[M+H]^+$, theoretical 314.1247 $[M+H]^+$, Δ = 0.0000. Purity HPLC (Method A): 98.3%.

*ethyl 5-amino-2-(piridin-4-yl)-[1,2,4]triazolo[1,5-c]pyrimidine-8-carboxylate (**5**):* flash chromatography eluent: EtOAc-MeOH 99:1. Yield 58% (83 mg); white solid; mp 268–270 °C (EtOEt-light petroleum). ^{1}H NMR (400 MHz, DMSO-d_6): δ 9.08 (bs, 1H), 8.82 (d, J = 5.9 Hz, 2H), 8.71–8.47 (m, 2H), 8.12 (d, J = 5.9 Hz, 2H), 4.34 (q, J = 7.1 Hz, 2H), 1.36 (t, J = 7.1 Hz, 3H). ^{13}C NMR (270 MHz, $CDCl_3$-CF_3COOD): δ 161.88, 152.73, 149.16, 146.08, 143.03, 142.45, 125.69, 123.71, 106.72, 63.09, 14.11. ES-MS (methanol) m/z: 284.9 $[M+H]^+$, 306.9 $[M+Na]^+$. HRMS (ESI-TOF) m/z: $C_{13}H_{12}N_6O_2$ experimental 285.1095 $[M+H]^+$, theoretical 285.1094 $[M+H]^+$, Δ = 0.0001. Purity HPLC (Method A): 96.3%.

*ethyl 5-amino-2-(4-(benzyloxy)phenyl)-[1,2,4]triazolo[1,5-c]pyrimidine-8-carboxylate (**6**):* flash chromatography eluent: DCM-methanol 95:5. Yield 93% (185 mg); white solid; mp 277–280 °C (EtOEt-light petroleum). ^{1}H NMR (400 MHz, DMSO-d_6): δ 8.86 (bs, 1H), 8.65–8.32 (m, 2H), 8.18 (d, J = 8.4 Hz, 2H), 7.44 (m, 5H), 7.22 (d, J = 8.4 Hz, 2H), 5.20 (s, 2H), 4.33 (q, J = 6.9 Hz, 2H), 1.35 (t, J = 6.9 Hz, 3H). ^{13}C NMR (68 MHz, $CDCl_3$): δ 163.26, 161.81, 160.57, 152.11, 151.99, 150.21, 136.92, 129.00, 128.66, 128.16, 128.04, 115.28, 102.98, 69.48, 60.18, 14.26. ES-MS (methanol) m/z: 390.2 $[M+H]^+$, 412.1 $[M+Na]^+$, 428.1 $[M+K]^+$. HRMS (ESI-TOF) m/z: $C_{21}H_{19}N_5O_3$ experimental 390.1557 $[M+H]^+$, theoretical 390.1560 $[M+H]^+$, Δ = 0.0003. Purity HPLC (Method A): 93.2%.

*ethyl 5-amino-2-(3-methoxyphenyl)-[1,2,4]triazolo[1,5-c]pyrimidine-8-carboxylate (**7**):* flash chromatography eluent: light petroleum-EtOAc 8:2. Yield 81% (127 mg); white solid; mp 200–204 °C (EtOEt-light petroleum). ^{1}H NMR (400 MHz, DMSO-d_6): δ 8.99 (s, 1H), 8.52 (bs, 2H), 7.89–7.74 (m, 2H), 7.50 (t, J = 7.9 Hz, 1H), 7.13 (d, J = 7.9 Hz, 1H), 4.34 (q, J = 7.0 Hz, 2H), 3.87 (s, 3H), 1.36 (t, J = 7.0 Hz, 3H). ^{13}C NMR (68 MHz, DMSO-d_6): δ 163.84, 163.18, 159.81, 152.24, 152.06, 150.31, 131.61, 130.35, 119.80, 116.57, 112.44, 103.15, 60.27, 55.31, 14.33. ES-MS (methanol) m/z: 286.3 $[M+2H-(CH_2CH_3)]^+$, 314.4 $[M+H]^+$, 336.3 $[M+Na]^+$. HRMS (ESI-TOF) m/z: $C_{15}H_{15}N_5O_3$ experimental 314.1245 $[M+H]^+$, theoretical 314.1247 $[M+H]^+$, Δ = 0.0002. Purity HPLC (Method A): 98.0%.

*ethyl 5-amino-2-(3-fluorophenyl)-[1,2,4]triazolo[1,5-c]pyrimidine-8-carboxylate (**8**):* flash chromatography eluent: DCM-MeOH

96:4. Yield 40% (60 mg); white solid; mp 223–225 °C (EtOEt-light petroleum). ^{1}H NMR (270 MHz, DMSO-d_6): δ 9.17–8.34 (m, 3H), 8.09 (d, J = 7.0 Hz, 1H), 7.95 (m, 1H), 7.70–7.59 (m, 1H), 7.42 (m, 1H), 4.34 (q, J = 7.0 Hz, 2H), 1.35 (t, J = 7.0 Hz, 3H). ^{13}C NMR (68 MHz, DMSO-d_6): δ 163.1, 162.8, 162.6 (d, J_{CF} = 244.1 Hz), 152.4, 152.2, 150.3, 132.5 (d, J_{CF} = 8.8 Hz), 131.4 (d, J_{CF} = 8.4 Hz), 123.5 (d, J_{CF} = 2.8 Hz), 117.7 (d, J_{CF} = 21.0 Hz), 113.75 (d, J_{CF} = 23.1 Hz), 103.2, 60.3, 14.25. ES-MS (methanol) m/z: 274.4 [M+2H-(CH_2CH_3)]$^+$, 302.5 [M+H]$^+$, 324.4 [M+Na]$^+$, 340.3 [M+K]$^+$. HRMS (ESI-TOF) m/z: $C_{14}H_{12}FN_5O_2$ experimental 302.1046 [M+H]$^+$, theoretical 302.1047 [M+H]$^+$, Δ = 0.0001. Purity HPLC (Method A): 95.6%.

*ethyl 5-amino-2-(3-nitrophenyl)-[1,2,4]triazolo[1,5-c]pyrimidine-8-carboxylate (**9**):* flash chromatography eluent: light petroleum-EtOAc 6:4. Yield 91% (149 mg); white solid; mp 275–280 °C (EtOEt-light petroleum). ^{1}H NMR (400 MHz, DMSO-d_6): δ 9.24–8.91 (m, 2H), 8.83–8.47 (m, 3H), 8.41 (d, J = 7.8 Hz, 1H), 7.91 (t, J = 7.9 Hz, 1H), 4.35 (q, J = 6.7 Hz, 2H), 1.36 (t, J = 6.7 Hz, 3H). ^{13}C NMR (68 MHz, DMSO-d_6): 163.06, 161.98, 152.63, 152.41, 150.38, 148.46, 133.40, 131.75, 131.06, 125.37, 121.70, 103.19, 60.42, 14.30. ES-MS (methanol) m/z: 329.4 [M+H]$^+$, 351.4 [M+Na]$^+$. HRMS (ESI-TOF) m/z: $C_{14}H_{12}N_6O_4$ experimental 302.0996 [M+H]$^+$, theoretical 329.0992 [M+H]$^+$, Δ = 0.0004. Purity HPLC: 95.1%.

*ethyl 5-amino-2-(3,5-dimethoxyphenyl)-[1,2,4]triazolo[1,5-c]pyrimidine-8-carboxylate (**10**):* flash chromatography eluent: from EtOAc-light petroleum 4:6 to EtOAc-light petroleum 8:2. Yield 87% (150 mg); white solid; mp 222–223 °C (EtOEt-light petroleum). ^{1}H NMR (400 MHz, DMSO) δ 8.94 (bs, 1H), 8.66–8.32 (m, 2H), 7.39 (d, J = 2.3 Hz, 2H), 6.67 (t, J = 2.3 Hz, 1H), 4.31 (q, J = 7.1 Hz, 2H), 3.83 (s, 6H), 1.34 (t, J = 7.1 Hz, 3H). ^{13}C NMR (101 MHz, DMSO) δ 163.41, 162.90, 160.75, 151.97, 151.76 (CH), 150.04, 131.85, 105.11 (2xCH), 102.99 (CH), 102.56, 60.19 (CH_2), 55.42 (2xCH_3), 14.27 (CH_3). MW = 343.13. ES-MS (methanol) m/z 344.2 [M+H]$^+$, 366.1 [M+Na]$^+$. HRMS (ESI-TOF) m/z: $C_{16}H_{17}N_5O_4$ experimental 344.1352 [M+H]$^+$, theoretical 344.1353 [M+H]$^+$, Δ = 0.0001; experimental 466.1175 [M+Na]$^+$, 366.1172 [M+Na]$^+$, Δ = 0.0003. Purity HPLC (Method A): 97.9%.

*ethyl 5-amino-2-(3-(benzyloxy)phenyl)-[1,2,4]triazolo[1,5-c]pyrimidine-8-carboxylate (**107**):* flash chromatography eluent: EtOAc-light petroleum 6:4. Yield 45% (88 mg); white solid; mp 196–198 °C (EtOEt-light petroleum). ^{1}H NMR (400 MHz, DMSO-d_6): δ 9.26–8.35 (m, 3H), 7.88 (m, 2H), 7.71–7.28 (m, 6H), 7.21 (s, 1H), 5.21 (s, 2H), 4.33 (bs, 2H), 1.35 (bs, 3H). ^{13}C NMR (68 MHz, DMSO-d_6): δ 163.4, 162.9, 158.6, 151.95, 151.78, 150.0, 136.9, 131.3, 130.1, 128.5, 127.9, 127.7, 119.8, 117.1, 113.4, 103.0, 69.3, 60.2, 14.3. ES-MS (methanol) m/z: 390.0 [M+H]$^+$, 412.0 [M+Na]$^+$. HPLC: 96.4%.

*ethyl 5-amino-2-(3,4-bis(benzyloxy)phenyl)-[1,2,4]triazolo[1,5-c] pyrimidine-8 carboxylate (**108**):* Flash chromatography eluent: DCM-MeOH 99:1. Yield 65% (161 mg); white solid; mp 200–202 °C (EtOEt-light petroleum). ^{1}H NMR (270 MHz; DMSO-d_6): δ 9.01–8.84 (m, 1H), 8.56–8.36 (m, 2H), 7.94–7.80 (m, 2H), 7.56–7.24 (m, 11H), 5.29–5.16 (m, 4H), 4.33 (q, J = 7.0 Hz, 2H), 1.36 (t, J = 7.0 Hz, 3H). ^{13}C NMR (68 MHz, DMSO-d_6): δ 163.5, 163.0, 151.9, 151.7, 150.5, 150.0, 148.2, 137.0, 136.9, 128.4, 127.9, 127.6, 122.9, 121.0, 114.1, 113.0, 102.9, 70.3, 70.0, 60.2, 14.3. ES-MS (methanol) m/z: 496.2 [M+H]$^+$, 518.2 [M+Na]$^+$, 534.1 [M+K]$^+$.

*ethyl 5-amino-2-(3,5-bis(benzyloxy)phenyl)-[1,2,4]triazolo[1,5-c] pyrimidine-8 carboxylate (**109**):* Flash chromatography eluent: DCM-MeOH 99:1. Yield 70% (173 mg); white solid; mp 245–248 °C (EtOEt-light petroleum). ^{1}H NMR (400 MHz; DMSO-d_6): δ 9.00–8.52 (m, 3H), 7.68–7.24 (m, 12H), 6.89 (s, 1H), 5.20 (s, 4H), 4.34 (q, J = 7.0 Hz, 2H), 1.35 (t, J = 7.0 Hz, 3H). ^{13}C NMR (68 MHz, DMSO-d_6): δ 163.6, 163.2, 160.05, 152.2, 152.0, 150.3, 137.0, 132.1, 128.7, 128.1, 127.9, 106.4, 104.2, 103.2, 69.55, 60.2, 14.3. ES-MS (methanol) m/z: 496.2 [M+H]$^+$, 518.2 [M+Na]$^+$, 534.2 [M+K]$^+$.

General procedure for the synthesis of the N^5-substituted 2-aryl-5-amino-8-ethoxycarbonyl-[1,2,4]triazolo[1,5-*c*]pyrimidine derivatives (**11**–**14**,**110**).

Compounds **98**,**102**–**104** (0.5 mmol) were dissolved in 4 mL of ethanol and reacted with 1.5 mmol of the required amine, heating at 90 °C for 3–12 h in a sealed tube. Once the reaction was completed, the solvent was evaporated and the crude products purified through flash chromatography.

*ethyl 5-((3,4-dimethoxybenzyl)amino)-2-phenyl-[1,2,4]triazolo [1,5-c]pyrimidine-8-carboxylate (**11**):* flash chromatography eluent: light petroleum-EtOAc 8:2. Yield 38% (82 mg); white solid; mp 163–166 °C (EtOEt-light petroleum). ^{1}H NMR (270 MHz, DMSO-d_6): δ 9.41 (t, J = 6.1 Hz, 1H), 8.58 (s, 1H), 8.39–8.13 (m, 2H), 7.70–7.42 (m, 3H), 7.08 (s, 1H), 6.95 (d, J = 7.9Hz, 1H), 6.88 (d, J = 7.9 Hz, 1H), 4.75 (d, J = 6.1 Hz, 2H), 4.34 (q, J = 6.8 Hz, 2H), 3.73 (s, 3H), 3.71 (s, 3H), 1.35 (t, J = 6.8 Hz, 3H). ^{13}C NMR (68 MHz, DMSO-d_6): δ 163.9, 163.2, 151.87, 151.7, 148.8, 148.5, 148.3, 130.9, 130.1, 129.1, 127.4, 120.0, 111.9, 103.4, 60.3, 55.6, 55.51, 43.9, 14.25. ES-MS (methanol) m/z: 434.1 [M+H]$^+$, 456.1 [M+Na]$^+$, 472.0 [M+K]$^+$. MW 433.46. $C_{23}H_{23}N_5O_4$. HRMS (ESI-TOF) m/z: $C_{23}H_{23}N_5O_4$ experimental 434.1825 [M+H]$^+$, theoretical 434.1822 [M+H]$^+$, Δ = 0.0003. Purity HPLC (Method A): 99.4%.

*ethyl 5-((3,4-dimethoxybenzyl)amino)-2-(4-fluorophenyl)-[1,2,4] triazolo[1,5-c]-8-carboxylate (**12**):* flash chromatography eluent: light petroleum-EtOAc 8:2. Yield 73% (165 mg); white solid; mp 156 °C (EtOEt-light petroleum). ^{1}H NMR (400 MHz, DMSO-d_6): δ 9.42 (bs, 1H), 8.58 (s, 1H), 8.29 (m, 2H), 7.43 (t, $J_{H,HF}$ = 8.4 Hz, 2H), 7.07 (s, 1H), 6.94 (d, J = 8.0 Hz, 1H), 6.88 (d, J = 8.0 Hz, 1H), 4.74 (d, J = 5.5 Hz, 2H), 4.34 (q, J = 6.8 Hz, 2H), 3.73 (s, 3H), 3.71 (s, 3H), 1.35 (t, J = 6.8 Hz, 3H). ^{13}C NMR (68 MHz, DMSO-d_6): δ 163.85 (d, J_{CF} = 247.3 Hz), 163.16, 163.05, 151.95, 151.81, 148.85, 148.45, 148.29, 130.82, 129.72 (d, J_{CF} = 8.7 Hz), 126.70 (d, J_{CF} = 2.7 Hz), 119.96, 116.21 (d, J_{CF} = 22.1 Hz), 111.92, 111.82, 103.40, 60.29, 55.56, 55.51, 43.91, 14.24. ES-MS (methanol) m/z: 452.1 [M+H]$^+$, 474.1 [M+Na]$^+$, 490.0 [M+K]$^+$. HRMS (ESI-TOF) m/z: $C_{23}H_{22}FN_5O_4$ experimental 452.1722 [M+H]$^+$, theoretical 452.1728 [M+H]$^+$, Δ = 0.0006. Purity HPLC (Method A): 97.3%.

*ethyl 5-(benzylamino)-2-(3-methoxyphenyl)-[1,2,4]triazolo[1,5-c]-8-carboxylate (**13**):* flash chromatography eluent: DCM-methanol 98.5:1.5. Yield 74% (149 mg); white solid; mp 159–160 °C (EtOEt-light petroleum). ^{1}H NMR (400 MHz, DMSO-d_6): δ 9.48 (s, 1H), 8.54 (s, 1H), 7.97–7.73 (m, 2H), 7.58–7.23 (m, 6H), 7.19–7.05 (m, 1H), 4.81 (s, 2H), 4.32 (q, J = 7.1 Hz, 2H), 3.84 (s, 3H), 1.33 (t, J = 7.1 Hz, 3H). ^{13}C NMR (101 MHz, DMSO-d_6): δ 164.03, 163.36, 159.99, 152.05, 151.91, 148.81, 138.82, 131.70, 130.62, 128.79, 127.86, 127.56, 120.07, 116.97, 112.62, 103.87, 60.82, 55.69, 44.50, 14.68. ES-MS (methanol) m/z: 404.2 [M+H]$^+$, 426.1 [M+Na]$^+$. HRMS (ESI-TOF) m/z: $C_{22}H_{21}N_5O_3$ experimental 404.1716 [M+H]$^+$, theoretical 404.1717 [M+H]$^+$, Δ = 0.0001. Purity HPLC (Method A): 98.5%.

*ethyl 5-(([1,1′-biphenyl]-4-ylmethyl)amino)-2-(3-methoxyphenyl)-[1,2,4]triazolo[1,5-c]-8-carboxylate (**14**):* flash chromatography eluent: DCM-methanol 99:1. Yield 68% (163 mg); white solid; mp 160 °C (EtOEt-light petroleum). ^{1}H NMR (270 MHz, DMSO-d_6): 9.52 (s, 1H), 8.56 (s, 1H), 7.98–7.73 (m, 2H), 7.71–7.29 (m, 10H), 7.21–7.05 (m, 1H), 4.85 (s, 2H), 4.32 (q, J = 7.1 Hz, 2H), 3.85 (s, 3H), 1.33 (t, J = 7.1 Hz, 3H). ^{13}C NMR (101 MHz, DMSO-d_6): δ 164.03, 163.39, 162.69, 160.25, 157.51, 151.93, 148.75, 138.07, 131.77, 131.19, 129.35, 128.52, 127.13, 127.03, 121.74, 117.03, 114.32, 112.60, 110.08, 104.00, 60.74, 55.57, 49.29, 14.82. ES-MS (methanol) m/z: 480.2 [M+H] $^+$, 502.2 [M+Na] $^+$. HRMS (ESI-TOF) m/z: $C_{28}H_{25}N_5O_3$ experimental 502.1852 [M+Na]$^+$, theoretical 502.1849 [M+Na]$^+$, Δ = 0.0003. Purity HPLC (Method A): 99.0%.

*ethyl 5-(methylamino)-2-(3-(benzyloxy)phenyl)-[1,2,4]triazolo [1,5-c]-8-carboxylate (**110**)*: flash chromatography eluent: light petroleum-EtOAc 8:2. Yield 29% (58 mg); white solid; mp

174–175 °C (EtOEt-light petroleum). ^{1}H NMR (400 MHz, DMSO-d_6): 8.85 (s, 1H), 8.57 (s, 1H), 7.96–7.76 (m, 2H), 7.61–7.26 (m, 6H), 7.26–7.12 (m, 1H), 5.20 (s, 2H), 4.33 (q, J = 7.1 Hz, 2H), 3.10 (s, 3H), 1.34 (t, J = 7.1 Hz, 3H). ^{13}C NMR (68 MHz, DMSO-d_6): δ 163.4, 163.1, 158.7, 151.7, 151.5, 148.6, 136.9, 131.4, 130.2, 128.5, 128.0, 127.7, 119.8, 117.2, 113.4, 102.9, 69.4, 60.3, 27.9, 14.4. ES-MS (methanol) m/z: 404.2 $[M+H]^+$, 426.1 $[M+Na]^+$.

General procedure for the removal of the 3,4-dimethoxybenzyl group (**15**–**16**).

To 0.2 mol of compounds **11** and **12**, TFA (1 mL), anisole (0.8 mmol) and trifluoromethanesulfonic acid (HOTf) (0.8 mmol) were added at 0 °C and the reaction proceeded for 12 h at room temperature. The solvent was evaporated, DCM added (15 mL), and washed with three aliquots of water (5 mL). After drying the organic phase over anhydrous sodium sulfate, the solvent is evaporated and the residue purified by flash chromatography.

*ethyl 5-amino-2-phenyl-[1,2,4]triazolo[1,5-c]pyrimidine-8-carboxylate (**15**):* flash chromatography eluent: DCM-EtOAc from 9:1 to 8:2. Yield 22% (12 mg); white solid; mp 195–198 °C (EtOEt-light petroleum). ^{1}H NMR (400 MHz, DMSO-d_6): δ 8.98 (bs, 1H), 8.52–8.33 (m, 2H), 8.25 (m, 2H), 7.58 (m, 3H), 4.34 (q, J = 7.1 Hz, 2H), 1.35 (t, J = 7.1 Hz, 3H). ^{13}C NMR (68 MHz, $CDCl_3$): δ 163.90, 163.20, 152.20, 152.07, 150.29, 130.84, 130.17, 129.08, 127.39, 103.14, 60.22, 14.26. ES-MS (methanol) m/z: 284.0 $[M+H]^+$, 305.9 $[M+Na]^+$, 321.9 $[M+K]^+$. HRMS (ESI-TOF) m/z: $C_{14}H_{13}N_5O_2$ experimental 309.0962 $[M+Na]^+$, theoretical 306.0961 $[M+Na]^+$, Δ = 0.0001. Purity HPLC (Method A): 99.0%.

*ethyl 5-amino-2-(4-fluorophenyl)-[1,2,4]triazolo[1,5-c]pyrimidine-8-carboxylate (**16**):* flash chromatography eluent: DCM-EtOAc from 9:1 to 8:2. Yield 73% (44.0 mg); pale pink solid; mp 263 °C (EtOEt-light petroleum). ^{1}H NMR (400 MHz, DMSO-d_6): δ 8.99 (bs, 1H), 8.61–8.37 (m, 2H), 8.28 (dd, J = 8.8 Hz, J_{HF} = 5.6 Hz, 2H), 7.43 (t, $J_{H,HF}$ = 8.8 Hz, 2H), 4.33 (q, J = 7.1 Hz, 2H), 1.35 (t, J = 7.1 Hz, 3H). ^{13}C NMR (68 MHz, DMSO-d_6): δ 163.84 (d, J_{CF} = 247.5 Hz), 163.19, 163.06, 152.29, 152.14, 150.29, 129.70 (d, J_{CF} = 8.8 Hz), 126.76 (d, J_{CF} = 1.2 Hz), 116.19 (d, J_{CF} = 22.0 Hz), 103.12, 60.22, 14.26. ES-MS (methanol) m/z: 323.9 $[M+Na]^+$. HRMS (ESI-TOF) m/z: $C_{14}H_{12}FN_5O_2$ experimental 302.1043 $[M+H]^+$, theoretical 302.1047 $[M+H]^+$, Δ = 0.0004. Purity HPLC (Method A): 95.0%.

General procedure for the removal of benzyl group (17–21) and the reduction of nitro group to amine (22).

To a stirred suspension of compounds **6**,**9**,**107**–**110** (0.2 mmol) and an equal weight of 10% Pd–C in dry methanol (10 mL), ammonium formate (2 mmol) was added in a single portion. The resulting reaction mixture was stirred under argon atmosphere at 60 °C for 3–12 h. Once completed, the catalyst was removed by filtration through a Celite pad, which was then washed with methanol. The solvent was evaporated under reduced pressure and the crude product dissolved in EtOAc (50 mL) and washed with water (3 × 15 mL). Finally, the organic phase was dried over anhydrous sodium sulfate, the solvent evaporated under *vacuum* and, if necessary, the residue purified by flash chromatography or precipitated with EtOEt and light petroleum to afford the desired derivatives.

*ethyl 5-amino-2-(4-hydroxyphenyl)-[1,2,4]triazolo[1,5-c]pyrimidine-8-carboxylate (**17**):* flash chromatography eluent: DCM-methanol from 98:2 to 95:5. Yield 72% (43 mg); white solid; mp > 300 °C (EtOEt-light petroleum). ^{1}H NMR (400 MHz, DMSO-d_6): δ 10.01 (bs, 1H), 8.89 (bs, 1H), 8.50–8.19 (m, 2H), 8.07 (d, J = 7.7 Hz, 2H), 6.93 (d, J = 7.7 Hz, 2H), 4.33 (q, J = 6.3 Hz, 2H), 1.35 (t, J = 6.3 Hz, 3H). ^{13}C NMR (68 MHz, DMSO-d_6): δ 164.2, 163.3, 160.0, 152.00, 151.9, 150.2, 129.15, 120.9, 115.8, 102.9, 60.2, 14.3. ES-MS (methanol) m/z: 322.1 $[M+Na]^+$, 338.0 $[M+K]^+$. HRMS (ESI-TOF) m/z: $C_{14}H_{13}N_5O_3$ experimental 300.1088 $[M+H]^+$, theoretical 300.1091 $[M+H]^+$, Δ = 0.0003. Purity HPLC (Method A): 95.1%.

*ethyl 5-amino-2-(3-hydroxyphenyl)-[1,2,4]triazolo[1,5-c]pyrimidine-8-carboxylate (**18**):* flash chromatography eluent: DCM-methanol 98:2. Yield 51% (30 mg); white solid; mp 282–284 °C (EtOEt-light petroleum). ^{1}H NMR (400 MHz, DMSO-d_6): δ 9.76 (s, 1H), 8.97 (bs, 1H), 8.64–8.25 (m, 2H), 7.76–7.63 (m, 2H), 7.36 (t, J = 8.1 Hz, 1H), 7.02–6.85 (m, 1H), 4.34 (q, J = 7.1 Hz, 2H), 1.36 (t, J = 7.1 Hz, 3H). ^{13}C NMR (68 MHz, DMSO-d_6): δ 164.0, 163.2, 157.9, 152.1, 152.0, 150.3, 131.4, 130.1, 118.2, 117.8, 114.25, 103.1, 60.2, 14.3. ES-MS (methanol) m/z: 299.8 $[M+H]^+$, 321.8 $[M+Na]^+$, 337.8 $[M+K]^+$. HRMS (ESI-TOF) m/z: $C_{14}H_{13}N_5O_3$ experimental 300.1098 $[M+H]^+$, theoretical 300.1091 $[M+H]^+$, Δ = 0.0007. Purity HPLC (Method A): 86.4%.

*ethyl 5-amino-2-(3,5-bis(hydroxy)phenyl)-[1,2,4]triazolo[1,5-c]pyrimidine-8 carboxylate (**19**):* yield 54% (34 mg); white solid; mp 255–260 °C (EtOEt-light petroleum). ^{1}H NMR (270 MHz, DMSO-d_6): 9.55 (bs, 2H), 8.50 (m, 3H), 7.20–7.11 (m, 2H), 6.36 (m, 1H), 4.33 (q, J = 7.1 Hz, 2H), 1.35 (t, J = 7.1 Hz, 3H). ^{13}C NMR (68 MHz, DMSO-d_6): δ 164.3, 163.2, 158.95, 152.1, 151.8, 150.2, 131.7, 105.7, 104.95, 103.1, 60.2, 14.3. ES-MS (methanol) m/z: 316.1 $[M+H]^+$, 338.0 $[M+Na]^+$. HRMS (ESI-TOF) m/z: $C_{14}H_{13}N_5O_4$ experimental 338.0857 $[M+Na]^+$, theoretical 338.0859 $[M+Na]^+$, Δ = 0.0002. Purity HPLC (Method A): 98.0%.

*ethyl 5-amino-2-(3,4-bis(hydroxy)phenyl)-[1,2,4]triazolo[1,5-c]pyrimidine-8 carboxylate (**20**):* yield 64% (40 mg); white solid; mp 270–272 °C (EtOEt-light petroleum). ^{1}H NMR (400 MHz, DMSO-d_6): δ 9.50–8.80 (m, 3H), 8.50–8.25 (m, 2H), 7.68 (s, 1H), 7.60–7.53 (m, 1H), 6.88 (d, J = 8.2 Hz, 1H), 4.33 (q, J = 7.1 Hz, 2H), 1.35 (t, J = 7.1 Hz, 3H). ^{13}C NMR (68 MHz, DMSO-d_6): δ 164.1, 163.0, 151.68, 151.57, 149.9, 148.0, 145.4, 121.1, 119.2, 115.8, 114.8, 102.8, 60.1, 14.3. ES-MS (methanol) m/z: 316.1 $[M+H]^+$, 338.1 $[M+Na]^+$. HRMS (ESI-TOF) m/z: $C_{14}H_{13}N_5O_4$ experimental 316.1036 $[M+H]^+$, theoretical 316.1040 $[M+H]^+$, Δ = 0.0004. Purity HPLC (Method A): 99.4%.

*ethyl 5-methylamino-2-(3-hydroxyphenyl)-[1,2,4]triazolo[1,5-c]pyrimidine-8-carboxylate (**21**):* yield 66%; white solid (41 mg); mp 234 °C (EtOEt-light petroleum). ^{1}H NMR (400 MHz, DMSO-d_6): δ 9.73 (s, 1H), 8.81 (bs, 1H), 8.56 (s, 1H), 7.75–7.61 (m, 2H), 7.34 (t, J = 8.1 Hz, 1H), 6.98–6.84 (m, 1H), 4.33 (q, J = 7.1 Hz, 2H), 3.10 (s, 3H), 1.34 (t, J = 7.1 Hz, 3H). ^{13}C NMR (68 MHz, DMSO-d_6) δ 163.0, 157.7, 153.9, 153.1, 151.5, 148.6, 131.1, 129.9, 117.9, 117.6, 114.0, 102.9, 60.2, 27.9, 14.3. ES-MS (methanol) m/z: 314.1 $[M+H]^+$, 336.1 $[M+Na]^+$. HRMS (ESI-TOF) m/z: $C_{15}H_{15}N_5O_3$ experimental 314.1251 $[M+H]^+$, theoretical 314.1247 $[M+H]^+$, Δ = 0.0004. Purity HPLC (Method A): 97.6%.

*ethyl 5-amino-2-(3-aminophenyl)-[1,2,4]triazolo[1,5-c]pyrimidine-8 carboxylate (**22**):* flash chromatography eluent: DCM-methanol 95:5. Yield 65% (39 mg); white solid; mp 245–250 °C (EtOEt-light petroleum). ^{1}H NMR (270 MHz, DMSO-d_6): δ 8.97–8.50 (m, 3H), 7.49 (s, 1H), 7.41 (d, J = 7.3 Hz, 1H), 7.18 (t, J = 7.9 Hz, 1H), 6.76–6.72 (m, 1H), 5.37 (s, 2H), 4.33 (q, J = 7.0 Hz, 2H), 1.35 (t, J = 7.0 Hz, 3H). ^{13}C NMR (68 MHz, DMSO-d_6): δ 164.74, 163.21, 151.99, 151.83, 150.24, 149.28, 130.67, 129.42, 116.20, 115.01, 112.83, 103.08, 60.18, 14.30. ES-MS (methanol) m/z: 299.1 $[M+H]^+$, 321.1 $[M+Na]^+$. HRMS (ESI-TOF) m/z: $C_{14}H_{14}N_6O_2$ experimental 299.1252 $[M+H]^+$, theoretical 299.1251 $[M+H]^+$, Δ = 0.0001. Purity HPLC (Method A): 98.8%.

General procedure for the synthesis of 2,5-disubstitited-[1,2,4]triazolo[1,5-*c*]pyrimidine-8-carboxylic acids (**23**,**111**–**113**).

A solution of boron tribromide (1 M in DCM, 12 equivalents) was slowly added to a cooled (−78 °C) solution of methoxy-derivatives **7**,**10**,**13**–**14** (1 equivalent) in DCM (5 mL/mmol of methoxy-derivatives) under argon atmosphere. The cooling bath was removed and the suspension was slowly warmed up to room temperature and stirred for 12 h. Once completed, an equal volume of cool methanol was added dropwise and the solution stirred for 15 min. Then the volatile species were removed under *vacuum*, thus

giving the corresponding carboxylic acids derivatives (**23**,**111**–**113**) that were suspended in methanol and filtered. Compounds **112**–**113** were obtained starting from 0.25 mmol of compounds **13** and **14** and immediately used in the next step without any characterization.

*5-amino-2-(3-hydroxyphenyl)-[1,2,4]triazolo[1,5-c]pyrimidine-8-carboxylic acid (**23**):*. Yield 92% (62 mg from 0.25 mmol of **7**); white solid; mp 290–295 °C. ^{1}H NMR (400 MHz, DMSO-D6) δ 12.69 (bs, 1H), 9.81 (s, 1H), 8.58 (bm, 3H), 7.89–7.53 (m, 2H), 7.34 (t, J = 7.9 Hz, 1H), 6.94 (d, J = 8.0 Hz, 1H). ^{13}C NMR (68 MHz, DMSO) δ 164.63, 163.85, 157.97, 152.20, 152.17, 150.15, 131.25, 130.17, 118.21, 117.88, 114.32, 103.65. ES-MS (methanol) m/z: 272.0 $[M+H]^+$, 294.0 $[M+Na]^+$. HRMS (ESI-TOF) m/z: $C_{12}H_9N_5O_3$ experimental 272.0776 $[M+H]^+$, theoretical 272.0778 $[M+H]^+$, Δ = 0.0002. Purity HPLC (Method A): 91.5%.

*5-amino-2-(3,5-dihydroxyphenyl)-[1,2,4]triazolo[1,5-c]pyrimidine-8-carboxylic acid (**111**)*: Yield: 98% (320 mg from 391 mg of **10**); grey solid. ^{1}H NMR (400 MHz, DMSO) δ 9.19–8.05 (m, 3H), 7.16 (d, J = 2.1 Hz, 2H), 6.35 (t, J = 2.1 Hz, 1H). ES-MS negative (methanol) m/z 286.0 $[M-H]^-$.

Synthesis of N^5-substituted ethyl 2-(3-hydroxyphenyl)-5-amino-[1,2,4]triazolo[1,5-*c*]pyrimidine-8-carboxylates **24**–**25**.

Carboxylic acids **112**–**113** (0.25 mmol) were reacted with thionyl chloride (1 mmol) and DMF (catalytic) in chloroform at reflux for 5 h. Then, the volatile species were removed under reduced pressure, the crude product was suspended in ethanol, and triethylamine was added (0.375 mmol), then the reaction was stirred at room temperature overnight. When completed, the solvent was removed under reduced pressure and the product purified by flash chromatography.

*ethyl 5-(benzylamino)-2-(3-hydroxyphenyl)-[1,2,4]triazolo[1,5-c] pyrimidine-8-carboxylate (**24**):* flash chromatography eluent: DCM-methanol 98.5:1.5. Yield 13% (12 mg); white solid; mp 219–220 °C (EtOEt-light petroleum). ^{1}H NMR (400 MHz, DMSO-d_6): δ 9.72 (s, 1H), 9.44 (s, 1H), 8.54 (s, 1H), 7.77–7.63 (m, 2H), 7.44–7.18 (m, 6H), 6.99–6.84 (m, 1H), 4.81 (s, 2H), 4.32 (q, J = 7.1 Hz, 2H), 1.33 (t, J = 7.1 Hz, 3H). ^{13}C NMR (101 MHz, DMSO-d_6): δ 164.3, 163.3, 158.1, 151.97, 151.82, 148.8, 138.8, 131.6, 130.4, 128.8, 127.8, 127.5, 118.4, 118.1, 114.6, 103.9, 60.7, 14.7. ES-MS (methanol) m/z: 390.1 $[M+H]^+$, 412.1 $[M+Na]^+$. HRMS (ESI-TOF) m/z: $C_{21}H_{19}N_5O_3$ experimental 390.1563 $[M+H]^+$, theoretical 390.1560 $[M+H]^+$, Δ = 0.0003. Purity HPLC (Method A): 99.7%.

*ethyl 5-(([1,1′-biphenyl]-4-ylmethyl)amino)-2-(3-hydroxyphenyl)-[1,2,4]triazolo[1,5-c] pyrimidine-8 carboxylate (**25**):* flash chromatography eluent: DCM-methanol 99.5:0.5. Yield 20% (23 mg); white solid; mp 227–229 °C (EtOEt-light petroleum). ^{1}H NMR (400 MHz, DMSO-d_6): δ 9.72 (s, 1H), 9.48 (s, 1H), 8.55 (s, 1H), 7.69 (s, 2H), 7.66–7.57 (m, 4H), 7.54–7.30 (m, 6H), 6.97–6.88 (m, 1H), 4.85 (s, 2H), 4.32 (q, J = 7.1 Hz, 2H), 1.33 (t, J = 7.1 Hz, 3H). ^{13}C NMR (68 MHz, DMSO-d_6): δ 163.8, 162.9, 157.7, 151.5, 151.35, 139.9, 139.8, 139.0, 137.6, 131.1, 129.9, 128.9, 128.0, 126.7, 126.6, 118.0, 117.7, 115.9, 114.1, 103.4, 60.2, 14.3. ES-MS (methanol) m/z: 465.9 $[M+H]^+$, 487.9 $[M+Na]^+$. HRMS (ESI-TOF) m/z: $C_{27}H_{23}N_5O_3$ experimental 488.1696 $[M+Na]^+$, theoretical 488.1693 $[M+Na]^+$, Δ = 0.0003. Purity HPLC (Method A): 95.6%.

General procedure for the synthesis of 5-amino-*N*-ethyl-2-substituted-[1,2,4]triazolo[1,5-*c*]pyrimidine-8-carboxamides (**26**–**27**).

The mixture of 100 mg of carboxylic acids **23**,**111** (0.37 mmol) dissolved in 2 mL of dry pyridine and 2 mL of dry THF was cooled to 0 °C and 0.405 mL (5.55 mmol) of thionyl chloride were added dropwise. The reaction was then allowed to warm up to 10 °C, and 2.78 mL of ethylamine 2 M in THF were added (5.55 mmol). The mixture was left to reach room temperature and stirred for 24 h. When the reaction was terminated, the pyridine was removed under reduced pressure, water (10 mL) and a saturated solution of sodium carbonate (10 mL) were added to the mixture and the product was extracted with EtOAc (5 × 5 mL). The organic layers were dried over anhydrous sodium sulfate and the compounds were concentrated under *vacuum*. The residues were purified with flash chromatography (ethyl acetate for compound **26** and ethyl acetate and dichloromethane 10% for compound **27**). Finally, the product was filtered to obtain white solids.

*5-amino-N-ethyl-2-(3-hydroxyphenyl)-[1,2,4]triazolo[1,5-c]pyrimidine-8-carboxamide (**26**):*Yield 9% (10 mg); white solid; mp 170–175 °C (EtOEt-light petroleum). ^{1}H NMR (400 MHz, DMSO-d_6): δ 9.80 (s, 1H), 8.99–8.13 (m, 4H), 7.79–7.74 (m, 2H), 7.38 (t, J = 7.6 Hz, 1H), 6.96 (d, J = 7.6 Hz, 1H), 3.48–3.41 (m, 2H), 1.23 (t, J = 6.5 Hz, 3H). ^{13}C NMR (68 MHz, DMSO-d_6): δ 174.4, 163.9, 162.9, 161.9, 157.9, 151.9, 149.41, 130.7, 118.3, 114.2, 108.3, 105.1, 33.7, 15.0. ES-MS (methanol) m/z: 299.1 $[M+H]^+$, 321.1 $[M+Na]^+$. HRMS (ESI-TOF) m/z: $C_{14}H_{14}N_6O_2$ experimental 321.1069 $[M+Na]^+$, theoretical 321.1070 $[M+Na]^+$, Δ = 0.0001. Purity HPLC (Method A): 97.2%.

*5-amino-2-(3,5-dihydroxyphenyl)-N-ethyl-[1,2,4]triazolo[1,5-c] pyrimidine-8-carboxamide (**27**):* Yield: 2,9% (3,2 mg); white solid; mp 258 d °C (EtOEt-methanol). ^{1}H NMR (400 MHz, DMSO-d_6) δ 9.57 (s, 2H), 8.98–8.00 (m, 4H), 7.16 (d, J = 2.2 Hz, 2H), 6.40 (t, J = 2.2 Hz, 1H), 3.48–3.38 (m, 2H), 1.23 (t, J = 7.2 Hz, 3H). ^{13}C NMR (101 MHz, CD_3OD) δ 163.97, 163.39, 158.59, 151.72, 149.64, 149.37, 131.10, 105.84, 105.01, 104.69, 33.99, 13.71. ES-MS (methanol) m/z 315.2 $[M+H]^+$, 337.1 $[M+Na]^+$. ES-MS negative (methanol) m/z 313.1 $[M-H]^-$. HRMS (ESI-TOF) m/z: $C_{14}H_{14}N_6O_3$ experimental 337.1017 $[M+Na]^+$, theoretical 337.1019 $[M+Na]^+$, Δ = 0.0002.

General procedure for the synthesis of *tert*-butyl (2-(5-amino-2-substituted-[1,2,4]triazolo[1,5-*c*]pyrimidine-8-carboxamido)ethyl) carbamate (**28**–**29**).

To carboxylic acid derivatives **23**,**111** (0.37 mmol) in chloroform (3 mL), and a catalytic amount of DMF (20 μL), thionyl chloride (0.107 mL, 1.48 mmol) was added at 0 °C. The mixture was heated under reflux for 5 h and under an argon atmosphere. The solvent was removed under reduced pressure to yield the corresponding chloride derivative (yellowish oil) which was immediately dissolved in THF (3 mL). The mixture was then cooled to 0 °C and an equimolar amount of triethylamine (0.051 mL, 0.37 mmol) was added to the solution; afterward, *tert*-butyl 2-aminoethylcarbamate (118 mg, 0.74 mmol) was added slowly. The solution was allowed to warm to room temperature and stirred overnight. Once completed, the solvent was then removed under reduced pressure and the residue was suspended in EtOAc (30 mL) and washed with water (3 × 10 mL). The organic phase was then dried over anhydrous sodium sulfate and concentrated at reduced pressure. The crude residue was purified with flash chromatography with methanol 2% in ethyl acetate affording compounds **28**–**29** as solids.

*tert-butyl (2-(5-amino-2-(3-hydroxyphenyl)-[1,2,4]triazolo[1,5-c] pyrimidine-8-carboxamido)ethyl)carbamate (**28**):* Yield 19% (29 mg); white solid; mp 220–223 °C (EtOEt-light petroleum). ^{1}H NMR (400 MHz, DMSO-d_6): δ 9.78 (s, 1H), 8.79 (s, 1H), 8.46 (s, 1H), 7.77 (d, J = 7.8 Hz, 1H), 7.70 (s, 1H), 7.36 (t, J = 7.9 Hz, 1H), 7.03–6.94 (m, 2H), 3.47 (d, J = 5.4 Hz, 2H), 3.16 (d, J = 5.6 Hz, 2H), 1.31 (m, 11H). ES-MS (methanol) m/z: 436.1 $[M+Na]^+$. HRMS (ESI-TOF) m/z: $C_{19}H_{23}N_7O_4$ experimental 436.1707 $[M+Na]^+$, theoretical 436.1703 $[M+Na]^+$, Δ = 0.0004. Purity HPLC (Method A): 91.2%.

*tert-butyl (2-(5-amino-2-(3,5-dihydroxyphenyl)-[1,2,4]triazolo [1,5-c]pyrimidine-8-carboxamido)ethyl)carbamate (**29**):* Yield 10% (16 mg); white solid; mp 232 d °C (EtOEt-methanol). ^{1}H NMR (400 MHz, CD_3OD) δ 8.55 (s, 1H), 7.28 (d, J = 2.2 Hz, 2H), 6.43 (t, J = 2.2 Hz, 1H), 3.60 (t, J = 6.0 Hz, 2H), 3.40–3.30 (m, 2H), 1.34 (s, 9H); ^{13}C NMR (101 MHz, CD_3OD) δ 197.78, 172.98, 166.01, 163.92, 160.02, 153.14, 151.11 (CH), 150.92, 107.43 (CH), 106.47, 106.09 (CH),

61.53, 41.10 (2xCH_2), 28.63 (3xCH_3). ES-MS (methanol) *m/z* 452.1 $[M + Na]^+$. HRMS (ESI-TOF) (negative) *m/z*: $C_{19}H_{23}N_7O_5$ experimental 428.1685 $[M - H]^+$, theoretical 428.1687 $[M - H]^+$, $\Delta = 0.0003$. Purity HPLC (Method A): 97.4%.

General procedure for the synthesis of 5-amino-*N*-(2-aminoethyl)-2-substituted-[1,2,4]triazolo[1,5-*c*]pyrimidine-8-carboxamide, trifluoroacetate salts (**30**–**31**).

The *N*-BOC derivatives **28**–**29** were suspended in a 10% solution of trifluoroacetic acid in DCM (2 mL every 0.5 mmol) and stirred at room temperature for 2 h. Once completed, the solvent was removed under reduced pressure and the residue precipitated from EtOAc-light petroleum to give the desired trifluoroacetate salts **30**–**31**.

*5-amino-N-(2-aminoethyl)-2-(3-hydroxyphenyl)-[1,2,4]triazolo [1,5-c]pyrimidine-8-carboxamide, trifluoroacetate salt (**30**):* Yield 95% (20 mg from 0.05 mol of **28**); white solid; mp 210–212 °C (EtOEt-light petroleum). ^{1}H NMR (270 MHz, DMSO-d_6): δ 9.84 (bs, 1H), 8.93–8.40 (m, 4H), 7.80 (m, 5H), 7.38 (m, 1H), 6.98 (s, 1H), 3.78–3.55 (m, 2H), 3.17–2.92 (m, 2H). ^{13}C NMR (68 MHz, DMSO-d_6): δ 163.0, 162.8, 157.7, 151.6, 150.0, 149.3, 130.5, 129.9, 118.4, 118.0, 114.3, 104.7, 56.4, 37.0. ES-MS (methanol) *m/z*: 314.1 $[M+H]^+$, 336.0 $[M+Na]^+$. HRMS (ESI-TOF) *m/z*: $C_{14}H_{15}N_7O_2$ experimental 314.1356 $[M+H]^+$, theoretical 314.1359 $[M+H]^+$, $\Delta = 0.0003$. Purity HPLC (Method A): 98.5%.

*5-amino-N-(2-aminoethyl)-2-(3,5-dihydroxyphenyl)-[1,2,4]triazolo[1,5-c]pyrimidine-8-carboxamide, trifluoroacetate salt (**31**):* Yield: 34%; (8 mg from 0.07 mol of **29**) white solid. ^{1}H NMR (400 MHz, dmso) δ 9.59 (s, 2H), 9.05–8.12 (m, 4H), 7.83 (bs, 3H), 7.20 (d, $J = 2.1$ Hz, 2H), 6.44 (t, $J = 2.1$ Hz, 1H), 3.76–3.57 (m, 2H), 3.14–2.98 (m, 2H). ^{13}C NMR (101 MHz, DMSO) δ 163.45, 159.10, 151.75, 149.76, 144.73, 134.33, 131.28, 106.11, 105.15, 39.34, 37.46. ES-MS (methanol) *m/z* 330.1 $[M+H]^+$. HRMS (ESI-TOF) *m/z*: $C_{14}H_{15}N_7O_3$ experimental 330.1306 $[M+H]^+$, theoretical 330.1309 $[M+H]^+$, $\Delta = 0.0003$. Purity HPLC (Method A): 95.1%.

*Synthesis of 2,5,7-trisubstituted [1,2,4]triazolo[1,5-c]pyrimidines (**32**–**37**).*

Synthesis of 2-amino-4,6-dichloro-pyrimidine (**115**).

To 10 g of 2-amino-4,6-dihydroxy-pyrimidine **114** (79 mmol) in 40 mL of acetonitrile, 22 mL of triethylamine were added (158 mmol) followed by the dropwise addition of 14.7 mL of phosphorous oxychloride (158 mmol). The solution was refluxed for 1 h, cooled to room temperature and ice was added. The resulting brown solid was filtered, washed with cold water to afford 12.9 g of a brown solid directly reacted in the subsequent step.

Synthesis of *N'*-(2-amino-6-chloropyrimidin-4-yl)- benzohydrazides (**116**–**117**).

4 g of 2-amino-4,6-dichloro-pyrimidine (**115**, 25 mmol) were reacted with appropriated benzohydrazides (**68,71**, 29 mmol) and DBU (5.05 mL, 34 mmol) in 40 mL of THF. The solution was stirred at room temperature overnight. After evaporation of the solvent under *vacuum*, the mixture was suspended with 300 mL of EtOAc and washed with three aliquots of water (3 × 100 mL). Then, the organic phase was dried over anhydrous sodium sulfate, concentrated and purified by flash chromatography, and the product obtained as a white solid (1.32 g).

*N'-(2-amino-6-chloropyrimidin-*4-yl*)-3-methoxybenzohydrazide (**116**):* flash chromatography eluent: dichloromethane-methanol from 98:2 to 95:5). Yield 18% (1.32 g); white solid; mp 253 °C (EtOEt-light petroleum). ^{1}H NMR (270 MHz, DMSO-d_6): δ 10.45 (s, 1H), 9.09 (s, 1H), 7.45 (m, 3H), 7.15 (d, $J = 8.0$ Hz, 1H), 6.64 (s, 2H), 5.80 (bs, 1H), 3.82 (s, 3H). ES-MS (methanol) *m/z*: 294.1 $[M+H]^+$.

*N'-(2-amino-6-chloropyrimidin-*4-yl*)-3,5-dimethoxybenzohydrazide (**117**):* flash chromatography eluent: EtOAc. Yield: 44% (3.6 g); white solid; mp 200 °C (EtOAc). ^{1}H NMR (400 MHz, DMSO) δ 10.41 (bs, 1H), 9.07 (bs, 1H), 7.07 (d, $J = 2.1$ Hz, 2H), 6.70 (s, 1H), 6.62 (bs, 2H), 5.79 (bs, 1H), 3.80 (s, 6H). ES-MS (methanol) *m/z* 324.1 $[M+H]^+$.

General procedure for the synthesis of 7-chloro-2-substituted-[1,2,4]triazolo[1,5-*c*]pyrimidine-5-amines (**118**–**119**).

7 mmol of *N'*-(2-amino-6-chloropyrimidin-4-yl)-benzohydrazide (**116**–**117**) in 270 mmol of BSA (bis(trimethylsilyl)acetamide, (69.5 mL) are refluxed under argon atmosphere for 12 h. When the starting material was consumed, 40 mL of ice methanol were added slowly keeping the temperature near 0 °C, and then the volatile species were removed under vacuum. The crude material, dissolved in dichloromethane (200 mL), was washed with water (3 × 65 mL). The organic phase was dried over anhydrous sodium sulfate, concentrated under reduced pressure and the mixture purified by flash chromatography.

*7-chloro-2-(3-methoxyphenyl)-[1,2,4]triazolo[1,5-c]pyrimidine-5-amine (**118**):* flash chromatography eluent: dichloromethane-methanol 99:1; solid phase: aluminum oxide. Yield 50% (0.96 g); white solid; mp 249–250 °C (EtOEt-light petroleum). ^{1}H NMR (400 MHz, DMSO-d_6): δ 8.43 (bs, 2H), 7.90–7.58 (m, 2H), 7.48 (s, 1H), 7.11 (s, 2H), 3.85 (s, 3H). ^{13}C NMR (68 MHz, DMSO-d_6): δ 163.99, 159.78, 154.71, 148.28, 147.27, 131.47, 130.31, 119.58, 116.76, 112.12, 96.92, 55.30. ES-MS (methanol) *m/z*: 276.0 $[M+H]^+$.

*7-chloro-2-(3,5-dimethoxyphenyl)-[1,2,4]triazolo[1,5-c]pyrimidin-5-amine (**119**)*: flash chromatography eluent: EtOAc-light petroleum 1:1. Yield: 42% (0.88 g); white solid; mp 251 °C (EtOAc-light petroleum). ^{1}H NMR (400 MHz, DMSO) δ 8.40 (bs, 2H), 7.35 (d, $J = 2.3$ Hz, 2H), 7.09 (s, 1H), 6.67 (t, $J = 2.3$ Hz, 1H), 3.83 (s, 6H). ^{13}C NMR (101 MHz, DMSO) δ 163.65, 160.74, 154.41, 148.05, 147.02, 131.80, 104.86, 102.73, 96.78, 55.42. ES-MS (methanol) *m/z* 306,1 $[M+H]^+$.

General synthesis of N^7-benzyl-2-substituted-[1,2,4]triazolo [1,5-*c*]pyrimidine-5,7-diamine (**32,33,36**).

Method A: 1.5 mmol of derivatives **118**–**119** were reacted with 3 mmol of benzylamine and 4.5 mmol of potassium carbonate in 8 mL of ethanol in a sealed tube at 95 °C for 4 days. When the reaction was completed, the solvent was evaporated and the crude material purified by chromatography.

in a gradient from DCM-MeOH 99.5:0.5 to 99:1.

Method B: 0.33 mmol of 7-chloro-2-(3,5-dimethoxyphenyl)-[1,2,4]triazolo[1,5-*c*]pyrimidin-5-amine (**119**, 100 mg) were added to 0.64 mmol (70 mg) of benzylamine, 0.98 mmol (135 mg) of potassium carbonate and 2 mL of butanol. The mixture was stirred for 36 h at the temperature of 100 °C. The solvent was removed under reduced pressure and the residue was purified with flash chromatography (light petroleum/ethyl acetate 40%). The compound was filtered with ethyl acetate and light petroleum to give a pale yellow solid.

*N^7-benzyl-2-(3-methoxyphenyl)-[1,2,4]triazolo[1,5-c]pyrimidine-5,7-diamine (**32**):* Method A. Yield 28% (131 mg); white solid; mp 207 °C (EtOEt-light petroleum). ^{1}H NMR (270 MHz, DMSO-d_6): δ 7.75–7.56 (m, 2H), 7.56–7.15 (m, 9H), 7.07–6.99 (m, 1H), 5.66 (s, 1H), 4.42 (d, $J = 6.0$ Hz, 2H), 3.82 (s, 3H). ^{13}C NMR (101 MHz, dmso) δ 162.71, 159.35, 157.51, 156.07, 146.51, 139.81, 132.35, 129.71, 128.28, 127.10, 126.67, 119.15, 115.79, 111.74, 73.75, 55.14, 44.74. ES-MS (methanol) *m/z*: 347.1 $[M+H]^+$. HRMS (ESI-TOF) *m/z*: $C_{19}H_{18}N_6O$ experimental 347.1614 $[M+H]^+$, theoretical 347.1614 $[M+H]^+$, $\Delta = 0.0000$. Purity HPLC (Method A): 99.4%.

*N^7-benzil-2-(3,5-dimethoxyphenyl)[1,2,4]triazolo[1,5-c]pyrimidin-5,7-diamine (**33**):* Method B. Yield: 17% (22 mg); pale yellow solid; mp 208 °C (EtOAc-light petroleum). ^{1}H NMR (400 MHz, CD_3OD) δ 7.40–7.35 (m, 2H), 7.34–7.28 (m, 4H), 7.23 (dt, $J = 9.3$, 4.3 Hz, 1H), 6.57 (t, $J = 2.3$ Hz, 1H), 5.73 (s, 1H), 4.49 (s, 2H), 3.84 (s, 6H). ^{13}C NMR (101 MHz, CD_3OD) δ 164.57, 162.48, 159.84, 157.70, 148.26, 140.65, 133.55, 129.51 (CH), 128.21 (CH), 128.01 (CH), 106.09 (CH), 103.59 (CH), 74.98 (CH), 55.92 (CH_3), 46.62 (CH_2). ES-MS

(methanol) *m/z* 377.2 $[M+H]^+$. HRMS (ESI-TOF) *m/z*: $C_{20}H_{20}N_6O_2$ experimental 377.1721 $[M+H]^+$, theoretical 377.1720 $[M+H]^+$, $\Delta = 0.0001$. Purity HPLC (Method A): 97.7%.

*2-(3,5-dimethoxyphenyl)-N^7,N^7-dimethyl-[1,2,4]triazolo[1,5-c]pyrimidine-5,7-diamine (**36**):* during synthesis of compound **33** using method A, 5 drops of DMF were added to the reaction mixture to solubilize the starting material and reaction was heated at 100 °C for 3 days. Compound 33 was not detected while the only product obtained was compound **36**. Yield: 30% (0.141 g), white solid; mp 242 °C (EtOEt-methanol). ^{1}H NMR (400 MHz, DMSO) δ 7.53 (bs, 2H), 7.30 (d, $J = 2.4$ Hz, 2H), 6.60 (t, $J = 2.4$ Hz, 1H), 5.84 (s, 1H), 3.81 (s, 6H), 3.03 (s, 6H). ^{13}C NMR (101 MHz, DMSO) δ 162.78, 160.54, 157.52, 156.24, 145.80, 132.95, 104.63 (CHx2), 102.03 (CH), 73.70 (CH), 55.32 (CH_3x2), 37.61 (CH_3x2). ES-MS (methanol) *m/z* 315.1 $[M+H]^+$. HRMS (ESI-TOF) *m/z*: $C_{15}H_{18}N_6O_2$ experimental 315.1559 $[M+H]^+$, theoretical 315.1564 $[M+H]^+$, $\Delta = 0.0005$. Purity HPLC (Method A): 96.0%.

General procedure for deprotection of 7-substituted [1,2,4]triazolo[1,5-*c*]pyrimidines (34,35–37).

12 equivalents of a 10 M solution of boron tribromide in DCM were slowly added to a cooled (−78 °C) solution of methoxy-derivatives (**32,33,36**1 equivalent) in dichloromethane (10 mL/mmol of methoxy derivatives) under argon atmosphere. The cooling bath was removed and the suspension was slowly warmed up to room temperature and stirred for 12 h. Once completed, at least an equal volume of cool methanol was added dropwise and the solution stirred for 15 minutes-1 hour. Then the volatile species were removed under reduced pressure, thus giving the corresponding deprotected derivatives (**34,35**–**37**).

*3-(5-amino-7-(benzylamino)-[1,2,4]triazolo[1,5-c]pyrimidin-2-yl) phenol (**34**):* Flash chromatography eluent: DCM-MeOH 98.5:1.5. Yield 39% (38 mg from 0.29 mmol of **32**); white solid; mp 267 °C (EtOEt-light petroleum). ^{1}H NMR (400 MHz, DMSO-d_6) δ 9.59 (s, 1H), 7.63–7.51 (m, 2H), 7.45 (bs, 2H), 7.41–7.12 (m, 7H), 6.95–6.72 (m, 1H), 5.66 (s, 1H), 4.42 (d, $J = 6.0$ Hz, 2H). ^{13}C NMR (101 MHz, dmso) δ 162.97, 157.47, 157.44, 156.00, 146.49, 139.85, 132.20, 129.55, 128.28, 127.08, 126.67, 117.66, 116.86, 113.70, 73.75, 44.73. ES-MS (methanol) *m/z*: 333.2 $[M+H]^+$. HRMS (ESI-TOF) *m/z*: $C_{18}H_{16}N_6O$ experimental 333.1459 $[M+H]^+$, theoretical 333.1458 $[M+H]^+$, $\Delta = 0.0001$. Purity HPLC (Method A): 95.7%.

*5-(5-amino-7-(benzylamino)-[1,2,4]triazolo[1,5-c]pyrimidin-2-yl) benzene-1,3-diol (**35**):* Yield 30% (6.6 mg from 0.058 mmol of **33**); white solid; mp 250-256 d °C (EtOEt-methanol). ^{1}H NMR (400 MHz, DMSO-d_6) δ 9.38 (s, 2H), 7.52–7.27 (m, 6H), 7.27–7.09 (m, 2H), 6.99 (s, 2H), 6.28 (s, 1H), 5.64 (s, 1H), 4.42 (d, $J = 5.7$ Hz, 2H). ^{13}C NMR (101 MHz, CD_3OD) δ 163.48, 158.41, 158.29, 156.14, 146.77, 139.24, 132.03, 128.08, 126.77, 126.57, 105.49, 104.06, 72.21, 45.20. ES-MS (methanol) *m/z* 349.2 $[M+H]^+$. HRMS (ESI-TOF) *m/z*: $C_{18}H_{16}N_6O_2$ experimental 349.1404 $[M+H]^+$, theoretical 349.1407 $[M+H]^+$, $\Delta = 0.0003$. Purity HPLC (Method A): 98.9%.

*5-(5-amino-7-(dimethylamino)-[1,2,4]triazolo[1,5-c]pyrimidin-2-yl)benzene-1,3-diol (**37**)*: Yield 82% (122 mg from 0.45 mmol of **36**); white solid; mp 268 d °C (EtOEt-methanol). 1H NMR (400 MHz, DMSO-d_6) δ 9.80 (s, 2H), 8.16 (s, 2H), 6.94 (d, $J = 2.0$ Hz, 2H), 6.51 (t, $J = 2.0$ Hz, 1H), 5.89 (s, 1H), 3.12 (s, 6H). ^{13}C NMR (101 MHz, DMSO) δ 159.55, 159.42, 146.73, 146.45, 106.59, 105.80, 71.50, 38.22 (some signals were not detected). ES-MS (methanol) *m/z* 287.1 $[M+H]^+$, 309.1 $[M+Na]^+$. HRMS (ESI-TOF) *m/z*: $C_{13}H_{14}N_6O_2$ experimental 287.1253 $[M+H]^+$, theoretical 287.1251 $[M+H]^+$, $\Delta = 0.0002$. Purity HPLC (Method A): 98.2%.

Synthesis of 2,5,7-trisubstituted [1,2,4]triazolo[1,5-a][1,3,5]triazines (**38**–**57**).

Synthesis of 2,4,6-triphenoxy-[1,3,5]triazine (**121**).

A mixture of 2,4,6-trichloro-[1,3,5]triazine (**120**, 184.4 g, 1.0 mol) was dissolved in phenol (3.0–4.0 mol) and refluxed for 5h. The hot reaction was extracted with methanol and a white solid (253.7 g) was obtained. Yield 71%; mp 235 °C (EtOAc-light petroleum); ^{1}H NMR (270 MHz, $CDCl_3$): δ 7.39 (m, 6H), 7.32–7.22 (m, 3H), 7.17 (m, 6H).

General procedure for the synthesis of substituted *N*'-(4,6-diphenoxy-1,3,5-triazin-2-yl)hydrazides (**123**–**127**).

2,4,6-triphenoxy-[1,3,5]triazine (**121**, 10.0 g, 0.028 mol) and the required hydrazide (**65**, **68**, **71**–**72**, **122**) (0.0476 mmol) was dissolved in anhydrous THF (200 mL) while DBU (7.1 mL, 0.0476 mmol) was added dropwise at 0 °C. The mixture was stirred at room temperature for 12 h. The solvent was then removed, the residue was dissolved in DCM (300 mL), and the resulting solution was washed with water (3 × 100 mL). The organic layer was concentrated, dried over anhydrous sodium sulfate, and purified by flash chromatography.

*N'-(4,6-diphenoxy-1,3,5-triazin-2-yl)-4-methoxybenzohydrazide (**123**):* flash chromatography eluent: DCM-EtOAc 98:2. Yield 48% (5.77 g); white solid; mp 220–221 °C (EtOEt-light petroleum). ^{1}H NMR (270 MHz, $CDCl_3$): δ 8.59 (bs, 1H), 7.68 (d, $J = 8.7$ Hz, 2H), 7.42–7.32 (m, 2H), 7.30–7.19 (m, 4H), 7.21–7.06 (m, 5H), 6.87 (d, $J = 8.7$ Hz, 2H), 3.84 (s, 3H). ES-MS (methanol) *m/z*: 430.2 $[M+H]^+$, 452.2 $[M+Na]^+$.

*N'-(4,6-diphenoxy-1,3,5-triazin-2-yl)-3-methoxybenzohydrazide (**124**):* flash chromatography eluent: DCM-EtOAc 95:5. Yield 39% (4.69 g); white solid; mp 182–184 °C (EtOEt-light petroleum). ^{1}H NMR (400 MHz, DMSO-d_6): δ 10.45 (s, 1H), 10.05 (s, 1H), 7.49–7.21 (m, 10H), 7.18–7.09 (m, 4H), 3.80 (s, 3H). ES-MS (methanol) *m/z*: 430.1 $[M+H]^+$, 452.1 $[M+Na]^+$.

*N'-(4,6-diphenoxy-1,3,5-triazin-2-yl)-3,5-dimethoxybenzohydrazide (**125**):* flash chromatography eluent: DCM-EtOAc 90:10. Yield 38% (4.89 g); white solid; mp 212–213 °C (EtOEt-light petroleum). ^{1}H NMR (270 MHz, DMSO-d_6): δ 10.45 (s, 1H), 10.05 (s, 1H), 7.53–7.35 (m, 2H), 7.35–7.04 (m, 8H), 7.04–6.89 (m, 2H), 6.73–6.68 (m, 1H), 3.79 (s, 6H). ES-MS (methanol) *m/z*: 460.2 $[M+H]^+$, 482.1 $[M+Na]^+$.

*N'-(4,6-diphenoxy-1,3,5-triazin-2-yl)benzohydrazide (**126**):* flash chromatography eluent: DCM-EtOAc 95:5. Yield 62% (4.95 g); white solid; mp 204–207 °C (EtOEt-light petroleum); ^{1}H NMR (270 MHz, $CDCl_3$): δ 8.54 (s, 1H), 7.66 (d, $J = 7.6$ Hz, 2H), 7.52 (q, $J = 7.0$ Hz, 1H), 7.46–7.31 (m, 4H), 7.31–7.19 (m, 4H), 7.11 (dd, $J = 12.8$, 7.8 Hz, 5H). ES-MS (methanol) *m/z*: 400.3 $[M+H]^+$, 422.2 $[M+Na]^+$, 438.2 $[M+K]^+$.

*N'-(4,6-diphenoxy-1,3,5-triazin-2-yl)-3,4-dimethoxybenzohydrazide (**127**):* flash chromatography eluent: DCM-EtOAc 90:10. Yield 25% (3.22 g); white solid; mp 146–149 °C (EtOEt-light petroleum). ^{1}H NMR (270 MHz, DMSO-d_6): δ 10.34 (s, 1H), 9.99 (s, 1H), 7.55–6.97 (m, 13H), 3.83 (s, 3H), 3.79 (s, 3H). ES-MS (methanol) *m/z*: 460.2 $[M+H]^+$, 482.2 $[M+Na]^+$.

General procedure for the synthesis of 5,7-diphenoxy-[1,2,4] triazolo[1,5-*a*][1,3,5]triazines (**128**–**132**) The mixture of phosphorous pentoxyde (0.045 mol, Method A or 0.075 mol, Method B) and hexamethyldisiloxane (0.045 mol, Method A or 0.075 mol Method B) in anhydrous xylene (150 mL) was heated to 90 °C over 1.5 h and then stirred for 1 h at 90 °C, under argon atmosphere. The well-dried hydrazides compounds (**123**–**127**) (0.015 mol, 1 equivalent) were then added to the clear solution and the temperature is increased to reflux and stirred for 2–4 h. The solvent was then removed, the residue dissolved in DCM (300 mL) and the resulting solution was washed with water (3 × 100 mL). The organic layer was concentrated, dried over anhydrous sodium sulfate, and purified to afford the desired compounds.

*2-(4-methoxyphenyl)-5,7-diphenoxy-[1,2,4]triazolo[1,5-a][1,3,5] triazine (**128**):* Method A. Flash chromatography eluent: DCM. Yield 39% (2.41 g); white solid; mp 216 °C (EtOEt-light petroleum). ^{1}H NMR (270 MHz, $CDCl_3$): δ 8.28 (d, $J = 8.8$ Hz, 2H), 7.56–7.47 (m, 2H),

7.44–7.34 (m, 5H), 7.24–7.15 (m, 3H), 7.00 (d, $J = 8.8$ Hz, 2H), 3.88 (s, 3H). ES-MS (acetonitrile) *m/z*: 412.2 $[M+H]^+$*0.2-(3-methoxyphenyl)-5,7-diphenoxy-[1,2,4]triazolo[1,5-a][1,3,5]triazine* (***129***):Method B. Flash chromatography eluent: DCM. Yield 71% (4.38 g); white solid; mp 235 °C (EtOEt-light petroleum). ^{1}H NMR (400 MHz, DMSO-d_6): δ 7.80 (d, J = 7.6 Hz, 1H), 7.70 (s, 1H), 7.65–7.39 (m, 8H), 7.32 (t, J = 7.3 Hz, 1H), 7.28–7.19 (m, 2H), 7.18–7.11 (m, 1H), 3.85 (s, 3H). ^{13}C NMR (68 MHz, $CDCl_3$): δ 167.51, 164.98, 160.68, 160.18, 155.03, 152.06, 150.78, 130.91, 130.35, 130.05, 129.90, 127.79, 126.47, 121.73, 121.42, 120.44, 118.42, 112.20, 55.59. ES-MS (acetonitrile) *m/z*: 412.1 $[M+H]^+$, 434.1 $[M+Na]^+$.

2-(3,5-dimethoxyphenyl)-5,7-diphenoxy-[1,2,4]triazolo[1,5-a][1,3,5]triazine (***130***)**:** Method B. Flash chromatography eluent: DCM. Yield 25% (1.65 g); white solid; mp 211 °C (EtOEt-light petroleum). ^{1}H NMR (270 MHz, $CDCl_3$): δ 7.59–7.47 (m, 4H), 7.47–7.34 (m, 5H), 7.34–7.12 (m, 3H), 6.68–6.55 (m, 1H), 3.86 (s, 6H). ^{13}C NMR (101 MHz, $CDCl_3$): δ 167.18, 164.67, 161.00, 160.32, 154.72, 151.77, 150.51, 131.19, 130.09, 129.64, 127.53, 126.22, 121.49,121.18, 105.27, 104.65, 55.64. ES-MS (acetonitrile) *m/z*: 442.2 $[M+H]^+$, 464.1 $[M+Na]^+$.

2-phenyl-5,7-diphenoxy-[1,2,4]triazolo[1,5-a][1,3,5]triazine (***131***): Method A. Flash chromatography eluent: DCM. Yield 75% (4.3 g); white solid; mp 246–250 °C (EtOEt-light petroleum); ^{1}H NMR (270 MHz, $CDCl_3$) δ: 8.38–8.28 (m, 2H), 7.65–7.34 (m, 9H), 7.34–7.10 (m, 4H). ^{13}C NMR (68 MHz, $CDCl_3$): δ 167.36, 164.72, 160.49, 154.80, 151.83, 150.55, 131.24, 130.08, 129.62, 129.41, 128.73, 127.81, 127.52, 126.20, 121.47, 121.17. ES-MS (methanol) *m/z*: 382.2 $[M+H]^+$, 404.2 $[M+Na]^+$, 420.1 $[M+K]^+$.

2-(3,4-dimethoxyphenyl)-5,7-diphenoxy-[1,2,4]triazolo[1,5-a][1,3,5]triazine (***132***)**:** Method B. Flash chromatography eluent: DCM-MeOH 99:1. Yield 51.5% (3.41 g); white solid; mp 248–249 °C (EtOEt-light petroleum). ^{1}H NMR (270 MHz, $CDCl_3$): δ 8.06–7.88 (m, 1H), 7.84 (m, 1H), 7.58–7.47 (m, 2H), 7.47–7.32 (m, 5H), 7.32–7.13 (m, 3H), 6.98 (m, 1H), 3.98 (s, 3H), 3.95 (s, 3H). ^{13}C NMR (68 MHz, DMSO-d_6): δ 165.5, 164.4, 160.4, 155.1, 152.0, 151.5, 150.7, 149.1, 130.2, 129.8127.4, 126.2, 121.9, 121.6, 121.4, 120.5, 112.0, 109.7, 55.6, 55.5. ES-MS (acetonitrile) *m/z*: 442.2 $[M+H]^+$, 464.2 $[M+Na]^+$.

General procedure for the synthesis of 5-phenoxy-[1,2,4]triazolo[1,5-*a*][1,3,5]triazin-7-amines (**133**–**137**).

A solution of the 5,7-diphenoxy-[1,2,4]triazolo[1,5-*a*][1,3,5] triazine derivative (2 mmol) in methanol (20 mL) with methanolic ammonia 7 N (12 mmol) was stirred for 2 h at room temperature. The solvent was removed under reduced pressure and the residue purified by flash chromatography, when required, or directly crystallized from EtOEt-light petroleum to afford the desired compounds as solids.

2-(4-methoxyphenyl)-5-phenoxy-[1,2,4]triazolo[1,5-a][1,3,5]triazin-7-amine (***133***): flash chromatography eluent: DCM-MeOH 99:1. Yield 86% (0.575 g); white solid; mp > 300 °C (EtOEt-light petroleum).^{1}H NMR (400 MHz, DMSO-d_6): δ 9.07 (s, 1H), 8.72 (s, 1H), 8.06 (d, J = 8.8 Hz, 2H), 7.46 (t, J = 7.9 Hz, 2H), 7.39–7.20 (m, 3H), 7.09 (d, J = 8.8 Hz, 2H), 3.83 (s, 3H). ^{13}C NMR (101 MHz, DMSO-d_6): δ 165.2, 164.2, 161.6, 159.4, 152.9, 152.3, 130.0, 128.8, 125.8, 123.1, 122.3, 114.7, 55.8. ES-MS (methanol) *m/z*: 335.1 $[M+H]^+$, 357.1 $[M+Na]^+$.

2-(3-methoxyphenyl)-5-phenoxy-[1,2,4]triazolo[1,5-a][1,3,5]triazin-7-amine (***134***): flash chromatography eluent: DCM-MeOH 99:1. Yield 91% (0.608 g); white solid; mp 226–229 °C (EtOEt-light petroleum). ^{1}H NMR (400 MHz, DMSO-d_6): δ 9.13 (s, 1H), 8.80 (s, 1H), 7.73 (d, J = 7.7 Hz, 1H), 7.67 (s, 1H), 7.57–7.40 (m, 3H), 7.37–7.19 (m, 3H), 7.10 (d, J = 7.7, 1H), 3.83 (s, 3H). ^{13}C NMR (101 MHz, DMSO-d_6): δ 165.3, 164.1, 159.9, 159.4, 152.9, 152.4, 132.0, 130.5, 130.0, 125.9, 122.3, 119.6, 116.9, 112.2, 55.7. ES-MS (methanol) *m/z*: 335.1 $[M+H]^+$, 357.1 $[M+Na]^+$, 373.0 $[M+K]^+$.

2-(3,5-dimethoxyphenyl)-5-phenoxy-[1,2,4]triazolo[1,5-a][1,3,5]triazin-7-amine (***135***): yield 95% (0.692 mg); white solid; mp 274 °C (EtOEt-light petroleum). ^{1}H NMR (400 MHz, DMSO-d_6): δ 9.12 (s, 1H), 8.78 (s, 1H), 7.46 (t, J = 7.8 Hz, 2H), 7.36–7.20 (m, 5H), 6.65 (s, 1H), 3.81 (s, 6H). ^{13}C NMR (101 MHz, DMSO-d_6): δ 165.3, 164.0, 161.1, 159.4, 152.8, 152.4, 132.5, 130.0, 125.9, 122.3, 110.0, 105.0, 103.1, 55.8. ES-MS (methanol) *m/z*: 365.1 $[M+H]^+$, 387.1 $[M+Na]^+$. MW 364.36. $C_{18}H_{16}N_6O_3$.

5-phenoxy-2-phenyl-[1,2,4]triazolo[1,5-a][1,3,5]triazin-7-amine (***136***): flash chromatography eluent: gradient from DCM-EtOAc 99:1 to 98:2. Yield 89% (0.133 g from 0.5 mmol of **131**); white solid. ^{1}H NMR (270 MHz, DMSO) δ 9.11 (s, 1H), 8.79 (s, 1H), 8.13 (d, J = 3.8 Hz, 2H), 7.74–7.38 (m, 5H), 7.38–7.03 (m, 3H). ES-MS (methanol) *m/z*: 305.2 $[M+H]^+$, 327.1 $[M+Na]^+$.

2-(3,4-dimethoxyphenyl)-5-phenoxy-[1,2,4]triazolo[1,5-a][1,3,5]triazin-7-amine (***137***): flash chromatography eluent: DCM-MeOH 99:1. Yield 89.5% (0.652 g); white solid; mp 276–278 °C (EtOEt-light petroleum). ^{1}H NMR (270 MHz, DMSO-d_6): δ 9.02 (bs, 1H), 8.83 (bs, 1H), 7.76–7.73 (m, 2H), 7.53–7.41 (m, 2H), 7.34–7.21 (m, 3H), 7.17–7.08 (m, 1H), 3.83 (s, 6H). ^{13}C NMR (101 MHz, DMSO-d_6): δ 165.2, 164.3, 159.4, 152.9, 152.3, 151.3, 149.2, 130.0, 125.8, 123.1, 122.3, 120.4, 112.2, 110.2, 56.0, 55.9. ES-MS (methanol) *m/z*: 365.2 $[M+H]^+$, 387.1 $[M+Na]^+$.

General procedure for the synthesis of N^5-benzyl-[1,2,4]triazolo[1,5-*a*][1,3,5]triazin-5,7-diamine (**38**,**39**,**41**–**47**) and N^7,N^5-dibenzyl-[1,2,4]triazolo[1,5-*a*][1,3,5]triazin-5,7-diamine (**40**).

Method A: A solution of 7-amino-5phenoxy-[1,2,4]triazolo[1,5-*a*][1,3,5]triazine derivatives (**133**–**134**, **136**–**137**) (2 mmol) with 6 mmol of the required amine in ethanol (20 mL) was stirred at 95–100 °C in a sealed tube for 24–72 h. The solvent was removed under reduced pressure and the residue was purified, when necessary, by flash chromatography or directly crystallized from EtOEt-light petroleum and washed with a small amount of methanol to afford the desired compounds as solids.

Method B: 0.750 mmol of 2-(3,5-dimethoxyphenyl)-5-phenoxy-[1,2,4]triazolo[1,5-*a*][1,3,5]triazine-7-amine (**135**) were dissolved in 5 mL of butanol, then 2.25 mmol of the desired amine were added. The reaction was allowed to react in a microwave (100 W) at 170 °C for 2 h. Once the reaction was completed, the solvent was removed under reduced pressure and the residue was purified by flash chromatography.

N^5-benzyl-2-(4-methoxyphenyl)-[1,2,4]triazolo[1,5-a][1,3,5]triazine-5,7-diamine (***38***): Method A. Flash chromatography eluent: DCM-MeOH 99:1. Yield 12% (21 mg); white solid; mp 266–269 °C (EtOEt-light petroleum). ^{1}H NMR (400 MHz, DMSO-d_6): δ 8.51–7.75 (m, 5H), 7.49–7.14 (m, 5H), 7.14–6.92 (m, 2H), 4.50 (d, J = 6.9 Hz, 2H), 3.81 (s, 3H). ^{13}C NMR (101 MHz, DMSO-d_6): δ 161.2, 160.1, 154.5, 140.4, 136.2, 132.9, 128.6, 127.5, 125.2, 123.7, 122.6, 114.5, 55.7, 44.2. ES-MS (methanol) *m/z*: 348.1 $[M+H]^+$, 370.1 $[M+Na]^+$. HRMS (ESI-TOF) *m/z*: $C_{18}H_{17}N_7O$ experimental 348.1570 $[M+H]^+$, theoretical 348.1567 $[M+H]^+$, Δ = 0.0003. Purity HPLC (Method A): 96.4%.

N^5-benzyl-2-(3-methoxyphenyl)-[1,2,4]triazolo[1,5-a][1,3,5]triazine-5,7-diamine (***39***): Method A. Flash chromatography eluent: DCM-MeOH 97:3. Yield 46% (80 mg); white solid; mp 271 °C (EtOEt-light petroleum). ^{1}H NMR (400 MHz, DMSO-d_6): δ 8.54–8.01 (m, 2H), 7.98 (t, J = 6.3 Hz, 1H) 7.73–7.61 (m, 2H), 7.42 (t, J = 7.9 Hz, 1H), 7.37–7.28 (m, 4H), 7.28–7.19 (m, 1H), 7.09–7.01 (m, 1H), 4.57–4.45 (m, 2H), 3.82 (s, 3H). ^{13}C NMR (101 MHz, DMSO-d_6): δ 162.94, 161.6, 159.8, 151.1, 150.6, 140.4, 132.6, 130.3, 128.6, 127.5, 127.0, 119.4, 116.5, 112.0, 55.6, 44.2. ES-MS (methanol) *m/z*: 348,1 $[M+H]^+$, 370,1 $[M+Na]^+$. HRMS (ESI-TOF) *m/z*: $C_{18}H_{17}N_7O$ experimental 348.1568 $[M+H]^+$, theoretical 348.1567 $[M+H]^+$, Δ = 0.0001. Purity HPLC (Method A): 98.8%.

In this case, also the *N^5,N^7-dibenzyl-2-(3-methoxyphenyl)-[1,2,4]triazolo[1,5-a][1,3,5]triazine-5,7-diamine* was isolated (***40***): Yield 15% (33 mg); white solid; mp 169–170 °C (EtOEt-light petroleum).

^{1}H NMR (400 MHz, DMSO-d_6): δ 9.22 + 9.07 (m, 1H), 8.20-8-09 (m, 1H), 7.70 (d, J = 7.6 Hz, 1H), 7.64 (s, 1H), 7.51–7.16 (m, 11H), 7.10–7.03 (m, 1H), 4.72–4.56 (m, 2H), 4.50 (d, J = 6.2 Hz, 2H), 3.82 (s, 3H). ^{13}C NMR (101 MHz, DMSO-d_6): δ 163.0, 161.4, 159.9, 149.2, 140.2, 138.9, 132.6, 130.3, 128.8, 128.6, 128.2, 127.9, 127.6, 127.5, 127.1, 119.4, 116.6, 111.9, 55.6, 44.3, 43.7. ES-MS (methanol) m/z: 438.2 $[M+H]^+$, 460.2 $[M+Na]^+$. HRMS (ESI-TOF) m/z: $C_{25}H_{23}N_7O$ experimental 438.2032 $[M+H]^+$, theoretical 438.2036 $[M+H]^+$, Δ = 0.0004. Purity HPLC (Method A): 95.1%.

*N^5-benzyl-2-(3,5-dimethoxyphenyl)-[1,2,4]triazolo[1,5-a][1,3,5] triazine-5,7-diamine (**41**)*: Method A. Flash chromatography eluent: EtOAc-light petroleum 7:3. Yield 10% (19 mg); white solid; mp 279–281 °C (EtOEt-light petroleum). ^{1}H NMR (400 MHz, DMSO-d_6): δ 8.46–7.84 (m, 3H), 7.43–7.13 (m, 7H), 6.59 (bs, 1H), 4.51 (bs, 2H), 3.79 (s, 6H). ES-MS (methanol) m/z: 378.1 $[M+H]^+$, 400.1 $[M+Na]^+$, 416.1 $[M+K]^+$. HRMS (ESI-TOF) m/z: $C_{19}H_{19}N_7O_2$ experimental 378.1672 $[M+H]^+$, theoretical 378.1672 $[M+H]^+$, Δ = 0.0000. Purity HPLC (Method A): 97.7%.

*N^5-(4-chlorobenzyl)-2-(3,5-dimethoxyphenyl)-[1,2,4]-triazolo-[1,5-a]-[1,3,5]-triazine-5,7-diamine (**42**):* Method B. flash chromatography eluent: DCM-MeOH 98:2. Yield: 39% (0.110 g); white solid; mp 285–287 °C (EtOEt-light petroleum). ^{1}H NMR (400 MHz, DMSO-d_6) δ 8.48–7.90 (m, 3H), 7.42–7.34 (m, 4H), 7.26 (d, J = 2.4 Hz, 2H), 6.61 (t, J = 2.4 Hz, 1H), 4.48 (d, J = 6.4 Hz, 2H), 3.80 (s, 6H). ^{13}C NMR (101 MHz, DMSO-d_6) δ 167.55, 161.59, 161.02, 159.65, 150.60, 139.49, 133.14, 131.53, 129.36 (2 x CH), 128.58 (2 x CH), 104.85 (2 x CH), 102.73 (CH), 55.79 (2 x CH_3), 43.64 (CH_2). MW = 411.1211. ES-MS (methanol) m/z: 412,1 $[M+H]^+$. HRMS (ESI-TOF) m/z: $C_{19}H_{18}ClN_7O_2$ experimental 412.2282 $[M+H]^+$, theoretical 412.1283 $[M+H]^+$, Δ = 0.0999; experimental 434.1101 $[M+Na]^+$, 434.1103 $[M+Na]^+$, Δ = 0.0002; $C_{19}H_{18}^{37}ClN_7O_2$ experimental 414.1260 $[M+H]^+$, theoretical 414.1253 $[M+H]^+$, Δ = 0.0007; experimental 436.1084 $[M+Na]^+$, 436.1073 $[M+Na]^+$, Δ = 0.0011. Purity HPLC (Method B): 96.1%

*N^5-(4-fluorobenzyl)-2-(3,5-dimetoxyphenyl)-[1,2,4]-triazolo-[1,5-a]-[1,3,5]-triazine-5,7-diamine (**43**):* Method B. flash chromatography eluent: DCM-MeOH 98:2. Yield: 41% (0.112 g); white solid; mp 264–266 °C (EtOEt-light petroleum). ^{1}H NMR (400 MHz, DMSO-d_6) δ 8.27–7.91 (m, 3H), 7.40–7.34 (m, 2H), 7.26 (d, J = 2.3 Hz, 2H), 7.17–7.09 (m, 2H), 6.61 (t, J = 2.3 Hz, 1H), 4.48 (d, J = 6.5 Hz, 2H), 3.80 (s, 6H). ^{13}C NMR (101 MHz, DMSO-d_6) δ 170.93, 161.14, 160.59, 159.24, 150.16, 136.11, 131.92 (d, $^1J_{CF}$ = 160.6 Hz), 131.11, 129.00 (d, $^2J_{CF}$ = 8.0 Hz, 2 x CH), 114.89 (d, $^3J_{CF}$ = 21.0 Hz, 2 x CH), 104.43 (2 x CH), 102.29 (CH), 55.34 (2 x CH_3), 43.12 (CH_2).

HRMS (ESI-TOF) m/z: $C_{19}H_{18}FN_7O_2$ experimental 396.1580 $[M+H]^+$, theoretical 396.1579 $[M+H]^+$, Δ = 0.0001; experimental 418.1395 $[M+Na]^+$, 418.1398 $[M+Na]^+$, Δ = 0.0003. Purity HPLC (Method B): 98.1%

*N^5-(3-methylbenzyl)-2-(3,5-dimethoxyphenyl)-[1,2,4]-triazolo-[1,5-a]-[1,3,5]-triazine-5,7-diamine (**44**):* Method B. flash chromatography eluent: DCM-MeOH 99:1. Yield: 13% (35.2 mg); white solid; mp 262–264 °C (EtOEt-light petroleum). ^{1}H NMR (400 MHz, DMSO-d_6) δ 8.16–7.89 (m, 3H), 7.27 (d, J = 2.4 Hz, 2H), 7.20 (t, J = 7.4 Hz, 1H), 7.15–7.10 (m, 2H), 7.04 (d, J = 7.4 Hz, 1H), 6.61 (t, J = 2.4 Hz, 1H), 4.47 (d, J = 6.4 Hz, 2H), 3.81 (s, 6H), 2.28 (s, 3H).^{13}C NMR (101 MHz, DMSO-d_6) δ 162.87, 161.60, 161.02, 159.71, 150.55, 140.33, 137.64, 133.17, 128.5 (CH), 127.99 (CH), 127.65 (CH), 124.56 (CH), 104.86 (2 x CH), 102.70 (CH), 55.77 (2 x CH_3), 44.17 (CH_2), 21.51 (CH_3). HRMS (ESI-TOF) m/z: $C_{20}H_{21}N_7O_2$ experimental 392.1828 $[M+H]^+$, theoretical 392.1829 $[M+H]^+$, Δ = 0.0001; experimental 414.1650 $[M+Na]^+$, theoretical 414.1649 $[M+Na]^+$, Δ = 0.0001. Purity HPLC (Method B): 96.7%.

*N^5-cyclohexyl-2-(3,5-dimethoxyphenyl)-[1,2,4]-triazolo-[1,5-a]-[1,3,5]-triazine-5,7-diamine (**45**):* Method B. flash chromatography eluent: DCM-MeOH 99:1. Yield: 16% (44.1 mg); white solid, mp 230–232 °C (EtOEt-light petroleum). ^{1}H NMR (400 MHz, DMSO-d_6) δ 8.48–7.82 (m, 2H), 7.39–7.18 (m, 2H), 6.61 (t, J = 2.4 Hz, 1H), 3.81 (s, 7H), 1.95–1.82 (m, 2H), 1.79–1.68 (m, 2H), 1.65–1.54 (m, 1H), 1.38–1.04 (m, 5H).^{13}C NMR (101 MHz, DMSO-d_6) δ 163.56, 160.57, 160.20, 159.35, 132.81, 132.19, 104.38 (2 x CH_2), 101.03 (CH), 78.33 (CH), 55.33 (2 x CH_3), 32.25 (2 x CH_2), 25.31 (CH_2), 24.92 (2 x CH_2). HRMS (ESI-TOF) m/z: $C_{18}H_{23}N_7O_2$ experimental 370.1988 $[M+H]^+$, theoretical 370.1987 $[M+H]^+$, Δ = 0.0001; experimental 392.1807 $[M+Na]^+$, 392.1805 $[M+Na]^+$, Δ = 0.0002. Purity HPLC (Method B): 98.3%.

*N^5-benzyl-2-phenyl-[1,2,4]triazolo[1,5-a][1,3,5]triazine-5,7-diamine (**46**):* Method A. Flash chromatography eluent: DCM-MeOH 99:1. Yield 27% (12 mg from 0.141 mmol of **136**); white solid. ^{1}H NMR (200 MHz, DMSO) δ 8.73–7.78 (m, 5H), 7.65–7.42 (m, 3H), 7.40–7.01 (m, 5H), 4.51 (d, J = 5.7 Hz, 2H). ES-MS (methanol) m/z: 318.2 $[M+H]^+$, 340.1 $[M+Na]^+$.

*N^5-benzyl-2-(3,4-dimethoxyphenyl)-[1,2,4]triazolo[1,5-a][1,3,5] triazine-5,7-diamine (**47**):* Method A. Flash chromatography eluent: DCM-MeOH 97:3. Yield 33% (62 mg); white solid; mp 234–235 °C (EtOEt-light petroleum). ^{1}H NMR (270 MHz, DMSO-d_6): δ 8.42–7.81 (m, 3H), 7.72–7.55 (m, 2H), 7.44–7.18 (m, 6H), 7.08 (d, J = 8.4 Hz, 1H), 4.50 (m, 1H), 3.82 (s, 6H). ^{13}C NMR (101 MHz, DMSO-d_6): δ 160.0, 159.6, 150.9, 150.5, 149.1, 140.5, 136.1, 130.7, 128.6, 127.5, 127.0, 120.1, 112.1, 110.2, 55.99, 55.81, 44.24. ES-MS (methanol) m/z: 378.2 $[M+H]^+$, 400.1 $[M+Na]^+$, 416.1 $[M+K]^+$. HRMS (ESI-TOF) m/z: $C_{19}H_{19}N_7O_2$ experimental 378.1669 $[M+H]^+$, theoretical 378.1672 $[M+H]^+$, Δ = 0.0003. Purity HPLC (Method B): 99.7%.

General procedure for deprotection of the hydroxyl group of 2,5,7-disubstituted [1,2,4]triazolo[1,5-*a*][1,3,5]triazines (**48**–**57**).

3 equivalents of a 1 M solution of boron tribromide in DCM were slowly added to a cooled (−78 °C) solution of methoxy-derivatives (**38**–**45,47,** 1 equivalent) in dichloromethane (10 mL/mmol of methoxy derivatives) under argon atmosphere. The cooling bath was removed and the suspension was slowly warmed up to room temperature and stirred for 12 h. Once completed, at least an equal volume of cool methanol was added dropwise and the solution stirred for 15 minutes-1 hour. Then the volatile species were removed under reduced pressure, thus giving the corresponding deprotected derivatives (**48**–**57**) that were purified by column chromatography or preparative TLC.

*4-(7-amino-5-(benzylamino)-[1,2,4]triazolo[1,5-a][1,3,5]triazin-2-yl)phenol (**48**):* flash chromatography eluent: DCM-MeOH 95:5. Yield 30% (25 mg from 0.25 mmol of **38**); white solid; mp 295 °C (EtOEt-light petroleum). ^{1}H NMR (400 MHz, DMSO-d_6): δ 9.87 (s, 1H), 8.51–7.80 (m, 5H), 7.41–7.15 (m, 5H), 6.86 (d, J = 8.2 Hz, 2H), 4.50 (d, J = 6.7 Hz, 2H). ^{13}C NMR (101 MHz, DMSO-d_6): δ 163.0, 161.6, 159.7, 150.5, 140.4, 138.5, 133.8, 128.7, 128.6, 127.5, 127.0, 115.8, 44.2. ES-MS (methanol) m/z: 334.1 $[M+H]^+$, 356.1 $[M+Na]^+$, 372.0 $[M+K]^+$. HRMS (ESI-TOF) m/z: $C_{17}H_{15}N_7O$ experimental 334.1409 $[M+H]^+$, theoretical 334.1410 $[M+H]^+$, Δ = 0.0001. Purity HPLC (Method A): 95.1%.

*3-(7-amino-5-(benzylamino)-[1,2,4]triazolo[1,5-a][1,3,5]triazin-2-yl)phenol (**49**):* flash chromatography eluent: DCM-MeOH 96:4. Yield 30% (25 mg from 0.25 mmol of **39**); white solid; mp 237–238 °C (EtOEt-light petroleum). ^{1}H NMR (400 MHz, DMSO-d_6): δ 9.65 (s, 1H), 8.50–7.82 (m, 3H), 7.61–7.45 (m, 2H), 7.45–7.17 (m, 6H), 6.86 (d, J = 7.1 Hz, 1H), 4.51 (d, J = 6.5 Hz, 2H). ^{13}C NMR (101 MHz, DMSO-d_6): δ 163.6, 163.2, 161.6, 157.9, 150.6, 140.4, 132.5, 130.1, 128.6, 127.5, 127.0, 117.9, 117.5, 114.0, 44.2. ES-MS (methanol) m/z: 334.1 $[M+H]^+$, 356.1 $[M+Na]^+$. HRMS (ESI-TOF) m/z: $C_{17}H_{15}N_7O$ experimental 334.1412 $[M+H]^+$, theoretical 334.1411 $[M+H]^+$, Δ = 0.0001. Purity HPLC (Method A): 99.7%.

*3-(5,7-bis(benzylamino)-[1,2,4]triazolo[1,5-a][1,3,5]triazin-2-yl) phenol (**50**):* flash chromatography eluent: DCM-MeOH 98:2 (stationary phase: alumina). Yield 15% (16 mg from 0.25 mmol of **40**);

white solid; mp 275–276 °C (EtOEt-light petroleum). ^{1}H NMR (400 MHz, DMSO-d_6): δ 9.65 (s, 1H), 9.09 (m, 1H), 8.12 (s, 1H), 7.69–7.08 (m, 13H), 6.87 (d, J = 8.2 Hz, 1H), 4.77–4.40 (m, 4H). ^{13}C NMR (101 MHz, DMSO-d_6): δ 161.4, 157.9, 151.7, 140.2, 138.9, 132.4, 130.1, 128.76, 128.72, 128.64, 128.1, 127.9, 127.64, 127.50, 127.1, 117.9, 117.6, 114.0, 44.3, 44.1. ES-MS (methanol) m/z: 424.2 $[M+H]^+$, 346.2 $[M+Na]^+$. MW 423.47. $C_{24}H_{21}N_7O$. HRMS (ESI-TOF) m/z: $C_{24}H_{21}N_7O$ experimental 424.1884 $[M+H]^+$, theoretical 424.1880 $[M+H]^+$, Δ = 0.0004. Purity HPLC (Method A): 99.7%.

*5-(7-amino-5-(benzylamino)-[1,2,4]triazolo[1,5-a][1,3,5]triazin-2-yl)benzen-1,3-diol (**51**):* flash chromatography eluent: DCM-MeOH 96:4. Yield 40% (35 mg from 0.25 mmol of **41**); white solid; mp > 300 °C (EtOEt-light petroleum). ^{1}H NMR (400 MHz, DMSO-d_6): δ 9.39 (s, 2H), 7.93–7.82 (m, 2H), 7.39–7.14 (m, 6H), 7.00–6.92 (m, 2H), 6.28 (bs, 1H), 4.57–4.43 (m, 2H). ^{13}C NMR (101 MHz, DMSO-d_6): δ 163.5, 161.5, 159.6, 158.9, 150.5, 140.5, 132.9, 128.6, 127.5, 127.0, 105.5, 104.7, 44.2. ES-MS (methanol) m/z: 350.1 $[M+H]^+$. HRMS (ESI-TOF) m/z: $C_{17}H_{15}N_7O_2$ experimental 350.1360 $[M+H]^+$, theoretical 350.1359 $[M+H]^+$, Δ = 0.0001. Purity HPLC (Method A): 99.4%.

*N^5-(4-chlorobenzyl)-2-(3,5-dihydroxyphenyl)-[1,2,4]-triazolo-[1,5-a][1,3,5]-triazine-5,7-diamine (**52**):* flash chromatography eluent: EtOAc-MeOH 90:10. Yield 80% (35 mg from 0.11 mmol of **42** using 12 equivalents of boron tribromide); white solid; mp 260 °C (EtOEt-light petroleum). ^{1}H NMR (400 MHz, DMSO-d_6) δ 9.43 (s, 2H), 8.58–7.75 (m, 3H), 7.43–7.29 (m, 4H), 6.98 (s, 2H), 6.31 (t, J = 2.2 Hz, 1H), 4.49 (d, J = 5.9 Hz, 2H) ^{13}C NMR (101 MHz, DMSO-d_6) δ 162.96, 161.09, 158.47 (2CH), 150.14, 139.06, 132.37, 131.10 (2CH), 128.93 (2CH), 128.13, 105.03 (2CH), 104.29 (CH), 43.17 (CH_2). ES- MS (methanol) m/z: 384.1 $[M+H]^+$. Purity HPLC (Method B): 97.7%.

*N^5-(4-fluorobenzyl)-2-(3,5-dihydroxyphenyl)-[1,2,4]-triazolo-[1,5-a][1,3,5]-triazine-5,7-diamine (**53**):* preparative TLC eluent: DCM-MeOH 97:3. Yield 8% (6.2 mg from 0.2 mmol of **43**); light brown solid; mp 269–271 °C (EtOEt-light petroleum). ^{1}H NMR (400 MHz, CD_3OD) δ 7.51–7.28 (m, 2H), 7.07 (d, J = 2.2 Hz, 2H), 7.02 (t, J = 8.8 Hz, 2H), 6.37 (t, J = 2.2 Hz, 1H), 4.59 (s, 2H).HRMS (ESI-TOF) m/z: $C_{17}H_{14}FN_7O_2$ experimental 368.1261 $[M+H]^+$, theoretical 368.1266 $[M+H]^+$, Δ = 0.0005. Purity HPLC (Method B): 97.1%.

*N^5-(3-methylbenzyl)-2-(3,5-dihydroxyphenyl)-[1,2,4]-triazolo-[1,5-a][1,3,5]-triazine-5,7-diamine (**54**):* preparative TLC eluent: DCM-MeOH 94:6. Yield 7% (11.4 mg from 0.43 mmol of **44**); white solid; mp > 300 °C (EtOEt-light petroleum). ^{1}H NMR (400 MHz, Methanol-d_4) δ 7.23–7.12 (m, 3H), 7.09–7.01 (m, 3H), 6.38 (t, J = 2.3 Hz, 1H), 4.58 (s, 2H), 2.32 (s, 3H). HRMS (ESI-TOF) m/z: $C_{18}H_{17}N_7O_2$ experimental 364.1516 $[M+H]^+$, theoretical 364.1522 $[M+H]^+$, Δ = 0.0006; experimental 386.1336 $[M+H]^+$, theoretical 386.1338 $[M+H]^+$, Δ = 0.0002. Purity HPLC (Method B): 98.5%.

N^5-cyclohexyl-2-(3,5-dihydroxyphenyl)-[1,2,4]-triazolo-[1,5-a][1,3,5]-triazine-5,7-diamine (**55**):

preparative TLC eluent: DCM-MeOH 94:6. Yield 43% (13.9 mg from 0.088 mmol of **45**); white solid; mp > 300 °C (EtOEt-light petroleum). ^{1}H NMR (400 MHz, CD_3OD) δ 7.07 (d, J = 1.6 Hz, 2H), 6.37 (s, 1H), 3.84 (s, 1H), 2.00 (s, 2H), 1.85–1.56 (m, 3H), 1.55–1.08 (m, 5H). HRMS (ESI-TOF) m/z: $C_{16}H_{19}N_7O_2$ experimental 342.1674 $[M+H]^+$, theoretical 342.1673 $[M+H]^+$, Δ = 0.0001; experimental 364.1496 $[M+H]^+$, theoretical 364.1492 $[M+H]^+$, Δ = 0.0004. Purity HPLC (Method B): 96.9%.

*N^5-cyclohexyl-2-(3-hydroxyphenyl)-(5-methoxyphenyl)-[1,2,4]-triazolo-[1,5-a][1,3,5]-triazine-5,7-diamine (**56**):* preparative TLC eluent: DCM-MeOH 94:6. Yield 32% (10.5 mg from 0.088 mmol of **45**); white solid; mp > 300 °C (EtOEt-light petroleum). ^{1}H NMR (400 MHz, CD_3OD) δ 7.29–7.07 (m, 2H), 6.46 (t, J = 2.2 Hz, 1H), 3.99–3.71 (m, 4H), 2.00 (s, 2H), 1.78 (m, 2H), 1.66 (m, 1H), 1.56–1.21 (m, 5H). HRMS (ESI-TOF) m/z: $C_{17}H_{21}N_7O_2$ experimental 356.1832 $[M+H]^+$, theoretical 356.1829 $[M+H]^+$, Δ = 0.0003. Purity HPLC (Method B): 98.7%.

*4-(7-amino-5-(benzylamino)-[1,2,4]triazolo[1,5-a][1,3,5]triazin-2-yl)benzen-1,2-diol (**57**):* flash chromatography eluent: EtOAc-MeOH 8:2. Yield 33% (29 mg from 0.5 mmol of **47**); white solid; mp 233 °C (EtOEt-light petroleum). ^{1}H NMR (270 MHz, DMSO-d_6): δ 9.32 (s, 1H), 9.19 (s, 1H), 8.36–7.77 (m, 4H), 7.65–7.16 (m, 6H), 6.81 (d, J = 8.2 Hz, 1H), 4.56–4.41 (m, 2H). ^{13}C NMR (101 MHz, DMSO-d_6): δ 163.4, 161.6, 159.6, 158.9, 150.5, 143.2, 140.4, 132.9, 128.6, 127.5, 127.0, 105.5, 104.7, 44.2. ES-MS (methanol) m/z: 350.1 $[M+H]^+$. HRMS (ESI-TOF) m/z: $C_{17}H_{15}N_7O_2$ experimental 350.1355 $[M+H]^+$, theoretical 350.1359 $[M+H]^+$, Δ = 0.0004. Purity HPLC: 99.1%.

7. Biochemistry

7.1. CK1δ activity assays

Assay with truncated *CK1δ*. Compounds were evaluated towards CK1δ (Merck Millipore, recombinant human, amino acids 1–294, with N-terminal GST-tagged) with the KinaseGlo® luminescence assay (Promega) following procedures reported in literature [20,59]. In detail, luminescent assays were performed in black 96-well plates, using the following buffer: 50 mM HEPES (pH 7.5), 1 mM EDTA, 1 mM EGTA, and 15 mM magnesium acetate. Compound CR8 (IC_{50} = 0.4 μM) was used as a positive control for CK1δ [44] while DMSO/buffer solution was used as a negative control. In a typical assay, 10 μL of inhibitor solution (dissolved in DMSO at 10 mM concentration and diluted in assay buffer to the desired concentration) and 10 μL (16 ng of CK1δ) of enzyme solution were added to the well, followed by 20 μL of assay buffer containing 0.1% casein substrate and 4 μM ATP (or 40 μM and 400 μM for ATP competition experiment). The final DMSO concentration in the reaction mixture did not exceed 1–2%. After 60 min of incubation at 30 °C for CK1δ the enzymatic reactions were stopped with 40 μL of Kinase-Glo reagent (Promega). Luminescence signal (relative light unit, RLU) was recorded after 10 min at 25 °C using Tecan Infinite M100 or FLUOstar Optima multimode readers. The activity is proportional to the difference of the total and consumed ATP. The inhibitory activities were calculated on the basis of maximal activities measured in the absence of inhibitor [63].

First, enzyme activity percentage was determined at 40 μM for each inhibitor with respect to DMSO; subsequently, for the most active compounds the IC_{50} values were determined. Data were analyzed using Excel and GraphPad Prism software (version 8.0).Assay with full length *CK1δ*. Compounds were evaluated towards CK1δ (full length, ThermoFisher) with the KinaseGlo® luminescence assay (Promega). In detail, luminescent assays were performed in black 96-well plates, using the following buffer: 50 mM HEPES (pH 7.5),1 mM EDTA, 1 mM EGTA, and 15 mM magnesium acetate. Compound PF-670462 was used as positive control for CK1δ while DMSO/buffer solution was used as negative control. In a typical assay, 10 μL of inhibitor solution (dissolved in DMSO at 10 mM concentration and diluted in assay buffer to the desired concentration) and 10 μL (26 nM) of enzyme solution were added to the well, followed by 20 μL of assay buffer containing 0.1% casein substrate and 4 μM ATP. The final DMSO concentration in the reaction mixture did not exceed 1–2%. After 10 min of incubation at 30 °C the enzymatic reactions were stopped with 40 μL of KinaseGlo ® reagent (Promega). Luminescence signal (relative light unit, RLU) was recorded after 10 min at 30 °C using Tecan Infinite M100. For IC_{50} determination, ten different inhibitor concentrations ranging from 100 to 0.026 μM were used. IC_{50} values are reported as means ± standard errors of three independent experiments. Data were analyzed using GraphPad Prism software (version 8.0).

7.2. Competition binding assays on other kinases

KINOMEscan™ platform by DiscoverX has been applied to 6 human protein kinase CK1 isoforms: CK1α1, CK1α1L, CK1γ1-3, CK1δ and CK1ε, by testing compound **51** at a concentration of 10 μM following a protocol reported in literature [60].

7.3. Cytotoxicity in non-tumoral cells

Peripheral blood lymphocytes (PBL) from healthy donors were obtained from human peripheral blood (leucocyte rich plasma-buffy coats) from healthy volunteers using the Lymphoprep (Fresenius KABI Norge AS) gradient density centrifugation.

Buffy coats were obtained from the Blood Transfusion Service, Azienda Ospedaliera of Padova and provided at this institution for research purposes. Therefore, no informed consent was further needed. In addition, buffy coats were provided without identifiers. The experimental procedures were carried out in strict accordance with approved guidelines.

After extensive washing, cells were resuspended (1.0×10^6 cells/mL) in RPMI-1640 with 10% FBS and incubated overnight. For cytotoxicity evaluations in proliferating PBL cultures, non-adherent cells were resuspended at 5×10^5 cells/mL in growth medium, containing 2.5 μg/mL Phytohematoagglutinin (PHA, Irvine Scientific). For cytotoxicity evaluations in resting PBL cultures, non-adherent cells were resuspended (5×10^5 cells/mL) and treated for 72 h with the test compounds, as described above.

Normal human adult fibroblast were purchased by ATCC (PCS-201-012) and were cultivated in DMEM additioned of 10% fetal Bovine serum. 2 × 104 cells were plated in 96 well plate and after 24 h, different concentrations of the test compounds were added, and viability was determined 72 h later. For both cell lines viability was evaluated by resazurin-based cell, measuring the relative fluorescence intensity at 590 nm with a Spark (Tecan) multiwell plate reader during a 4 h timespan.

7.4. CNS permeation prediction: PAMPA-BBB assay

Prediction of the brain penetration of active compounds was evaluated using a parallel artificial membrane permeability assay (PAMPA) [62]. Ten drugs of known BBB permeability (2–6 mg of Caffeine, Enoxacine, Hydrocortisone, Desipramine, Ofloxacine, Piroxicam, Testosterone, 12–15 mg of Promazine and Verapamil and 23 mg of Atenolol dissolved in 1000 μL of ethanol) were included in each experiment to validate the analysis set. Compounds were dissolved in a 70/30 PBS pH = 7.4 buffer/ethanol solution in a concentration that ensures adequate absorbance values in the UV-VIS light spectrum. 5 mL of these solutions were filtered with PDVF membrane filters (diameter 30 mm, pore size 0.45 μm). The acceptor indented 96-well microplate (MultiScreen 96-well Culture Tray clear, Merck Millipore) was filled with 180 μL of PBS/ethanol (70/30). The donor 96-well filtrate plate (Multiscreen® IP Sterile Plate PDVF membrane, pore size is 0.45 μM, Merck Millipore) was coated with 4 μL of porcine brain lipid (Spectra 2000) in dodecane (20 mg/mL) and after 5 min, 180 μL of each compound solution were added. Then the donor plate was carefully put on the acceptor plate to form a "sandwich", which was left undisturbed for 2.5 h at 25 °C. During this time the compounds diffused from the donor plate through the brain lipid membrane into the acceptor plate. After incubation, the donor plate was removed. The concentrations of compounds and commercial drugs were determined by measuring the absorbance in the donor (before the incubation) and the acceptor wells (after the incubation) with UV plate reader Tecan Infinite M1000. Every sample was analyzed at two to five wavelengths in 3 replicates and in two independent experiments. The permeability coefficient (*Pe*) of each drug, in centimeter per second, was calculated applying the following formula [64]:

$$Pe\frac{Vd \quad Vr}{(Vd \quad Vr).\ S.\ t} \quad \frac{100.Vd}{100.Vd - \%T(Vd \quad Vr)}$$

$$\%T = \frac{Vr\ .\ Ar}{Ad\ .\ Vd}100$$

where Vd and Vr are the volumes of the donor and the receptor solutions (0.18 cm^3), S is the membrane area (0.266 cm^2), t is the time of incubation (2.5 h = 9000 s), Ar is the absorbance of the receptor plate after the experiment and Ad0 is the absorbance in the donor compartment before incubation. Results are given as the mean and the average of the two runs ± standard deviation (SD) is reported.

Obtained results for quality control drugs were then correlated to permeability data found in the literature. The linear correlation between experimental and literature permeability values was used for the classification of compounds in those able to cross the BBB by passive permeation (CNS + which correlate with a bibliographic Pe > 4) and those not (CNS- which correlate with a bibliographic Pe < 2).

Compounds correlating with reported Pe values from 2 to 4 10^{-6} cm s^{-1} are classified as CNS+/-. Complete data were reported in supporting information.

7.5. Molecular modeling

Most of the in-silico operations described in the following paragraphs were performed on a Desktop Linux workstation (Intel® Core™ CPU i9-9820 × 3.30 GHz). The collection of MD trajectories instead was made possible using a Linux Server equipped with a Titan V GPU.

7.6. Three-dimensional structures of CK1δ

Among the 31 crystallographic structures available for the human protein kinase *CK1δ*, two were selected for this computational study. For molecular docking calculations, as well as for SuMD simulations, the holo-form of the protein kinase (PDB ID: 4HNF) was chosen, while for the investigation of the hydrodynamic behavior of the solvent within the catalytic binding pocket, the apo-form (PDB ID: 5IH4) was instead selected. The two structures were retrieved from the RCSB Protein Data Bank database and were processed with the protein preparation tool as implemented in the Molecular Operating Environment (MOE) suite 2019.01 version [65,66]. In detail, missing hydrogen atoms were added, establishing the more probable ionization states for all titratable residues at pH 7.4 using the Protonate-3D tool [67]. Missing atoms in protein side chains were built according to AMBER14 force field topology and non-natural N-terminal and C-terminal were capped to mimic the previous residue. Crystallographic co-solvents or ligand were subsequently removed.

7.7. Molecular docking

Three-dimensional structures of the ligands were built by the MOE-builder tool. Ionization states were predicted using the MOE-protonate 3D tool and structures were minimized by the MMFF94x until the root mean square (RMS) gradient fell below 0.1 kcal $mol^{-1}Å^{-1}$. PLANTS docking protocol was selected as a conformational search program and ChemPLP as a scoring function [68,69]. For each compound investigated, 20 docking simulation runs were performed, searching on a sphere of 10 Å radius, build

around the coordinates of ligand 16W center of mass (PDB ID: 4HNF).

7.8. Docking results analysis

For each derivate herein investigated, a single conformation was chosen as representative of the bound state, based on the docking score and a visual inspection of each complex, in such a way to optimize the ligand-protein interaction network. Electrostatic and hydrophobic interactions, respectively IE_{ele} and IE_{hyd}, were computed between each selected ligand pose and each protein residue involved in binding (residues within 10 Å with respect to the binding site center of mass). Both these contributions were computed using MOE software and, in particular, IE_{ele} were calculated as non-bonded electrostatic interactions energy term of the force field (expressed in kcal/mol). Instead, IE_{hyd} were computed as contact hydrophobic surfaces and are associated with an adimensional score (the higher the better). The data obtained by this analysis were reported in a graphic, representing residues (x-axis) in the form of equally high rectangles rendered according to a colorimetric scale. As regards IE_{ele}, colors from blue to red represent energy values ranging from negative to positive values; for IE_{hyd}, colors from white to dark green depict scores going from 0 to positive values.

7.9. Molecular dynamics (MD)simulations setup

The tleap software, as part of the AmberTools20 suite, was exploited to explicitly solvate each molecular system by a cubic water box with cell borders placed at least 15 Å away from any protein or ligand atoms [70]. The protein force field parameters were assigned using the AMBER ff14SB and the TIP3P water model was used [71,72]. In the case also small organic molecules were present (e.g. SuMD simulations), parameters were assigned by means of parmchk tools, as implementer on AmberTools20 package, using the GAFF. The compound partial charges were instead calculated using the semiempirical method AM1-BCC [70,73,74]. To neutralize the total charge of each system, Na^+/Cl^- counterions were added to a final salt concentration of 0.154 M. The energy of each system was minimized by performing 500 steps with the conjugate-gradient method, then sampling 500000 MD steps (1 ns) in the canonical ensemble (NVT) followed by 500000 steps (1 ns) in the isothermal-isobaric ensemble (NPT), in both of the cases using 2 fs as a time step. Harmonic positional constraints have been applied during the system equilibration phases on protein-heavy atoms, with a force constant of 1 kcal mol^{-1} $Å^{-2}$, gradually reduced with a scaling factor of 0.1. The temperature was maintained at 273 K by a Langevin thermostat and the pressure at 1 atm by a Monte Carlo barostat [75,76]. All MD simulations were performed exploiting ACEMD3 platform, which is based on the OpenMM 7.4.2 engine [77,78].

7.10. AquaMMapS analysis

To characterize the hydrodynamic behavior of water molecules within the CK1δ binding site, 100 ns of classical MD simulation were sampled in the NVT ensemble with the temperature set at 273 K. The trajectory has then been superposed and aligned on the α-carbons atoms of the protein at the first frames and wrapped into an image of the system simulated under periodic boundary conditions (PBC). AquaMMapS algorithm was then exploited to analyze this trajectory and only the hydration spots characterized by a water occupancy (% O_{RMSF}) higher than 15% were retained and used in this study [79].

7.11. Supervised molecular dynamics (SuMD) setup

SuMD is a computational protocol written in python programming language allowing the exploration of the entire ligand-receptor binding mechanism, from the unbound to the bound state by collecting short unbiased MD simulations (hereinafter defined SuMD steps) at the end of which variations in the ligand-receptor distances is checked [80,81]. The supervision, more specifically, acts accepting all those SuMD steps in which a shortening in ligand-receptor distances has been sampled while rejecting and simulating again from the previous set of coordinates the other. When the ligand-protein center of mass distance falls below a defined cut-off (here 5 Å), the supervision algorithm is switched off and classical MD is exploited to relax the predicted complex. The merging of all the collected SuMD steps hence results in a SuMD trajectory describing a putative binding mechanism. SuMD code has several input parameters user-editable, such as the MD time-step (here, 2 fs), the number of MD steps within a SuMD step (here, 300000−600ps), and the residues were chosen to dynamically define the binding site location (here I23, A36 and I148). The SuMD trajectory discussed was analyzed exploiting an in-house tool written in tcl and python languages, deeply described in the original publication [82].

Declaration of competing interest

None.

Acknowledgments

MMS lab is very grateful to Chemical Computing Group, OpenEye, and Acellera for the scientific and technical partnership. MMS lab gratefully acknowledges the support of NVIDIA Corporation with the donation of the Titan V GPU used for this research. This scientific work has been financially supported by MIUR (PRIN 2010−2011, n.20103W4779_006; PRIN2017, n. 2017MT3993).

Supplementary material

additional experimental data, video 1 description and all spectra of final compounds were reported in supplementary material.

References

[1] G. Manning, D.B. Whyte, R. Martinez, T. Hunter, S. Sudarsanam, The protein kinase complement of the human genome, Science 298 (80-) (2002) 1912−1934, https://doi.org/10.1126/science.1075762.

[2] K. Yasojima, J. Kuret, A.J. Demaggio, E. McGeer, P.L. McGeer, Casein kinase 1 delta mRNA is upregulated in Alzheimer disease brain, Brain Res. 865 (2000) 116−120, https://doi.org/10.1016/S0006-8993(00)02200-9.

[3] G. Cozza, L.A. Pinna, Casein kinases as potential therapeutic targets, Expert Opin. Ther. Targets 8222 (2015) 1−22, https://doi.org/10.1517/14728222.2016.1091883.

[4] Y. Xu, Q.S. Padiath, R.E. Shapiro, C.R. Jones, S.C. Wu, N. Saigoh, K. Saigoh, L.J. Ptáček, Y.-H. Fu, Acknowledgements We Thank M. Rees for Comments on Statistical Analyses Functional Consequences of a CKId Mutation Causing Familial Advanced Sleep Phase Syndrome, 2005. www.nature.com/nature.

[5] K.C. Brennan, E.A. Bates, R.E. Shapiro, J. Zyuzin, W.C. Hallows, Y. Huang, H.Y. Lee, C.R. Jones, Y.H. Fu, A.C. Charles, L.J. Ptáček, Casein kinase Iδ mutations in familial migraine and advanced sleep phase, Sci. Transl. Med. 5 (2013), https://doi.org/10.1126/scitranslmed.3005784, 183ra56-183ra56.

[6] F. Vena, S. Bayle, A. Nieto, V. Quereda, M. Aceti, S.M. Frydman, S.S. Sansil, W. Grant, A. Monastyrskyi, P. McDonald, W.R. Roush, M. Teng, D. Duckett, Targeting casein kinase 1 delta sensitizes pancreatic and bladder cancer cells to gemcitabine treatment by upregulating deoxycytidine kinase, Mol. Canc.

Therapeut. 19 (2020) 1623–1635, https://doi.org/10.1158/1535-7163.MCT-19-0997.
[7] I. Bar, A. Merhi, L. Larbanoix, M. Constant, S. Haussy, S. Laurent, J.-L. Canon, P. Delrée, Silencing of Casein Kinase 1 Delta Reduces Migration and Metastasis of Triple Negative Breast Cancer Cells, 2018. www.oncotarget.com.
[8] T. Liu, D. Vergara, E. Laura Mazzoldi, S. Pavan, A. Pastò, E. Ceppelli, G. Pilotto, V. Barbieri, A. Amadori, Casein kinase 1 delta regulates cell proliferation, response to chemotherapy and migration in human ovarian cancer cells, Front. Oncol. | Www.Frontiersin.Org. 9 (2019) 1211, https://doi.org/10.3389/fonc.2019.01211.
[9] Y.C. Lin, M.C. Chen, T.H. Hsieh, J.P. Liou, C.H. Chen, CK1δ as a potential therapeutic target to treat bladder cancer, Aging 12 (2020) 5764–5780, https://doi.org/10.18632/aging.102966.
[10] U. Knippschild, M. Krüger, J. Richter, P. Xu, Balbina García-Reyes, C. Peifer, J. Halekotte, V. Bakulev, J. Bischof, The CK1 family: contribution to cellular stress response and its role in carcinogenesis, Front. Oncol. 4 (2014) 1–33, https://doi.org/10.3389/fonc.2014.00096. MAY.
[11] M.B. Batty, R.B. Schittenhelm, D. Dorin-Semblat, C. Doerig, J.F. Garcia-Bustos, Interaction of Plasmodium falciparum casein kinase 1 with components of host cell protein trafficking machinery, IUBMB Life 72 (2020) 1243–1249, https://doi.org/10.1002/iub.2294.
[12] E. Durieu, E. Prina, O. Leclercq, N. Oumata, N. Gaboriaud-Kolar, K. Vougogiannopoulou, N. Aulner, A. Defontaine, J.H. No, S. Ruchaud, A.-L. Skaltsounis, H. Galons, G.F. Späth, L. Meijer, N. Rachidi, From Drug Screening to Target Deconvolution: a Target-Based Drug Discovery Pipeline Using Leishmania Casein Kinase 1 Isoform 2 to Identify Compounds with Anti-leishmanial Activity, 2016, https://doi.org/10.1128/AAC.00021-16.
[13] P. Gami-Patel, I. Van Dijken, Lieke H. Meeter, S. Melhem, H.J. Tjado, Morrema, Wiep Scheper, J.C. Van Swieten, J.M. Annemieke, Rozemuller, A.A. Dijkstra, J.M. Jeroen, Hoozemans, J.J.M. Hoozemans, Unfolded protein response activation in C9orf72 frontotemporal dementia is associated with dipeptide pathology and granulovacuolar degeneration in granule cells, Brain Pathol. 31 (2021) 163–173, https://doi.org/10.1111/bpa.12894.
[14] C. Schwab, A.J. Demaggio, N. Ghoshal, L.I. Binder, J. Kuret, P.L. McGeer, Casein kinase 1 delta is associated with pathological accumulation of tau in several neurodegenerative diseases, Neurobiol. Aging 21 (2000) 503–510, https://doi.org/10.1016/S0197-4580(00)00110-X.
[15] P. Xu, C. Ianes, F. Gärtner, C. Liu, T. Burster, V. Bakulev, N. Rachidi, U. Knippschild, J. Bischof, Structure, regulation, and (patho-)physiological functions of the stress-induced protein kinase CK1 delta (CSNK1D), Gene 715 (2019), https://doi.org/10.1016/j.gene.2019.144005, 144005.
[16] P. Adler, J. Mayne, K. Walker, Z. Ning, D. Figeys, Therapeutic targeting of casein kinase 1δ/ε in an alzheimer's disease mouse model, J. Proteome Res. 18 (2019) 3383–3393, https://doi.org/10.1021/acs.jproteome.9b00312.
[17] D.P. Hanger, H.L. Byers, S. Wray, K.Y. Leung, M.J. Saxton, A. Seereeram, C.H. Reynolds, M.A. Ward, B.H. Anderton, Novel phosphorylation sites in Tau from Alzheimer brain support a role for casein kinase 1 in disease pathogenesis, J. Biol. Chem. 282 (2007) 23645–23654, https://doi.org/10.1074/jbc.M703269200.
[18] G. Li, H. Yin, J. Kuret, Casein kinase 1 delta phosphorylates tau and disrupts its binding to microtubules*, J. Biol. Chem. 279 (2004) 15938–15945, https://doi.org/10.1074/jbc.M314116200.
[19] K. Yasojima, J. Kuret, A.J. Demaggio, E. Mcgeer, P.L. Mcgeer, Casein kinase 1 delta mRNA is upregulated in Alzheimer disease brain. www.elsevier.com/locate/bres, 2000.
[20] I.G. Salado, M. Redondo, M.L. Bello, C. Perez, N.F. Liachko, B.C. Kraemer, L. Miguel, M. Lecourtois, C. Gil, A. Martinez, D.I. Perez, Protein kinase CK-1 inhibitors as new potential drugs for amyotrophic lateral sclerosis, J. Med. Chem. 57 (2014), https://doi.org/10.1021/jm500065f.
[21] C. Alquezar, I.G. Salado, A. De La Encarnación, D.I. Pérez, F. Moreno, C. Gil, A. López De Munain, A. Martínez, Á. Martín-Requero, Targeting TDP-43 Phosphorylation by Casein Kinase-1δ Inhibitors: a Novel Strategy for the Treatment of Frontotemporal Dementia, 2016, https://doi.org/10.1186/s13024-016-0102-7.
[22] L. Martínez-González, C. Rodríguez-Cueto, D. Cabezudo, F. Bartolomé, P. Andrés-Benito, I. Ferrer, C. Gil, Á. Martín-Requero, J. Fernández-Ruiz, A. Martínez, E. de Lago, Motor Neuron Preservation and Decrease of in Vivo TDP-43 Phosphorylation by Protein CK-1δ Kinase Inhibitor Treatment, Sci .Rep. 10, 2020, 4449, https://doi.org/10.1038/s41598-020-61265-y.
[23] M. Bissaro, S. Federico, V. Salmaso, M. Sturlese, G. Spalluto, S. Moro, Targeting protein kinase CK1δ with Riluzole: could it be one of the possible missing bricks to interpret its effect in the treatment of ALS from a molecular point of view? ChemMedChem (2018) https://doi.org/10.1002/cmdc.201800632.
[24] J. Kosten, A. Binolfi, M. Stuiver, S. Verzini, F.-X. Theillet, B. Bekei, M. Van Rossum, P. Selenko, Efficient modification of alpha-synuclein serine 129 by protein kinase CK1 requires phosphorylation of tyrosine 125 as a priming event, ACS Chem. Neurosci. 5 (2014), https://doi.org/10.1021/cn5002254.
[25] M. Okochi, J. Walter, A. Koyama, S. Nakajo, M. Baba, T. Iwatsubo, L. Meijer, P.J. Kahle, C. Haass, Constitutive phosphorylation of the Parkinson's disease associated a-synuclein, J. Biol. Chem. 275 (2000) 390–397, https://doi.org/10.1074/jbc.275.1.390.
[26] T. De Wit, & V Baekelandt, E. Lobbestael, Inhibition of LRRK2 or Casein Kinase 1 Results in LRRK2 Protein Destabilization, (2035). doi:10.1007/s12035-018-1449-2.
[27] Y. Qiao, T. Chen, H. Yang, Y. Chen, H. Lin, W. Qu, F. Feng, W. Liu, Q. Guo, Z. Liu, H. Sun, Small molecule modulators targeting protein kinase CK1 and CK2, Eur. J. Med. Chem. 181 (2019), https://doi.org/10.1016/j.ejmech.2019.111581.
[28] T. Chijiwa, M. Hagiwara, H. Hidaka, A newly synthesized selective casein kinase I inhibitor, N-(2-aminoethyl)-5-chloroisoquinoline-8-sulfonamide, and affinity purification of casein kinase I from bovine testis, J. Biol. Chem. 264 (1989) 4924–4927, https://doi.org/10.1016/s0021-9258(18)83679-1.
[29] G. Rena, J. Bain, M. Elliott, P. Cohen, D4476, A cell-permeant inhibitor of CK1, suppresses the site-specific phosphorylation and nuclear exclusion of FOXO1a, EMBO Rep. 5 (2004) 60–65, https://doi.org/10.1038/sj.embor.7400048.
[30] L. Behrend, D.M. Milne, M. Stoè Ter, W. Deppert, L.E. Campbell, D.W. Meek, U. Knippschild, IC261, a speci®c inhibitor of the protein kinases casein kinase 1-delta and-epsilon, triggers the mitotic checkpoint and induces p53-dependent postmitotic e€ects. www.nature.com/onc.
[31] S.D. Gross, R.A. Anderson, Casein kinase I: spatial organization and positioning of a multifunctional protein kinase family, Cell. Signal. 10 (1998) 699–711.
[32] U. Knippschild, A. Gocht, S. Wolff, N. Huber, M. St, The casein kinase 1 family : participation in multiple cellular processes in eukaryotes 17 (2005) 675–689, https://doi.org/10.1016/j.cellsig.2004.12.011.
[33] L. Badura, T. Swanson, W. Adamowicz, J. Adams, J. Cianfrogna, K. Fisher, J. Holland, R. Kleiman, F. Nelson, L. Reynolds, K.S. Germain, E. Schaeffer, B. Tate, J. Sprouse, An inhibitor of casein kinase I induces phase delays in circadian rhythms under, Free-Running and Entrained Conditions 322 (2007) 730–738, https://doi.org/10.1124/jpet.107.122846.loops.
[34] T.T. Wager, R.Y. Chandrasekaran, J. Bradley, D. Rubitski, H. Berke, S. Mente, T. Butler, A. Doran, C. Chang, K. Fisher, J. Knafels, S. Liu, J. Ohren, M. Marconi, G. DeMarco, B. Sneed, K. Walton, D. Horton, A. Rosado, A. Mead, Casein kinase 1δ/ε inhibitor PF-5006739 attenuates opioid drug-seeking behavior, ACS Chem. Neurosci. 5 (2014) 1253–1265, https://doi.org/10.1021/cn500201x.
[35] N. Oumata, K. Bettayeb, Y. Ferandin, L. Demange, A. Lopez-Giral, M.L. Goddard, V. Myrianthopoulos, E. Mikros, M. Flajolet, P. Greengard, L. Meijer, H. Galons, Roscovitine-derived, dual-specificity inhibitors of cyclin-dependent kinases and casein kinases 1, J. Med. Chem. 51 (2008) 5229–5242, https://doi.org/10.1021/jm800109e.
[36] M. Bibian, R.J. Rahaim, J.Y. Choi, Y. Noguchi, S. Schürer, W. Chen, S. Nakanishi, K. Licht, L.H. Rosenberg, L. Li, Y. Feng, M.D. Cameron, D.R. Duckett, J.L. Cleveland, W.R. Roush, Development of highly selective casein kinase 1δ/1ε (CK1δ/ε) inhibitors with potent antiproliferative properties, Bioorg, Med. Chem. Lett. 23 (2013) 4374–4380, https://doi.org/10.1016/j.bmcl.2013.05.075.
[37] C.R. Keenan, S.Y. Langenbach, F. Jativa, T. Harris, M. Li, Q. Chen, Y. Xia, B. Gao, M.J. Schuliga, J. Jaffar, D. Prodanovic, Y. Tu, A. Berhan, P.V.S. Lee, G.P. Westall, A.G. Stewart, Casein kinase 1δ/ε inhibitor, PF670462 attenuates the fibrogenic effects of transforming growth factor-β in pulmonary fibrosis, Front. Pharmacol. 9 (2018) 738, https://doi.org/10.3389/fphar.2018.00738.
[38] H. Zuo, M. Trombetta-Lima, I.H. Heijink, C.H.T.J. Van Der Veen, L. Hesse, K.N. Faber, W.J. Poppinga, H. Maarsingh, V.O. Nikolaev, M. Schmidt, A-kinase anchoring proteins diminish TGF-β 1/cigarette smoke-induced epithelial-to-mesenchymal transition, 9 (n.d) 356. doi:10.3390/cells9020356.
[39] S. Sundaram, S. Nagaraj, H. Mahoney, A. Portugues, W. Li, K. Millsaps, J. Faulkner, A. Yunus, C. Burns, C. Bloom, M. Said, L. Pinto, S. Azam, M. Flores, A. Henriksen, J. Gamsby, D. Gulick, Inhibition of Casein Kinase 1δ/ε Improves Cognitive-Affective Behavior and Reduces Amyloid Load in the APP-PS1 Mouse Model of Alzheimer's Disease Open, 2019, https://doi.org/10.1038/s41598-019-50197-x.
[40] P. Janovska, J. Verner, J. Kohoutek, L. Bryjova, M. Gregorova, M. Dzimkova, H. Skabrahova, T. Radaszkiewicz, P. Ovesna, O.V. Blanarova, T. Nemcova, Z. Hoferova, K. Vasickova, L. Smyckova, A. Egle, S. Pavlova, L. Poppova, K. Plevova, S. Pospisilova, V. Bryja, Casein Kinase 1 Is a Therapeutic Target in Chronic Lymphocytic Leukemia, 2018. http://ashpublications.org/blood/article-pdf/131/11/1206/1405389/blood786947.pdf.
[41] D.W. Kim, C. Chang, X. Chen, A.C. Doran, F. Gaudreault, T. Wager, G.J. DeMarco, J.K. Kim, Systems approach reveals photosensitivity and <scp>PER</scp> 2 level as determinants of clock-modulator efficacy, Mol. Syst. Biol. 15 (2019), https://doi.org/10.15252/msb.20198838 e8838.
[42] T. Ihara, Y. Nakamura, T. Mitsui, S. Tsuchiya, M. Kanda, S. Kira, H. Nakagomi, N. Sawada, M. Kamiyama, E. Shigetomi, Y. Shinozaki, M. Yoshiyama, A. Nakao, S. Koizumi, M. Takeda, Intermittent Restraint Stress Induces Circadian Misalignment in the Mouse Bladder, Leading to Nocturia, Sci. Rep (9), 2019, 10069, https://doi.org/10.1038/s41598-019-46517-w.
[43] A. Alli, L. Yu, M. Holzworth, J. Richards, K.-Y. Cheng, I. Jeanette Lynch, C.S. Wingo, M.L. Gumz, Direct and indirect inhibition of the circadian clock protein Per1: effects on ENaC and blood pressure, Am. J. Physiol. Ren. Physiol. 316 (2019) 807–813, https://doi.org/10.1152/ajprenal.00408.2018.-Circadian.
[44] K. Bettayeb, N. Oumata, A. Echalier, Y. Ferandin, J.A. Endicott, H. Galons, L. Meijer, CR8, a potent and selective, roscovitine-derived inhibitor of cyclin-dependent kinases, Oncogene 27 (2008) 5797.
[45] A. Monastyrskyi, N. Nilchan, V. Quereda, Y. Noguchi, C. Ruiz, W. Grant, M. Cameron, D. Duckett, W. Roush, Development of dual casein kinase 1δ/1ε (CK1δ/ε) inhibitors for treatment of breast cancer, Bioorg. Med. Chem. 26 (2018) 590–602, https://doi.org/10.1016/j.bmc.2017.12.020.
[46] L.H. Rosenberg, M. Lafitte, V. Quereda, W. Grant, W. Chen, M. Bibian, Y. Noguchi, M. Fallahi, C. Yang, J.C. Chang, W.R. Roush, J.L. Cleveland, D.R. Duckett, Therapeutic targeting of casein kinase 1δ in breast cancer, Sci. Transl. Med. 7 (2015) 1–13, https://doi.org/10.1126/scitranslmed.aac8773.

[47] S. Federico, A. Ciancetta, N. Porta, S. Redenti, G. Pastorin, B. Cacciari, K.N. Klotz, S. Moro, G. Spalluto, Scaffold decoration at positions 5 and 8 of 1,2,4- triazolo [1,5-c]Pyrimidines to explore the antagonist profiling on adenosine receptors: a preliminary Structure–Activity relationship study, J. Med. Chem. 57 (2014) 6210–6225.

[48] S. Federico, E. Margiotta, V. Salmaso, G. Pastorin, S. Kachler, K.N. Klotz, S. Moro, G. Spalluto, [1,2,4]Triazolo[1,5-c]pyrimidines as adenosine receptor antagonists: modifications at the 8 position to reach selectivity towards A3adenosine receptor subtype, Eur. J. Med. Chem. 157 (2018) 837–851, https://doi.org/10.1016/j.ejmech.2018.08.042.

[49] S. Federico, S. Paoletta, S.L. Cheong, G. Pastorin, B. Cacciari, S. Stragliotto, K.N. Klotz, J. Siegel, Z.-G. Gao, K.A. Jacobson, S. Moro, G. Spalluto, Synthesis and biological evaluation of a new series of 1,2,4-triazolo[1,5-a]-1,3,5-triazines as human A(2A) adenosine receptor antagonists with improved water solubility, J. Med. Chem. 54 (2011) 877–889, https://doi.org/10.1021/jm101349u.

[50] G. Deganutti, A. Zhukov, F. Deflorian, S. Federico, G. Spalluto, R.M. Cooke, S. Moro, J.S. Mason, A. Bortolato, Impact of protein–ligand solvation and desolvation on transition state thermodynamic properties of adenosine A2A ligand binding kinetics, Silico Pharmacol 5 (2017) 16, https://doi.org/10.1007/s40203-017-0037-x.

[51] A. Dalpiaz, B. Cacciari, C.B. Vicentini, F. Bortolotti, G. Spalluto, S. Federico, B. Pavan, F. Vincenzi, P.A. Borea, K. Varani, A novel conjugated agent between dopamine and an A 2A adenosine receptor antagonist as a potential anti-Parkinson multitarget approach, Mol. Pharm. 9 (2012) 591–604, https://doi.org/10.1021/mp200489d.

[52] S. Federico, A. Ciancetta, N. Porta, S. Redenti, G. Pastorin, B. Cacciari, K.N. Klotz, S. Moro, G. Spalluto, 5,7-Disubstituted-[1,2,4]triazolo[1,5-a][1,3,5]triazines as pharmacological tools to explore the antagonist selectivity profiles toward adenosine receptors, Eur. J. Med. Chem. 108 (2016), https://doi.org/10.1016/j.ejmech.2015.12.019.

[53] H. Tsumoki, J. Shimada, H. Imma, A. Nakamura, H. Nonaka, S. Shiozaki, S. Ichikawa, T. Kanda, Y. Kuwana, M. Ichimura, F. Suzuki, [1,2,4]Triazolo[1,5-c] Pyrimidine Derivatives, EP0976753A1, 1998.

[54] J. Hutton, Chemical Process, US 5 (1994). https://patents.google.com/patent/US5326869/pt.

[55] C. Slobutsey, L. Audrieth, R. Campbell, Acid catalysis in liquid ammonia in ammonolysis of diethylmalonate, Proc. Natl. Acad. Sci. U.S.A. 23 (1937) 611–615.

[56] J. Matasi, J. Caldwell, D. Tulshian, L. Silverman, B. Neustadt, Adenosine A2a Receptor Antagonists, EP1453835, 2006.

[57] O. Píša, S. Rádl, Synthesis of 4-quinolones: *N* , *O* -Bis(trimethylsilyl)acetamide-Mediated cyclization with cleavage of aromatic C-O bond, Eur. J. Org Chem. 2016 (2016) 2336–2350, https://doi.org/10.1002/ejoc.201600178.

[58] P.W. Caulkett, G. Jones, M. McPartlin, N. Renshaw, S. Stewart, B. Wright, Adenine isosteres with bridgehead nitrogen. Part 1. Two independent syntheses of the [1,2,4]triazolo[1,5-a]triazine ring system leading to a range of substituents in the 2,5 and 7 positions, J. Chem. Soc. Perkin Trans. 1 (1995) 801–808.

[59] S. Redenti, I. Marcovich, T. De Vita, C. Pérez, R. De Zorzi, N. Demitri, D.I. Perez, G. Bottegoni, P. Bisignano, M. Bissaro, S. Moro, A. Martinez, P. Storici, G. Spalluto, A. Cavalli, S. Federico, A triazolotriazine-based dual GSK-3β/CK-1δ ligand as a potential neuroprotective agent presenting two different mechanisms of enzymatic inhibition, ChemMedChem 14 (2019) 310–314, https://doi.org/10.1002/cmdc.201800778.

[60] M.A. Fabian, W.H. Biggs, D.K. Treiber, C.E. Atteridge, M.D. Azimioara, M.G. Benedetti, T.A. Carter, P. Ciceri, P.T. Edeen, M. Floyd, J.M. Ford, M. Galvin, J.L. Gerlach, R.M. Grotzfeld, S. Herrgard, D.E. Insko, M.A. Insko, A.G. Lai, J.-M. Lélias, S.A. Mehta, Z.V. Milanov, A.M. Velasco, L.M. Wodicka, H.K. Patel, P.P. Zarrinkar, D.J. Lockhart, A small molecule–kinase interaction map for clinical kinase inhibitors, Nat. Biotechnol. 23 (2005) 329–336, https://doi.org/10.1038/nbt1068.

[61] J.T. Henderson, M. Piquette-Miller, Blood-brain barrier: an impediment to neuropharmaceuticals, Clin. Pharmacol. Ther. 97 (2015) 308–313, https://doi.org/10.1002/cpt.77.

[62] L. Di, E.H. Kerns, K. Fan, O.J. McConnell, G.T. Carter, High throughput artificial membrane permeability assay for blood-brain barrier, Eur. J. Med. Chem. 38 (2003) 223–232, https://doi.org/10.1016/S0223-5234(03)00012-6.

[63] S. Redenti, I. Marcovich, T. De Vita, C. Pérez, R. De Zorzi, N. Demitri, D.I. Perez, G. Bottegoni, P. Bisignano, M. Bissaro, S. Moro, A. Martinez, P. Storici, G. Spalluto, A. Cavalli, S. Federico, A triazolotriazine-based dual GSK-3β/CK-1δ ligand as a potential neuroprotective agent presenting two different mechanisms of enzymatic inhibition, ChemMedChem 14 (2019) 310–314, https://doi.org/10.1002/cmdc.201800778.

[64] A. Avdeef, Absorption and Drug Development, John Wiley & Sons, Inc., Hoboken, NJ, USA, 2012, https://doi.org/10.1002/9781118286067.

[65] R. Wang, X. Fang, Y. Lu, C.Y. Yang, S. Wang, The PDBbind database: methodologies and updates, J. Med. Chem. 48 (2005) 4111–4119, https://doi.org/10.1021/jm048957q.

[66] Molecular Operating Environment (MOE), (2019).

[67] P. Labute, Protonate 3D: Assignment of Macromolecular Protonation State and Geometry, Chem. Comput. Gr. Inc., 2007.

[68] O. Korb, T. Stützle, T.E. Exner, An ant colony optimization approach to flexible protein–ligand docking, Swarm Intell (2007), https://doi.org/10.1007/s11721-007-0006-9.

[69] O. Korb, T. Stützle, T.E. Exner, Empirical scoring functions for advanced Protein-Ligand docking with PLANTS, J. Chem. Inf. Model. (2009), https://doi.org/10.1021/ci800298z.

[70] D.M. Y. and P.A.K. D.A. Case, K. Belfon, I.Y. Ben-Shalom, S.R. Brozell, D.S. Cerutti, T.E. Cheatham, III, V.W.D. Cruzeiro, T.A. Darden, R.E. Duke, G. Giambasu, M.K. Gilson, H. Gohlke, A.W. Goetz, R. Harris, S. Izadi, S.A. Izmailov, K. Kasavajhala, A. Kovalenko, R. Krasny, T, AmberTools20, (2020).

[71] J.A. Maier, C. Martinez, K. Kasavajhala, L. Wickstrom, K.E. Hauser, C. Simmerling, ff14SB: improving the accuracy of protein side chain and backbone parameters from ff99SB, J. Chem. Theor. Comput. 11 (2015) 3696–3713, https://doi.org/10.1021/acs.jctc.5b00255.

[72] W.L. Jorgensen, J. Chandrasekhar, J.D. Madura, R.W. Impey, M.L. Klein, Comparison of simple potential functions for simulating liquid water, J. Chem. Phys. (1983), https://doi.org/10.1063/1.445869.

[73] K.G. Sprenger, V.W. Jaeger, J. Pfaendtner, The general AMBER force field (GAFF) can accurately predict thermodynamic and transport properties of many ionic liquids, J. Phys. Chem. B 119 (2015) 5882–5895, https://doi.org/10.1021/acs.jpcb.5b00689.

[74] A. Jakalian, B.L. Bush, D.B. Jack, C.I. Bayly, Fast, efficient generation of high-quality atomic charges. AM1-BCC model: I. Method, J. Comput. Chem. 21 (2000) 132–146, https://doi.org/10.1002/(SICI)1096-987X(20000130)21:2<132::AID-JCC5>3.0. CO;2-P.

[75] R.J. Loncharich, B.R. Brooks, R.W. Pastor, Langevin dynamics of peptides: the frictional dependence of isomerization rates ofN-acetylalanyl-N?-methylamide, Biopolymers 32 (1992) 523–535, https://doi.org/10.1002/bip.360320508.

[76] W.L. Jorgensen, J. Chandrasekhar, J.D. Madura, R.W. Impey, M.L. Klein, Comparison of simple potential functions for simulating liquid water, J. Chem. Phys. 79 (1983) 926–935, https://doi.org/10.1063/1.445869.

[77] M.J. Harvey, G. Giupponi, G. De Fabritiis, ACEMD: accelerating biomolecular dynamics in the microsecond time scale, J. Chem. Theor. Comput. 5 (2009) 1632–1639.

[78] P. Eastman, J. Swails, J.D. Chodera, R.T. McGibbon, Y. Zhao, K.A. Beauchamp, L.-P. Wang, A.C. Simmonett, M.P. Harrigan, C.D. Stern, R.P. Wiewiora, B.R. Brooks, V.S. Pande, OpenMM 7: rapid development of high performance algorithms for molecular dynamics, PLoS Comput. Biol. 13 (2017), e1005659, https://doi.org/10.1371/journal.pcbi.1005659.

[79] A. Cuzzolin, G. Deganutti, V. Salmaso, M. Sturlese, S. Moro, AquaMMapS: an alternative tool to monitor the role of water molecules during protein-ligand association, ChemMedChem 13 (2018) 522–531, https://doi.org/10.1002/cmdc.201700564.

[80] D. Sabbadin, S. Moro, Supervised molecular dynamics (SuMD) as a helpful tool to depict GPCR–ligand recognition pathway in a nanosecond time scale, J. Chem. Inf. Model. 54 (2014) 372–376.

[81] A. Cuzzolin, M. Sturlese, G. Deganutti, V. Salmaso, D. Sabbadin, A. Ciancetta, S. Moro, Deciphering the complexity of ligand–protein recognition pathways using supervised molecular dynamics (SuMD) simulations, J. Chem. Inf. Model. 56 (2016) 687–705, https://doi.org/10.1021/acs.jcim.5b00702.

[82] V. Salmaso, M. Sturlese, A. Cuzzolin, S. Moro, Exploring protein-peptide recognition pathways using a supervised molecular dynamics approach, Structure 25 (2017) 655–662.e2, https://doi.org/10.1016/j.str.2017.02.009.